

FINAL REPORT  
Sheathing Braced Design of Wall Studs

February 2013

B.W. Schafer  
Johns Hopkins University

This report was prepared as part of the American Iron and Steel Institute sponsored project: Sheathing Braced Design of Wall Studs. The project also received supplementary support and funding from the Steel Stud Manufacturers Association. Additional project information and documentation is available at [www.ce.jhu.edu/bschafer/sheathedwalls](http://www.ce.jhu.edu/bschafer/sheathedwalls). Any opinions, findings, and conclusions or recommendations expressed in this publication are those of the author and do not necessarily reflect the views of the American Iron and Steel Institute, nor the Steel Stud Manufacturers Association.

## Table of Contents

Introduction.....	4
Publications.....	5
Basic Design Formulation .....	7
Basic Illustration for Definition of Sheathed Wall Variables.....	8
Draft Ballot 1: Lateral Restraint Provided by Fastener-Sheathing System ( $k_x$ ).....	9
Draft Ballot 2: Testing for Local Lateral Restraint of Sheathed Members ( $k_{x\ell}$ ).....	10
Draft Ballot 3: Vertical Restraint Provided by Fastener-Sheathing System ( $k_y$ ).....	15
Draft Ballot 4: Rotational Restraint Provided by Fastener-Sheathing System ( $k_\phi$ ) .....	17
Draft Ballot 5: New Test Standard, Similar to AISI S901, for Rotational Restraint ( $k_\phi$ ).....	20
Draft Ballot 6: Commentary Addition to Appendix 1 Direct Strength Method for Elastic Stability of Sheathed Walls with emphasis on using the Finite Strip Method .....	26
Draft Ballot 7: Clean up Distortional buckling notation in AISI-S100 C3.1.4 and C4.2.....	30
Draft Ballot 8: Add new section to C4.1 for Flexural-Torsional Buckling with Sheathing.....	31
Draft Ballot 9: Add new section to C3.1.2.3 for Lateral-Torsional Buckling with Sheathing.....	34
Draft Ballot 10: Clean up Sheathing-Braced Design Charging Language in S100.....	35
Draft Ballot 11: Fastener (Bearing and Pull-through) Demands [Required Loads].....	36
Draft Ballot 12: Fastener (Bearing and Pull-through) Capacity [Available Loads].....	41
Draft Ballot 13: Strength Table (Mock Up) for COFS or Design Manual.....	43
Appendix: Design Example.....	44-1 to 44-18
Appendix: CUFSM Elastic Buckling Analysis for Design Example .....	45
Appendix: Project Monitoring Task Group Responses.....	52
Appendix: Vieira Jr., L.C.M., Schafer, B.W. (2013). “Behavior and Design of Sheathed Cold-Formed Steel Stud Walls under Compression.” ASCE, <i>Journal of Structural Engineering</i> (DOI: 10.1061/(ASCE)ST.1943-541X.0000731). <i>In Press</i> .....	57
Appendix: Peterman, K.D., Schafer, B.W. “Sheathed Cold-Formed Steel Studs Under Axial and Lateral Load.” Submitted to <i>Journal of Structural Engineering</i> (Submitted 2 January 2013).....	58

## Introduction

This report provides a summary document and final report for the multi-year project on Sheathing Braced Design of Wall Studs conducted at Johns Hopkins University. This project examined the axial behavior and axial + bending behavior of cold-formed steel stud walls braced solely by sheathing connected to the stud and track flanges. This report is a practical summary of the work: the history of sheathing braced design, derivations of new analytical methods, testing on components and full sheathing-braced walls, modeling of sheathing-braced members, and the development of the proposed design method are all provided in accompanying documents. Here the focus is on the proposed design method and its application.

The research resulted in an extensive series of publications that are summarized in the next section. Comprehensive summaries of the work are available in the Ph.D. thesis of Dr. Vieira and the M.S. essay of Ms. Peterman. These documents provide a complete recording of the conducted work. Two journal publications: Vieira and Schafer (2013) and Peterman and Schafer (2013) provide the most concise summaries of the total work, and are thus included as appendices to this report.

An important step in the translation of the work from research to practice is the creation of draft Specification language, i.e., draft ballots. The existing publications provide recommendations, but not in Specification language, and in some cases not all details are provided. This final report provides a complete set of draft ballots encompassing all of the work conducted. The effort is significant and thirteen different draft ballots are provided. The ballots may be broken into four groups:

- Ballots 1-5 address the determination of the stiffness supplied by the fastener-sheathing restraint to the stud wall. Both analytical and test methods are addressed.
- Ballots 6-9 determine the elastic buckling load and/or moment when a stud has additional sheathing-based restraint. This is best summarized in a commentary on elastic buckling determination written to accompany the Appendix 1 Direct Strength Method.
- Ballots 11-12 determine fastener demands and capacity (in bearing and pull-through).
- Ballots 10,13 make a clear path for sheathing-braced design from COS to COFS standards and simplify the design in COFS standards with proposed strength tables.

An expanded design example follows the ballots. The design example illustrates the basic methodology and demonstrates how the sheathing-braced design check would work in compression and bending. The example is provided in Mathcad and provides a basis for the creation of the strength tables addressed in Ballot 13.

The first appendix provides an exchange between the project PI and the project monitoring task group on certain key aspects of implementing the research. The exchange is included as a reference for the Specification committee as the ballots go forward. Finally, the two key manuscripts for the research: Vieira and Schafer (2013) and Peterman and Schafer (2013) are included.

## Publications

As of this writing, the following publications are derived wholly or in part from research associated with this project. Most publications are available at the website [www.ce.jhu.edu/bschafer/sheathedwalls](http://www.ce.jhu.edu/bschafer/sheathedwalls) for the project. In some cases, due to copyright the articles cannot be posted directly. Please contact the author of this report for a personal copy if needed.

## Dissertations

Vieira Jr., L.C.M. (2011) Behavior and design of cold-formed steel stud walls under axial compression, Department of Civil Engineering, Ph.D. Dissertation, Johns Hopkins University.

Peterman, K.D.P. (2012) Experiments on the stability of sheathed cold-formed steel stud under axial load and bending, M.S. Essay, Department of Civil Engineering, Johns Hopkins University.

## Journal Articles

### Submitted

\*\*\*Peterman, K.D., Schafer, B.W. "Sheathed Cold-Formed Steel Studs Under Axial and Lateral Load." Submitted to *Journal of Structural Engineering* (Submitted 2 January 2013).

### Published/In Press

\*\*\*Vieira Jr., L.C.M., Schafer, B.W. (2013). "Behavior and Design of Sheathed Cold-Formed Steel Stud Walls under Compression." ASCE, *Journal of Structural Engineering* (DOI: 10.1061/(ASCE)ST.1943-541X.0000731). *In Press*

Vieira Jr., L.C.M., Schafer, B.W. (2012). "On the design methods of cold-formed steel wall studs by the AISI specification." *Revista da Estrutura de Aço*. 1 (2) 79-94.

Vieira Jr., L. C. M., Schafer, B.W. (2012). "Lateral Stiffness and Strength of Sheathing Braced Cold-Formed Steel Stud Walls." Elsevier, *Engineering Structures*. 37, 205 - 213 (doi:10.1016/j.engstruct.2011.12.029)

Vieira Jr., L. C. M., Shifferaw, Y., Schafer, B.W. (2011) "Experiments on Sheathed Cold-Formed Steel Studs in Compression." Elsevier, *Journal of Constructional Steel Research*. 67 (10) 1554-1566 (doi:10.1016/j.jcsr.2011.03.029).

## Conference Proceedings

Vieira Jr., L.C.M., Schafer, B.W. (2010) "Behavior and Design of Axially Compressed Sheathed Wall Studs." *Proceedings of the 20<sup>th</sup> Int'l. Spec. Conf. on Cold-Formed Steel Structures*, St. Louis, MO. November, 2010. 475-492.

Vieira Jr., L.C.M., Schafer, B.W. (2010). "Bracing Stiffness and Strength in Sheathed Cold-Formed Steel Stud Walls." *Proceedings SDSS'Rio 2010 STABILITY AND DUCTILITY OF STEEL STRUCTURES*, E. Batista, P. Vellasco, L. de Lima (Eds.), Rio de Janeiro, Brazil, September 8 - 10, 2010. 1069-1076.

Shifferaw, Y., Vieira<sup>†</sup> Jr., L.C.M., Schafer, B.W. (2010). "Compression testing of cold-formed steel columns with different sheathing configurations." *Proceedings of the Structural Stability Research Council - Annual Stability Conference*, Orlando, FL. 593-612.

Vieira Jr., L.C.M., Schafer, B.W. (2010). "Full-scale testing of sheathed cold-formed steel wall stud systems in axial compression." *Proceedings of the Structural Stability Research Council - Annual Stability Conference*, Orlando, FL. 533-552.

### **Miscellaneous Reports**

The following reports are unpublished works derived by students during the course of the project. The work is available in report form and was presented to the AISI COFS Design Methods committee or the Project Monitoring Task Group during the course of the research.

Iuorio, O., Schafer, B.W. (2008). "FE Modeling of Elastic Buckling of Stud Walls." Supplemental report to AISI-COFS Design Methods Subcommittee, September 2008

Blum et al. (2011). "A few thoughts on bracing and accumulation." Supplemental report to AISI-COFS Design Methods Subcommittee, February 2011

Post, B. (2012). "Fastener Spacing Study of Cold-Formed Steel Wall Studs Using Finite Strip and Finite Element Methods." Research Report, December 2012.

\*\*\* These two papers are provided in the Appendices of this report.

## Basic Design Formulation

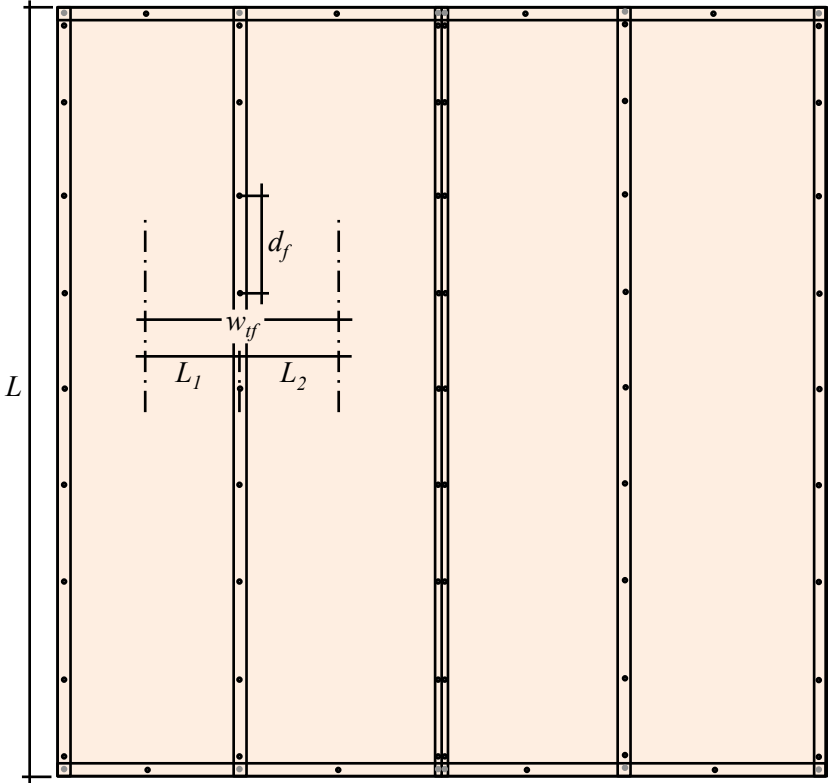
The basic design formulation for determining the available strength of a sheathed wall is as follows.

1. Determine the stiffness of the fastener-sheathing systems that provide bracing restraint to the studs. This may be completed by testing (preferred) or from closed-form design expressions that are generally geared to providing a lowerbound estimate to the stiffness. In general, the stiffness to be determined include  $k_x$ ,  $k_y$ , and  $k_z$  springs at every fastener location.
2. Determine the elastic stability ( $P_{cr}$  and/or  $M_{cr}$ ) of the studs with the bracing restraint included. This includes local ( $P_{cr\ell}$  and/or  $M_{cr\ell}$ ), distortional ( $P_{crd}$  and/or  $M_{crd}$ ), and global buckling ( $P_{cre}$  and/or  $M_{cre}$ ). This may be completed by finite strip analysis (preferred) or shell finite element analysis or from closed-form design expressions. The closed-form expressions can be lengthy and are only provided in the commentary. A closed-form expression for global buckling (i.e., LTB) in bending with the bracing restraint in place is not currently available.
3. Assess the member limit states utilizing the appropriate increased elastic stability load or moment.
  - 3a. For the Direct Strength Method (AISI-S100 Appendix 1) the local, distortional, and global buckling loads and moments are used in the existing formulas directly, and no further change is needed.
  - 3b. For conventional, Effective Width Method (AISI-S100 Main Body) design, the global buckling load or moment replaces  $F_e$  in the main Specification (for columns and for beams as appropriate) in determining  $F_n$ . Local buckling  $A_e$  and  $S_e$  is determined at the appropriate  $F_n$ . Distortional buckling utilizes the existing provisions.
4. Assess the fastener demands and limit states. For bending, torsional bracing dominates and fastener demand is based on the applied torsion created by having loads that are not applied at the shear center. For axial, stability bracing dominates and the fastener demand is based on a simplification of the forces that develop in a second order analysis. For both bending and axial load the demands are converted into fastener demands in bearing and pull-through. These demands are compared against capacities in these two limit states to assess the adequacy of the fasteners for the applied load and/or moment.

The following sections provide the first draft of specification language for completion of steps 1 through 4. In many cases the method can be formulated in tables or other derivative presentations to simplify its design use, see ballot 13 for a specific presentation of such a derivative presentation, here the fundamental formulas are provided.

**Basic Illustration for Definition of Sheathed Wall Variables**

All variables are defined in the draft ballots that follow. The illustrations provided here attempt to summarize key variables with respect to the larger design problem.



Basic illustration of a sheathed stud wall. Example wall has two full sheets as would be typical in an 8' x 8' wall with studs spaced 24 in. o.c. Basic variables for a fastener attached to one of the field studs is illustrated.

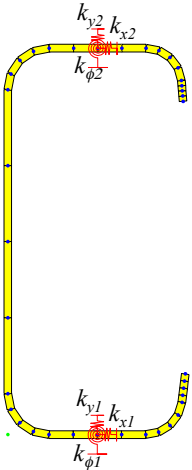


Illustration of the springs that are developed at the fastener locations on the two faces of the stud. These springs provide bracing for the stud and determination of their stiffness is the first major step of the design method.



## Draft Ballot 1: Lateral Restraint Provided by Fastener-Sheathing System ( $k_x$ )

### X.1 Sheathing Braced Member - Available Lateral Stiffness at Fastener ( $k_x$ )

The available lateral stiffness provided at a fastener location from a fastener-sheathing combination providing bracing restraint to a member shall be determined as follows.

$$k_x = \frac{1}{\frac{1}{k_{xl}} + \frac{1}{k_{xd}}} \quad (\text{X.1.1})$$

where:

$k_{xd}$  = Lateral stiffness supplied to the fastener by the sheathing under diaphragm action

$$k_{xd} = \frac{\pi^2 G_b t_b d_f w_{ff}}{L^2} \quad (\text{X.1.2})$$

$d_f$  = distance between fasteners

$w_{ff}$  = width of sheathing tributary to the fastener

$G_b$  = shear modulus of the sheathing, and shall be determined via testing (ASTM-D2719-89 or utilizing tabulated values from NDS (NDS 2005) or APA Panel Design Specification.

$t_b$  = thickness of the sheathing board

$L$  = sheathing height

and

$k_{xl}$  = localized lateral stiffness developed at the fastener during tilting and bearing,  $k_{xl}$  may be determined through testing per AISI S990-13, or as follows:

$$k_{xl} = \frac{3\pi E d^4 t^3}{4t_b^2 (9\pi d^4 + 16t_b t^3)} \quad (\text{X.1.3})$$

$E$  = Young's modulus of the CFS member (stud, joist, girt, etc.)

$t$  = thickness of the flange of the CFS member

$d$  = diameter of the fastener

$t_b$  = thickness of the sheathing board

*Commentary:* Resistance of a stud to lateral movement (as developed from weak-axis buckling, torsion, etc.) is developed from two distinct mechanisms, in series, in a sheathed wall: local and diaphragm. The diaphragm stiffness develops as the sheathing undergoes shear. The local stiffness develops as the fastener bears against the sheathing and tilts at its attachment point. The expressions and guidance provided here are detailed in Vieira and Schafer (2012). The method may be extended to purlins, girts, joists, or any member in which restraint is provided, in part, by the lateral stiffness that develops at the connection between a cold-formed steel member and sheathing.

Vieira Jr., L. C. M., Schafer, B.W. (2012). "Lateral Stiffness and Strength of Sheathing Braced Cold-Formed Steel Stud Walls." Elsevier, *Engineering Structures*. 37, 205–213.

## Draft Ballot 2: Testing for Local Lateral Restraint of Sheathed Members ( $k_{xl}$ )

### AISI S990-13 TEST STANDARD FOR DETERMINATION OF LOCAL LATERAL STIFFNESS OF FASTENER-SHEATHING RESTRAINT

#### 1. Scope

This Standard shall apply for the determination of the local lateral stiffness ( $k_{xl}$ ) supplied by sheathing, fastened to cold-formed steel members.

This Standard shall include Sections 1 through 10 inclusive.

*Commentary:* Wall studs braced solely by sheathing primarily rely on the lateral bracing restraint that is experimentally determined in this test standard. The use of this simple test for determining lateral restraint began with Winter (1960) and an updated treatment and discussion is available in Vieira and Schafer (2012). The test method may be extended to purlins, girts, joists, or any member in which restraint is provided, in part, by the localized lateral stiffness that develops at the connection between a cold-formed steel member and sheathing.

Winter, G. (1960). "Lateral Bracing of Beams and Columns." ASCE, *J. of the Structural Division*.  
Vieira Jr., L. C. M., Schafer, B.W. (2012). "Lateral Stiffness and Strength of Sheathing Braced Cold-Formed Steel Stud Walls." Elsevier, *Engineering Structures*. 37, 205-213.

#### 2. Referenced Documents

The following documents or portions thereof are referenced within this Standard and shall be considered as part of the requirements of this document.

- a. American Iron and Steel Institute (AISI), Washington, DC:
  - S100-12, North American Specification for the Design of Cold Formed Steel Structural Members, 2012 Edition.
  - S200-12, North American Standard for Cold-Formed Steel Framing - General Provisions, 2012 Edition.
- b. ASTM International (ASTM), West Conshohoken, PA:
  - A370-~~latest edition~~, Standard Test Methods and Definitions for Mechanical Testing of Steel Products
  - ASTM E6-~~latest edition~~, Standard Terminology Relating to Methods of Mechanical Testing
  - IEEE/ASTM-SI-10-~~latest edition~~, American National Standard for Use of the International System of Units (SI): The Modern Metric System

#### 3. Terminology

Where the following terms appear in this standard they shall have the meaning as defined in AISI S100, AISI S200, or as defined herein. Terms not defined in Section 3 of this standard, or AISI S100, or AISI S200 shall have the ordinary accepted meaning for the context for which they

are intended.

#### 4 Symbols

$P_{test}$  = lateral force at peak load for complete test specimen

$P_i$  = lateral force at an individual fastener

$\Delta_{0.4}$  = lateral displacement at 0.4 $P_{test}$  as measured in test

$\Delta_i$  = lateral displacement at an individual fastener

$k_{xl}$  = local lateral stiffness of fastener-sheathing system

#### 5 Precision

5.1 Loads shall be recorded to a precision of 1 percent of the ultimate load during application of test loads.

5.2 Deflections shall be recorded to a precision of 0.001 in. (0.025 mm).

#### 6 Test Fixture

6.1 The test may be conducted in a Universal Testing Machine or similar.

6.2 The test consists of two horizontal studs connected by sheathing fastened to the flanges (4 fasteners on a side) where the studs are pulled apart (perpendicular to the long axis of the stud). An example test setup is provided in Figure 1.

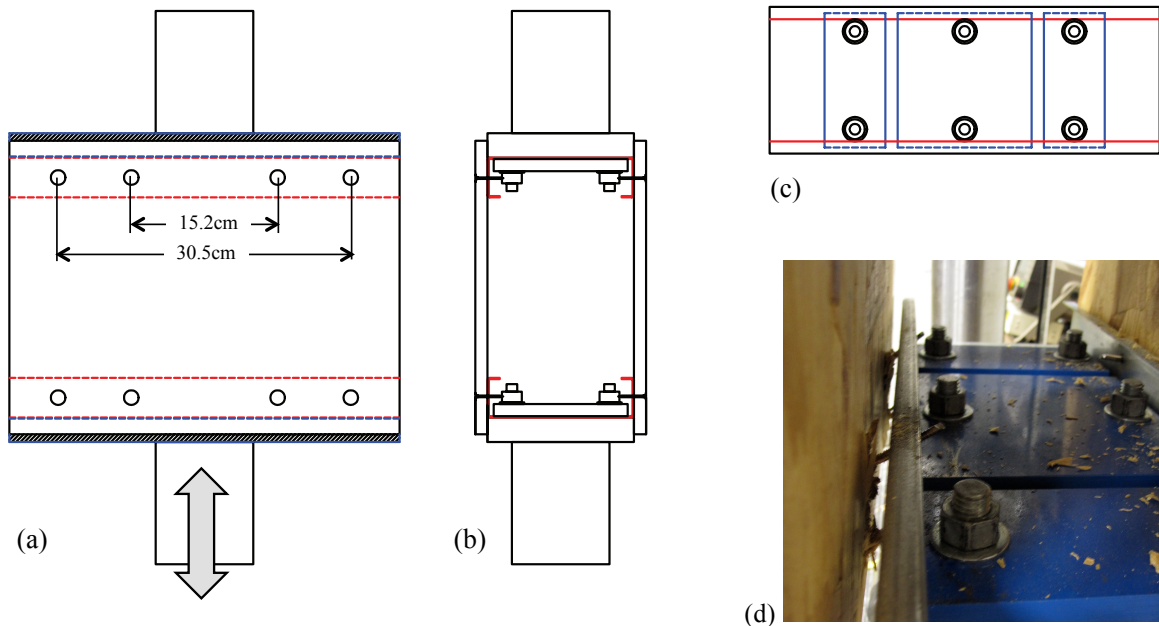


**Figure 1** (a) Front view of rig and specimen, dashed lines indicate hidden stud, arrow indicates location and direction of loading (note circles indicate potential fastening locations not actual holes in sheathing) (b) Side view of specimen in rig (c) Inside view of stud clamping system (d) photograph of clamping system

6.3 Bending in the web of the studs shall be minimized by use of clamping plates or other

means.

- 6.4 Fasteners shall be free to tilt.

## 7 Test Specimen

The test specimen consists of the studs, fasteners, and sheathing.

- 7.1 The stud should be representative of intended end use. However, the stud web depth does not have to match intended end use, as web deformation is minimized by the test fixture. The stud thickness shall not be greater than 20% above the design value. The stud length should be at least twice the fastener spacing.
- 7.2 The fasteners should be representative of intended end use. Fastener diameter shall not be greater than 20% above the design value. All fasteners should be driven to flush using the same installation methods as intended end use. Fasteners are not allowed to have their tips bear against the flange web as they tilt, if this condition occurs the fasteners should be shortened and the test redone.
- 7.3 The sheathing should be representative of intended end use. The sheathing material should be environmentally conditioned to a cited standard. The sheathing thickness shall not be greater than 20% above the design value. The sheathing width shall match the stud length. The sheathing length shall be at least equal to the fastener spacing, but not greater than the stud spacing in intended end use.

*Commentary:* The basic premise of the test specimen is the construction of a small segment of the wall consistent with final application. However, this analogy is incomplete and the test standard recognizes that the primary variables are the stud thickness, the fastener diameter (and local details of the fastener and the fastener head), and the sheathing thickness and material properties of the sheathing. Fastener spacing and stud spacing are not typically critical variables. Note, as discussed in Section 1, the stud may be replaced by a purlin, girt, joist, or any member in which restraint is provided, in part, by the localized lateral stiffness that develops at the connection between a cold-formed steel member and sheathing.

## 8 Test Procedure

- 8.1 The test should be conducted under pseudo-static monotonic load until a peak (failure) load is reached. A specific loading rate is not prescribed, but the test shall not reach peak load in less than 5 minutes.
- 8.2 Displacement shall be measured across the test specimen. Machine displacements (from the internal LVDT that drives the actuator of the Universal Testing Machine) may be used as the specimen displacement.
- 8.3 The test procedure shall be consistent with AISI S100, that is “Evaluation of the test results shall be made on the basis of the average value of test data resulting from tests of not fewer than three identical specimens, provided the deviation of any individual test result from the average value obtained from all tests does not exceed  $\pm 15$  percent. If such deviation from the average value exceeds 15 percent, more tests of the same kind shall be made until the deviation of any individual test result from the average value obtained from all tests does not exceed  $\pm 15$  percent, or until at least three additional tests have been made. No test result shall be eliminated unless a rationale for its exclusion can be given.” For this criteria, the evaluation of consistency is made on the stiffness  $k_{xL}$ .

## 9 Data Evaluation

9.1 The local lateral stiffness of the fastener-sheathing system ( $k_{xl}$ ) is determined at 40% of the ultimate strength (i.e., peak load or  $P_{test}$ ) of the specimen. Specifically:

$$P_{0.4} = 0.4P_{test} \quad (1)$$

$$P_i = P_{0.4} / 4 \quad (2)$$

$$\Delta_{0.4} = \Delta(0.4P_{test}) \quad (3)$$

$$\Delta_i = \Delta_{0.4} / 2 \quad (4)$$

$$k_{xl} = P_i / \Delta_i \quad (5)$$

where

$P_{test}$  = lateral force at peak load for complete test specimen

$P_i$  = lateral force at an individual fastener

$\Delta_{0.4}$  = lateral displacement at  $0.4P_{test}$  as measured in test

$\Delta_i$  = lateral displacement at an individual fastener

$k_{xl}$  = local lateral stiffness of fastener-sheathing system

9.2 No test result shall be eliminated unless a rationale for its exclusion can be given.

*Commentary:* Free body diagrams for the conversion from the specimen to the individual fastener values are provided in Figure 2 and 3 below. Additional discussion of the determination of the stiffness may be found in Vieira and Schafer (2012).

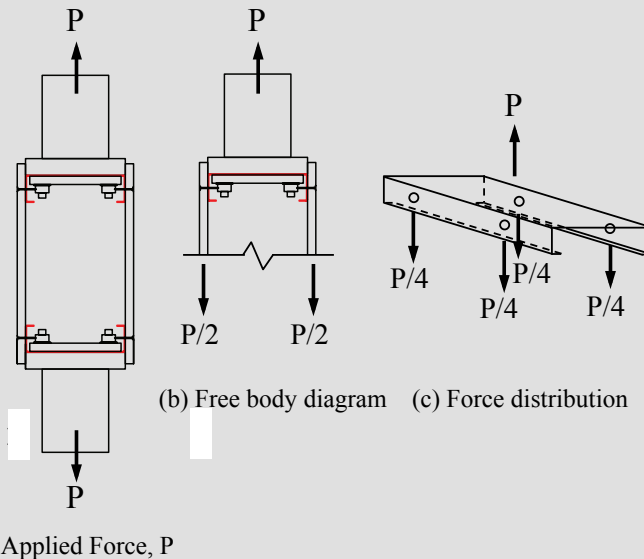
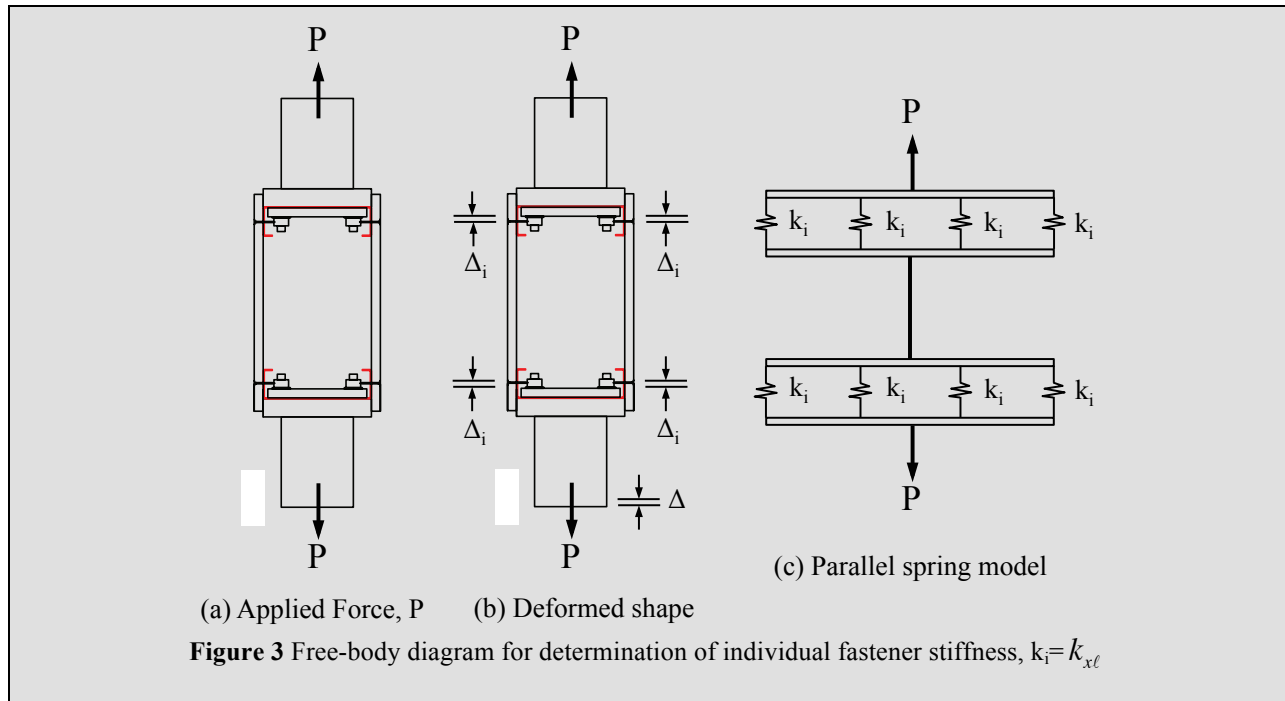


**Figure 2** Free-body diagrams for determination of individual fastener forces,  $P_i$



## 10 Report

- 10.1 The test report shall include a description of the tested specimens, including a drawing detailing all pertinent dimensions.
- 10.2 The test report shall include the measured physical properties consistent with the limitations outlined in Section 7.
- 10.3 The test report shall include a detailed drawing of the test setup, depicting location and direction of load application, location of displacement instrumentation and their point of reference, and details of any deviations from the test requirements. Additionally, photographs shall supplement the detailed drawings of the test setup.
- 10.4 The test report shall include individual and average load-versus-deformation values and curves, as plotted directly, or as reprinted from data acquisition systems.
- 10.5 The stiffness determined at 40% of the peak load ( $k_{x\ell}$ ) shall also be drawn on the load-versus-deformation curves. Values of  $k_{x\ell}$  shall be provided for all tested specimens.
- 10.5 The test report shall include individual and average maximum test load values observed (i.e.,  $P_{test}$ ). Description of the nature, type and location of failure exhibited by each specimen tested, and a description of the general behavior of the test fixture during load application. Additionally, photographs shall supplement the description of the failure mode(s).
- 10.6 The test report shall include a description of the test method and loading procedure used, rate of loading or rate of motion of the crosshead movement, and time to maximum load.

## Draft Ballot 3: Vertical Restraint Provided by Fastener-Sheathing System ( $k_y$ )

### Y.1 Sheathing Braced Member - Available Vertical Stiffness at Fastener ( $k_y$ )

The available vertical stiffness provided at a fastener location from a fastener-sheathing combination providing bracing restraint to a member shall be determined as follows.

$$k_y = \frac{(EI)_w \pi^4 d_f}{L^4} \quad (\text{Y.1.1})$$

where:

$d_f$  = distance between fasteners

$L$  = sheathing height

$(EI)_w$  = additional bending rigidity contributed by the sheathing

if composite action between the member and sheathing *is ignored*:

$(EI)_w$  = bending sheathing rigidity per APA-D510C for OSB and plywood sheathing, and GA-235-10 for gypsum sheathing

if composite action between the member and sheathing *is included*, then the additional bending rigidity shall be determined from a composite wall system test using the same test configuration as ASTM-E72:

$$(EI)_w = \frac{1}{2} [(EI)_{system} - (EI)_{stud}] \quad (\text{Y.1.2})$$

where:

$(EI)_{stud}$  = major-axis bending rigidity of the stud

$(EI)_{system}$  = major-axis bending rigidity of the tested, sheathed, wall

Depending on the test configuration employed

$$(EI)_{system} = \frac{11HL^3}{384\delta} \quad (\text{two point loads}) \quad (\text{Y.1.3})$$

$$(EI)_{system} = \frac{5wL^4}{384\delta} \quad (\text{uniform distributed load}) \quad (\text{Y.1.4})$$

where

$H$  = concentrated load applied perpendicular to the wall,

$L$  = height of the wall,

$w$  = uniform load perpendicular to the wall, and

$d$  = maximum measured displacement for the respective loading case ( $H$  or  $w$ )

*Commentary:* In the method developed here the vertical spring,  $k_y$ , does not represent the pull-out stiffness of the fastener, but rather the additional stiffness that the sheathing adds to the major-axis bending rigidity of the stud. This stiffness can be an important restriction in flexural-torsional buckling of the stud. The composite action of the sheathing is only utilized to develop the bracing restraint, the maximum member strength is still limited to the stud properties alone.

See Vieira and Schafer (2012, 2013) for further discussion included expressions for  $(EI)_w$  if full composite action is included (this provides an upper bound solution that can be useful in some instances).

Vieira Jr., L. C. M., Schafer, B.W. (2012). "Lateral Stiffness and Strength of Sheathing Braced Cold-Formed Steel Stud Walls." Elsevier, *Engineering Structures*. 37, 205–213.

Vieira Jr., L.C.M., Schafer, B.W. (2013). "Behavior and Design of Sheathed Cold-Formed Steel Stud Walls under Compression." ASCE, *Journal of Structural Engineering* (DOI: 10.1061/(ASCE)ST.1943-541X.0000731). *In Press*



## Draft Ballot 4: Rotational Restraint Provided by Fastener-Sheathing System ( $k_\phi$ )

*Note:* Determination of rotational restraint is already provided in AISI-COFS standards. However, it likely makes the most sense to move that material to be parallel with the  $k_x$  and  $k_y$  springs – to that end a draft ballot is provide here that provides this information. The ballot is a modified form of that already available in AISI COFS standards.

In addition, some care must be taken with the current use of  $k_\phi$  and whether this quantity is a spring stiffness or a foundation stiffness (i.e. the spring stiffness divided by a tributary length). Existing provisions for distortional buckling in the main Specification of AISI-S100 require a foundation stiffness, but  $k_x$  and  $k_y$  are spring stiffness values. The notation developed in Vieira and Schafer (2013) is extended here:  $k_x, k_y, k_\phi$  refer to spring stiffness and  $\underline{k}_x, \underline{k}_y, \underline{k}_\phi$  refers to foundation stiffness, i.e., the spring stiffness divided by the fastener spacing. Foundation stiffness  $\underline{k}_x, \underline{k}_y, \underline{k}_\phi$  is also what is utilized in an FSM analysis.

Vieira Jr., L.C.M., Schafer, B.W. (2013). "Behavior and Design of Sheathed Cold-Formed Steel Stud Walls under Compression." ASCE, *Journal of Structural Engineering* (DOI: 10.1061/(ASCE)ST.1943-541X.0000731). *In Press*

### Z.1 Sheathing Braced Member - Available Rotational Stiffness at Fastener ( $k_\phi$ )

The available vertical stiffness provided at a fastener location from a fastener-sheathing combination providing bracing restraint to a member shall be determined as follows.

The rotational stiffness  $k_\phi$  shall be determined per test using AISI-S991, or as follows:

$$k_\phi = \underline{k}_\phi d_f \quad (\text{Eq. Z.1-1})$$

where

$d_f$  = fastener spacing

$$\underline{k}_\phi = (1/\underline{k}_{\phi w} + 1/\underline{k}_{\phi c})^{-1} \quad (\text{Eq. Z.1-2})$$

where

$\underline{k}_{\phi w}$  = Sheathing rotational restraint

=  $EI_w/L_1 + EI_w/L_2$  for interior members (joists or rafters) with *structural sheathing* fastened on both sides (Eq. Z.1-3)

=  $EI_w/L_1$  for exterior members (joists or rafters) with *structural sheathing* fastened on one side (Eq. Z.1-4)

where

$EI_w$  = Sheathing bending rigidity

= Values as given in Table Z.1-1(a) for plywood and OSB

Values as given in Table Z.1-1(b) for gypsum board.

$L_1, L_2$  = One half joist spacing to the first and second sides respectively, as illustrated in Figure Z.1-1

$\underline{k}_{\phi c}$  = Connection rotational restraint

= Values as given in Table Z.1-2 for fasteners spaced 12 in. o.c. or closer (Eq. Z.1-5)

**Table Z.1-1 (a)<sup>1,2</sup>**  
**Plywood and OSB Sheathing Bending Rigidity,  $EI_w$  (lbf-in<sup>2</sup>/ft)**

Span Rating	Strength Parallel to Strength Axis				Stress Perpendicular to Strength Axis			
	Plywood			OSB	Plywood			OSB
	3-ply	4-ply	5-ply		3-ply	4-ply	5-ply	
24/0	66,000	66,000	66,000	60,000	3,600	7,900	11,000	11,000
24/16	86,000	86,000	86,000	86,000	5,200	11,500	16,000	16,000
32/16	125,000	125,000	125,000	125,000	8,100	18,000	25,000	25,000
40/20	250,000	250,000	250,000	250,000	18,000	39,500	56,000	56,000
48/24	440,000	440,000	440,000	440,000	29,500	65,000	91,500	91,500
16oc	165,000	165,000	165,000	165,000	11,000	24,000	34,000	34,000
20oc	230,000	230,000	230,000	230,000	13,000	28,500	40,500	40,500
24oc	330,000	330,000	330,000	330,000	26,000	57,000	80,500	80,500
32oc	715,000	715,000	715,000	715,000	75,000	615,000	235,000	235,000
48oc	1,265,000	1,265,000	1,265,000	1,265,000	160,000	350,000	495,000	495,000

Note:

- To convert to lbf-in<sup>2</sup>/in., divide table values by 12.  
 To convert to N-mm<sup>2</sup>/m, multiply the table values by 9415.  
 To convert to N-mm<sup>2</sup>/mm, multiply the table values by 9.415.
- Above Plywood and OSB bending rigidity is obtained in accordance APA, Panel Design Specification (2004).

**Table Z.1-1 (b)<sup>1</sup>**  
**Gypsum Board Bending Rigidity**  
**Effective Stiffness (Typical Range),  $EI_w$**

Board Thickness (in.) (mm)	$EI$ (Lb-in <sup>2</sup> /in) of width (N-mm <sup>2</sup> /mm)
0.5 (12.7)	1500 to 4000 (220,000 to 580,000)
0.625 (15.9)	3000 to 8000 (440,000 to 1,160,000)

Note:

- Above Gypsum board bending rigidity is obtained from Gypsum Association, GA-235-01 (2001). See commentary for further information.

**Table Z.1-2<sup>1</sup>**  
**Connection Rotational Restraint**

t (mils)	t (in.)	$k_c$ (lbf-in./in./rad)	$k_c$ (N-mm/mm/rad)
18	0.018	78	348
27	0.027	83	367
30	0.03	84	375
33	0.033	86	384
43	0.043	94	419
54	0.054	105	468
68	0.068	123	546
97	0.097	172	766

Note:

- Fasteners spaced 12 in. (25.4 mm) o.c. or less.

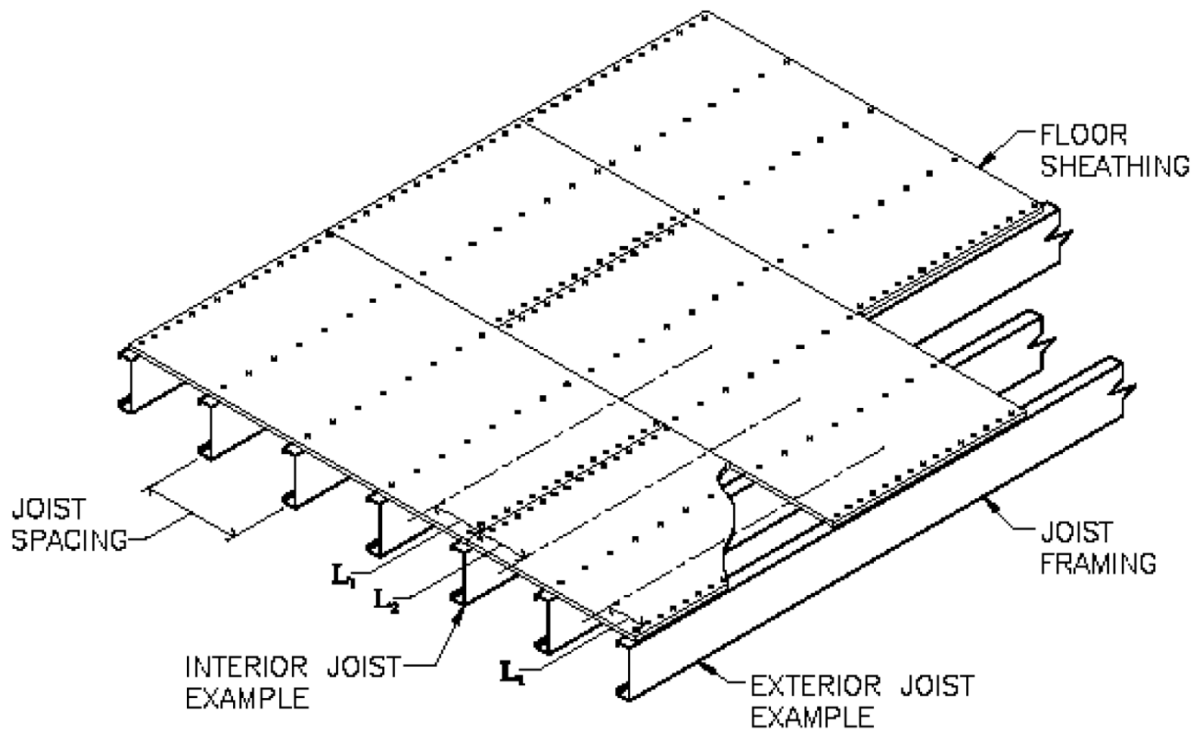


Figure Z.1-1, Illustration of  $L_1$  and  $L_2$  for Sheathing Rotational Restraint

## Draft Ballot 5: New Test Standard, Similar to AISI S901, for Rotational Restraint ( $k_\phi$ )

*Note:* AISI S901 provides several test methods for determining rotational restraint. This standard was used as the experimental basis for finding  $k_\phi$ , the rotational restraint against distortional buckling, but the test standard was never updated. This same rotational restraint is also used in the sheathing braced design of wall studs. S901 is a relative complex test standard, it is proposed that the simplest method is to create a new standard, a draft of that new standard is provided here.

### AISI S991-13 TEST STANDARD FOR DETERMINATION OF FASTENER-SHEATHING ROTATIONAL RESTRAINT

#### 1. Scope

This Standard shall apply for the determination of the rotational restraint ( $k_\phi$ ) supplied by sheathing, fastened to cold-formed steel members.

This Standard shall include Sections 1 through 10 inclusive.

*Commentary:* This test standard is conceptually related to AISI S901; however, the specifics of the test and instrumentation are modified for the use intended here. When a cold-formed steel member is connected to sheathing the sheathing can provide beneficial rotational restraint of the member (stud, joist, etc.). One direct mechanism for developing such rotational restraint is a combination of bearing between the flange and sheathing, and pull-through resistance at a fastener location, as the member rotates. This mechanical combination may be idealized as a rotational restraint at the fastener location. This rotational restraint provides the primary bracing restraint against distortional buckling. See Schafer et al. (2010) for a complete discussion.

Schafer, B. W. Vieira Jr., L. C. M., Sangree, R. H., Guan, Y. (2010) "Rotational Restraint and Distortional Buckling in Cold-Formed Steel Framing Systems." Revista Sul-Americana de Engenharia Estrutural (South American Journal of Structural Engineering), Special issue on cold-formed steel structures, 7 (1) 71-90.

#### 2. Referenced Documents

The following documents or portions thereof are referenced within this Standard and shall be considered as part of the requirements of this document.

- a. American Iron and Steel Institute (AISI), Washington, DC:
  - S100-12, North American Specification for the Design of Cold Formed Steel Structural Members, 2012 Edition.
  - S200-12, North American Standard for Cold-Formed Steel Framing - General Provisions, 2012 Edition.
- b. ASTM International (ASTM), West Conshohocken, PA:

A370-*<latest edition>*, Standard Test Methods and Definitions for Mechanical Testing of Steel Products

ASTM E6-*<latest edition>*, Standard Terminology Relating to Methods of Mechanical Testing

IEEE/ASTM-SI-10-*<latest edition>*, American National Standard for Use of the International System of Units (SI): The Modern Metric System

### 3. Terminology

Where the following terms appear in this standard they shall have the meaning as defined in AISI S100, AISI S200, or as defined herein. Terms not defined in Section 3 of this standard, or AISI S100, or AISI S200 shall have the ordinary accepted meaning for the context for which they are intended.

### 4 Symbols

$d_f$  = distance between fasteners

$P$  = vertical force applied a distance  $h_o$  from member-sheathing connection

$h_o$  = out-to-out distance of the web of member

$w$  = width of the test specimen

$\Delta_v$  = vertical displacement at face of flange where load  $P$  is applied

$\Delta_h$  = horizontal displacement of sheathing at connector location

$L$  = length (height) of the sheathing from fixed end to connector location

### 5 Precision

5.1 Loads shall be recorded to a precision of 1 percent of the ultimate load during application of test loads.

5.2 Deflections shall be recorded to a precision of 0.001 in. (0.025 mm).

### 6 Test Fixture

6.1 The test consists of a cantilevered piece of sheathing fastened to a horizontally oriented member (i.e., joist, stud, etc.). An example test setup is provided in Figure 1.

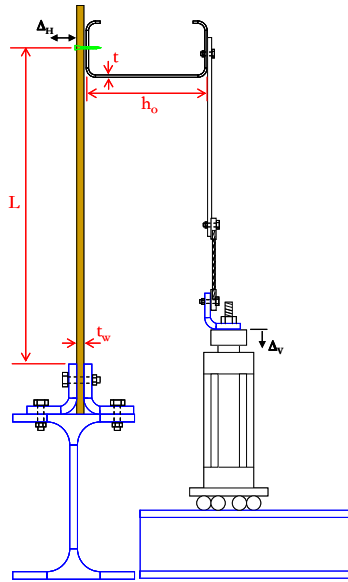


**Figure 1** Side view of cantilever specimen.

6.2 The actuator that supplies the force to the end of the member must be free to translate.

## 7 Test Specimen

The test specimen consists of the sheathing, fasteners, and CFS member (joist, stud, etc.).

7.1 The sheathing should be representative of intended end use. The sheathing material should be environmentally conditioned to a cited standard. The sheathing thickness shall not be greater than 20% above the design value. The sheathing width shall match the member length. The sheathing length shall be at least equal to  $\frac{1}{2}$  the spacing between CFS members, but not less than 12 in. [305mm].

7.2 The fasteners should be representative of intended end use. Fastener diameter shall not be greater than 20% above the design value. All fasteners should be driven to flush using the same installation methods as intended end use. At least three fasteners shall be used per test. Fastener spacing shall match intended end use.

7.3 The CFS member should be representative of intended end use. The stud thickness shall not be greater than 20% above the design value. The stud length should be at least four times the fastener spacing.

## 8 Test Procedure

8.1 The test should be conducted under pseudo-static monotonic load until a peak (failure) load is reached. A specific loading rate is not prescribed, but the test shall not reach peak load in less than 5 minutes.

8.2 Displacement shall be measured in the test specimen. Actuator displacements (from the internal LVDT of the actuator) may be used as the vertical displacement,  $\Delta_v$ . If the rotational stiffness is to be separated into connector and sheathing components (as utilized in AISI-COFS standards) then the horizontal displacement,  $\Delta_{Hr}$ , must also be recorded.

8.3 The test procedure shall be consistent with AISI S100, that is "Evaluation of the test

results shall be made on the basis of the average value of test data resulting from tests of not fewer than three identical specimens, provided the deviation of any individual test result from the average value obtained from all tests does not exceed  $\pm 15$  percent. If such deviation from the average value exceeds 15 percent, more tests of the same kind shall be made until the deviation of any individual test result from the average value obtained from all tests does not exceed  $\pm 15$  percent, or until at least three additional tests have been made. No test result shall be eliminated unless a rationale for its exclusion can be given." For this criteria, the evaluation is made on the stiffness  $\underline{k}_\phi$ , or  $\underline{k}_{\phi c}$ , or  $\underline{k}_{\phi w}$ .

## 9 Data Evaluation

- 9.1 The rotational stiffness of the fastener-sheathing system is determined at 40% of the ultimate strength (i.e., peak load or  $P_{test}$ ) of the specimen. Specifically,  $P = 0.4P_{test}$  and  $\Delta_v$  and  $\Delta_h$  are determined at  $0.4P_{test}$ :

Rotational stiffness if separation between connector and sheathing is not needed:

$$k_\phi = \underline{k}_\phi d_f \quad (1)$$

$$\underline{k}_\phi = \underline{M} / \theta \quad (2)$$

$$\underline{M} = (P / w) h_o \quad (3)$$

$$\theta = \tan^{-1}(\Delta_v / h_o) \quad (4)$$

where

$d_f$  = distance between fasteners

$P$  = vertical force applied a distance  $h_o$  from member-sheathing connection

$h_o$  = out-to-out distance of the web of member

$w$  = width of the test specimen

$\Delta_v$  = vertical displacement at face of flange where load  $P$  is applied

Rotational stiffness if separation between connector and sheathing is desired:

connector:

$$k_{\phi c} = \underline{k}_{\phi c} d_f \quad (5)$$

$$\underline{k}_{\phi c} = \underline{M} / \theta_c = \underline{M} / (\theta - \theta_w) \quad (6)$$

$$\theta_w = 2\Delta_h / L$$

where

$\Delta_h$  = horizontal displacement of sheathing at connector location

$L$  = length (height) of the sheathing from fixed end to connector location

sheathing:

$$k_{\phi w} = \underline{k}_{\phi w} d_f \quad (7)$$

$$\underline{k}_{\phi w} = \underline{M} / \theta_w = \underline{M} / (2\Delta_h / L) \quad (8)$$

total:

$$k_{\phi} = \underline{k}_{\phi} d_f \quad (9)$$

$$\underline{k}_{\phi} = 1 / [(1 / \underline{k}_{\phi c}) + (1 / \underline{k}_{\phi w})] \quad (10)$$

9.2 No test result shall be eliminated unless a rationale for its exclusion can be given.

*Commentary:* Separation of the rotational restraint into connector and sheathing restraint is conceptually summarized in Figure 2. In existing testing (Schafer et al. 2010) the total rotational restraint was found to be highly variable due principally to large variations in sheathing properties; however, connector rotational stiffness was found to be more repeatable. Both connector and sheathing rotational restraint are utilized in AISI COFS standards, and may be replaced by the experimental values developed here.

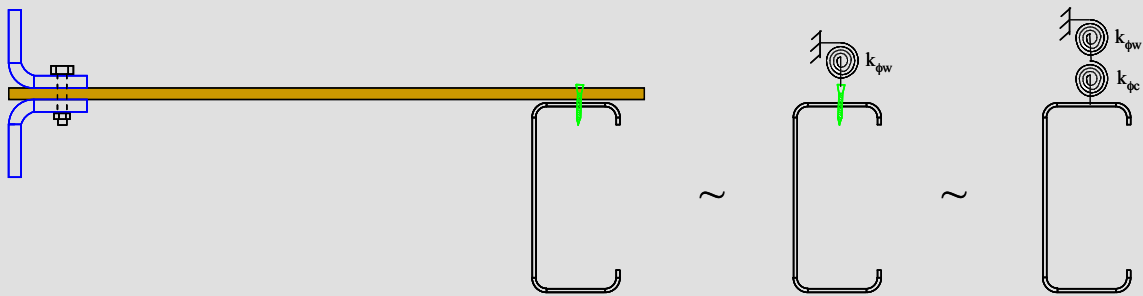


**Figure 2** Separation of rotational resistance into connector and sheathing components

## 10 Report

- 10.1 The test report shall include a description of the tested specimens, including a drawing detailing all pertinent dimensions.
- 10.2 The test report shall include the measured physical properties consistent with the limitations outlined in Section 7.
- 10.3 The test report shall include a detailed drawing of the test setup, depicting location and direction of load application, location of displacement instrumentation and their point of reference, and details of any deviations from the test requirements. Additionally, photographs shall supplement the detailed drawings of the test setup.
- 10.4 The test report shall include individual and average load-versus-deformation values and curves, as plotted directly, or as reprinted from data acquisition systems.
- 10.5 The test report shall include individual and average moment-versus-rotation values and curves, as plotted directly, or as reprinted from data acquisition systems.
- 10.6 The stiffness determined at 40% of the peak load ( $\underline{k}_{\phi}$ ) shall also be drawn on the moment-versus-rotation curves. Values of  $\underline{k}_{\phi}$  shall be provided for all tested specimens.
- 10.7 The test report shall include individual and average maximum test load values observed (i.e.,  $P_{test}$ ). Description of the nature, type and location of failure exhibited by each specimen tested, and a description of the general behavior of the test fixture during load application. Additionally, photographs shall supplement the description of the failure



mode(s).

- 10.8 The test report shall include a description of the test method and loading procedure used, rate of loading or rate of motion of the crosshead movement, and time to maximum load.

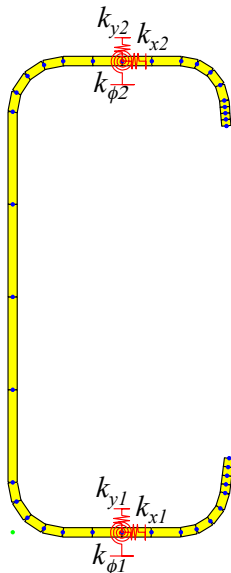
## Draft Ballot 6: Commentary Addition to Appendix 1 Direct Strength Method for Elastic Stability of Sheathed Walls with emphasis on using the Finite Strip Method

### 1.1.2 Elastic Buckling

#### *Members with Sheathing*

In addition to finding the stability of bare cold-formed steel members it is also possible to model, and determine the elastic buckling loads of members which have semi-rigid restraints developed through attachments to panels, sheathing, or discrete braces. Such restraint can greatly increase the elastic stability loads and moments of a cross-section and even alter the observed buckling modes.

For the specific case of light steel framing, e.g. a cold-formed steel stud wall braced by sheathing, research has been conducted to determine (a) how to characterize the semi-rigid restraints developed at the fastener-sheathing connection to the cold-formed steel member, and (b) how to model the elastic stability of the resulting section (Vieira and Schafer 2013, Peterman and Schafer 2013). AISI-COFS standards provide guidance in terms of design expressions and test standards to determine the key springs:  $k_x, k_y, k_\phi$  that are developed in a sheathing braced member, Figure C-1.1.2-3 summarizes.



$k_x, k_y, k_\phi$  springs are included at fastener locations and reflect the stiffness developed through deformations at in the flange-fastener-sheathing system. The stiffness may be different for the two sides (1 and 2) of the member if the sheathing or fastening details vary across the two sides.

$k_x$  is the lateral restraint developed through bearing and tilting of the fastener against the sheathing acting in series with shearing of the sheathing as a diaphragm, see AISI-COFS X.1 and AISI S990 for further information on this restraint.

$k_y$  is the vertical restraint developed as composite action of the member and sheathing occurs in major-axis bending, see AISI-COFS Y.1 for further information on this restraint.

$k_\phi$  is the rotational restraint developed as the flange attempts to rotate against the face of the sheathing, see AISI-COFS Z.1 and AISI S991 for further information on this restraint.

Figure C-1.1.2-3 Cold-formed steel cross-section partially restrained by sheathing, introduced as springs

Peterman, K.D., Schafer, B.W. “Sheathed Cold-Formed Steel Studs Under Axial and Lateral Load.” Submitted to *Journal of Structural Engineering* (Submitted 2 January 2013). [to be updated after final publication, see Peterman M.S. thesis or research report in the interim]

Vieira Jr., L.C.M., Schafer, B.W. (2013). “Behavior and Design of Sheathed Cold-Formed Steel Stud Walls under Compression.” ASCE, *Journal of Structural Engineering* (DOI: 10.1061/(ASCE)ST.1943-541X.0000731). *In Press*

#### 1.1.2.1 Elastic Buckling Numerical Solutions

##### *Members with Sheathing*

It is possible to construct full shell finite element models of members, fasteners, and sheathing and use these models to determine the elastic buckling loads and moments. However, since much of the

deformations are developed locally at the fastener locations (often through damage in the sheathing material) it is difficult to properly capture the stiffness and interactions between the components (Vieira and Schafer 2012). Modeling and experimentation has shown that the complex member-fastener-sheathing interaction can be simplified to a series of springs at the fastener locations as indicated in Figure C-1.1.2-3.

Shell finite element models of the member with springs added at the fastener locations can provide an accurate prediction of the elastic critical loads and moments, see Vieira (2011) or Post (2013). In addition, such models readily allow for a mixture of discrete bracing (springs) and sheathing-based springs. In that sense, this approach is the most general. However, startup time for developing and analyzing such models is relatively significant. Further, identification of the individual local, distortional, and global buckling modes must be done visually, and can be time consuming. As a result, the finite strip method is generally preferred.

Finite strip models of members with springs may be completed in CUFSM. However, it is important to note that the springs in CUFSM are foundation springs, i.e. continuous along the length of the member, not discrete at the fastener locations. Conversion of discrete  $k_x, k_y, k_\phi$  springs to foundation  $\underline{k}_x, \underline{k}_y, \underline{k}_\phi$  springs only requires dividing the discrete springs by the fastener spacing. The accuracy of this smeared spring stiffness or (foundation) stiffness approximation is addressed in sections 1.1.2.1.1 - .3 for local, distortional, and global buckling respectively. For practical dimensions it is found to work well.

Vieira Jr., L. C. M., Schafer, B.W. (2012). "Lateral Stiffness and Strength of Sheathing Braced Cold-Formed Steel Stud Walls." Elsevier, *Engineering Structures*. 37, 205 - 213 (doi:10.1016/j.engstruct.2011.12.029)

Vieira Jr., L.C.M. (2011) Behavior and design of cold-formed steel stud walls under axial compression, Department of Civil Engineering, Ph.D. Dissertation, Johns Hopkins University.

Post, B. (2012). "Fastener Spacing Study of Cold-Formed Steel Wall Studs Using Finite Strip and Finite Element Methods." Research Report, December 2012.

### 1.1.2.1.1 Local Buckling via Finite Strip ( $P_{cr\ell}$ , $M_{cr\ell}$ )

#### *Members with Sheathing*

Due to its short wavelength sheathing has little impact on local buckling and it is recommended to ignore the any bracing restraint. Theoretically,  $\underline{k}_x$  and  $\underline{k}_\phi$  (if located at the exact mid-width of the flange) have no influence on local buckling, only  $\underline{k}_y$ . The out-of-plane stiffness,  $\underline{k}_y$ , is derived consistent with global bending resistance and not localized resistance. Due to the short wavelength of the buckling mode, end conditions also have little influence on local buckling. Thus, a conventional finite strip signature curve result completed on the bare stud (or similar shell finite element model) is adequate for finding the local elastic buckling load or moment. For industry standard studs local elastic buckling loads and moments have been tabled (Li and Schafer 2011).

Li, Z., Schafer, B.W. (2011). "Local and Distortional Elastic Buckling Loads and Moments for SSMA Stud Sections." Cold-Formed Steel Engineers Institute, Tech Note G103-11, 5pp.

### 1.1.2.1.2 Distortional Buckling via Finite Strip ( $P_{crd}$ , $M_{crd}$ )

#### *Members with Sheathing*

Sheathing provides beneficial rotational restraint against distortional buckling, and  $k_z$  should be included when determining the elastic distortional buckling load or moment. For studs with deep webs (and narrow flanges) the additional restraint supplied by  $k_x$  may also be influential – its inclusion is optional, but if included requires the use of computational stability solutions (finite strip, finite element, etc.). Stiffness  $k_y$  should not be included when determining distortional buckling. In distortional buckling  $k_y$  would be engaged, but as derived,  $k_y$ 's deformations are consistent with strong-axis stud flexure, not rotation of the flange. Further,  $k_z$  already accounts for the moment couple that develops between  $k_y$  at the fastener and bearing between the flange and sheathing.

End conditions have influence on distortional buckling at practical lengths. General end conditions may be treated in the (CUFSM) finite strip solution directly (Li and Schafer 2010), in shell finite element models, or by using a correction factor ( $D_{boost}$  in Moen 2008) for fixed-fixed end conditions on a simply-supported model, i.e. a correction to the conventional signature curve FSM. In some cases the distortional buckling mode can be difficult to identify in a finite strip model, in such cases the constrained FSM is recommended (Li and Schafer 2010b). For industry standard studs, tables are provided to aid in the determination of  $k_z$  and  $P_{crd}$  and  $M_{crd}$  along with full design examples of the available analytical hand solutions (Li and Schafer 2011, Schafer 2008) including the  $P_{crd}$  and  $M_{crd}$  solutions adopted in the main Specification of AISI-S100.

The use of the smeared foundation stiffness ( $k_s$  as opposed to  $k_z$ , see the discussion in Section 1.1.2.1) in the prediction of distortional buckling has been shown to be adequate for a large variety of members with fastener spacing of 12 in. [305mm]. In general the fastener spacing ( $d_f$ ) should be less than the distortional buckling half-wavelength ( $L_{crd}$ ) and it is generally recommended that  $d_f/L_{crd} \leq 0.5$  for the use of the smeared foundation stiffness. Otherwise the bracing should be ignored, or a model capable of accounting for the discrete spacing (e.g., shell finite element model) should be employed.

Li, Z., Schafer, B.W. (2010b). "Application of the finite strip method in cold-formed steel member design." Elsevier, *Journal of Constructional Steel Research*. 66 (8-9) 971-980. (doi:10.1016/j.jcsr.2010.04.001)

Li, Z., Schafer, B.W. (2010) "Buckling analysis of cold-formed steel members with general boundary conditions using CUFSM: conventional and constrained finite strip methods." *Proceedings of the 20<sup>th</sup> Int'l. Spec. Conf. on Cold-Formed Steel Structures*, St. Louis, MO. November, 2010. 17-32.

Moen, C. D. (2008). "Direct strength design for cold-formed steel members with perforations." Ph.D., Johns Hopkins University, Baltimore, MD USA.

Li, Z., Schafer, B.W. (2011). "Local and Distortional Elastic Buckling Loads and Moments for SSMA Stud Sections." Cold-Formed Steel Engineers Institute, Tech Note G103-11, 5pp.

Schafer, B.W. (2008) "Design Aids and Examples for Distortional Buckling" Cold-Formed Steel Engineers Institute, Tech Note G100-08, 22 pp.

### 1.1.2.1.3 Global (Euler) Buckling via Finite Strip ( $P_{cre}$ , $M_{cre}$ )

#### *Members with Sheathing*

Sheathing greatly influences the global buckling load or moment. For determining  $P_{cre}$  or  $M_{cre}$  inclusion of all available fastener-sheathing springs ( $k_x$ ,  $k_y$ ,  $k_z$ ) is recommended, but  $k_x$  is critical as it provides the primary fastener-sheathing restraint for both weak-axis flexure and torsion (when present on both flanges).

It is generally beneficial to account for end conditions. To include the impact of fixed end conditions the finite strip model for general end conditions (Li and Schafer 2010, CUFSM v4 or higher) or shell finite element models may be utilized. Alternatively, classical analytical solutions with appropriate effective length factors may be employed as discussed in Section 1.1.2.2 below.

The use of smeared foundation stiffness as opposed to discrete springs (see the discussion in Section 1.1.2.1) in the elastic buckling prediction has been shown to be adequate when the fastener spacing ( $d_f$ ) is less than the global buckling half-wavelength ( $L_{cre}$ ). Specifically it is recommended that  $d_f/L_{cre} \leq 0.25$  in Post (2012). Otherwise the bracing should be ignored, or a model capable of accounting for the discrete spacing (e.g., shell finite element model, or beam model with discrete springs) should be employed.

Post, B. (2012). “Fastener Spacing Study of Cold-Formed Steel Wall Studs Using Finite Strip and Finite Element Methods.” Research Report, December 2012.

### 1.1.2.2 Elastic Buckling – Manual Solutions

#### *Members with Sheathing*

*Local buckling:* As discussed in Section 1.1.2.1.1 the sheathing is ignored, and solutions based on the bare section as previously described should be employed.

*Distortional buckling:* If  $k_x$  and  $k_y$  are included (Figure C-1.1.2-3, also see discussion in Section 1.1.2.1.2) no readily available manual solution exists and computational stability solutions should be pursued. If only  $k_y$  is included the previously provided discussion on distortional buckling is to be followed – namely see AISI S100 C3.1.4 and C4.2.

*Global buckling:* For axial load an analytical solution that follows the general treatment of Timoshenko and Gere (1961) for the buckling of an unsymmetric section with multiple foundation springs has recently been made available (Vieira and Schafer 2013). The solution does not model each individual bracing spring, but rather uses the same foundation stiffness approximation as used in the FSM analysis. Buckling load determination still requires solution of a 3x3 eigenvalue problem or the related cubic equation. However, the solution is analytical and may be solved in Mathcad, Excel, etc. Application and validation of the solution are provided in Vieira and Schafer (2013). Further details are discussed in the commentary to Section C4.1.6.

For major-axis bending a purely analytical solution to lateral-torsional buckling, including the influence of bracing springs is not generally available. Numerical solutions such as the finite strip method discussed in Section 1.1.2.1.3 are recommended.

Vieira Jr., L.C.M., Schafer, B.W. (2013). “Behavior and Design of Sheathed Cold-Formed Steel Stud Walls under Compression.” ASCE, *Journal of Structural Engineering* (DOI: 10.1061/(ASCE)ST.1943-541X.0000731). *In Press*

Timoshenko, S. P., Gere, James M. (1961). *Theory of Elastic Stability*, McGraw-Hill, New York.

## Draft Ballot 7: Clean up Distortional buckling notation in AISI-S100 C3.1.4 and C4.2

Note: Cleanup notation and make reference to new provisions for  $\underline{k}_\phi$

### C3.1.4 Distortional Buckling Strength [Resistance]

Modified definition of  $k_\phi$ : change to  $\underline{k}_\phi$  and modestly amend definition.

$\underline{k}_\phi$  = Rotational foundation (i.e., per unit length) stiffness provided by an ~~restraining~~ element (brace, panel, sheathing) ~~that restrains rotation about the flange/web juncture of a member.~~ (~~z~~Zero if the compression flange is unrestrained). Also, may be taken as zero if this restraint is conservatively ignored. For sheathing-based restraint, see AISI-S200 Z.1 for determining  $\underline{k}_\phi$  analytically, or AISI S991 for determining  $\underline{k}_\phi$  by testing.

Also, update notation in Eq. C3.1.4-6.

$$F_d = \beta \frac{\underline{k}_{\phi fe} + \underline{k}_{\phi we} + \underline{k}_\phi}{\underline{k}_{\phi fg} + \underline{k}_{\phi wg}} \quad (\text{Eq. C3.1.4-6})$$

Also, update definitions and expressions for  $\underline{k}_{\phi fe}$  and  $\underline{k}_{\phi we}$  in C3.1.4 (notation change only).

### C4.2 Distortional Buckling Strength [Resistance]

Modified definition of  $k_\phi$ : change to  $\underline{k}_\phi$  and modestly amend definition.

$\underline{k}_\phi$  = Rotational foundation (i.e., per unit length) stiffness provided by an ~~restraining~~ element (brace, panel, sheathing) ~~that restrains rotation about the flange/web juncture of a member.~~ (~~z~~Zero if the flange is unrestrained). Also, may be taken as zero if this restraint is conservatively ignored. If rotational stiffness provided to the two flanges is dissimilar, the smaller rotational stiffness is used. For sheathing-based restraint, see AISI-S200 Z.1 for determining  $\underline{k}_\phi$  analytically, or AISI S991 for determining  $\underline{k}_\phi$  by testing.

Also, update notation in Eq. C4.2-6.

$$F_d = \beta \frac{\underline{k}_{\phi fe} + \underline{k}_{\phi we} + \underline{k}_\phi}{\underline{k}_{\phi fg} + \underline{k}_{\phi wg}} \quad (\text{Eq. C4.2-6})$$

Also, update definitions and expressions for  $\underline{k}_{\phi fe}$  and  $\underline{k}_{\phi we}$  in C4.2 (notation change only).

## Draft Ballot 8: Add new section to C4.1 for Flexural-Torsional Buckling with Sheathing

*Note:* AISI S100 covers global buckling strength of concentrically loaded compression members. A new section should be added, proposed as C4.1.6, to cover sheathed compression members. Alternatively these provisions could be added to Chapter D under assemblies, but since it is all about calculating  $F_e$ , it may make more sense to have it with the other  $F_e$  expressions. Given the complexity of  $F_e$ , a preference is for computational solutions, so the analytical solution is in the commentary only.

### C4 Concentrically Loaded Compression Members

#### C4.1 Nominal Strength for Yielding, Flexural, Flexural-torsional, and Torsional Buckling

[The following section is entirely new]

##### C4.1.6 Sections with sheathing attached to the flanges

The elastic buckling stress  $F_e$ , for a section with sheathing attached to the member shall be determined by rational elastic buckling analysis.

*Commentary:* The elastic buckling stress of a member with sheathing attached is often significantly greater than the bare section. The fastener-sheathing restraint may be modeled as a series of springs, see AISI COFS X.1, Y.1, Z.1 and AISI S990, and 991 for further details. Numerical methods for rational elastic buckling analysis of a section with sheathing attached to the flanges are covered in detail in the Commentary to Appendix 1, Section 1.1.2. See Section 1.1.2.1.3 for specific guidance on finite strip modeling. An analytical rational elastic buckling analysis is provided here.

For axial load an analytical solution that follows the general treatment of Timoshenko and Gere (1961) for the buckling of an unsymmetric section with multiple foundation springs has recently been made available (Vieira and Schafer 2013) and is provided here. Consider a cross-section which at any location “ $i$ ” in its section has springs  $k_x, k_y$ , and  $k_\phi$ . These springs are foundation stiffness values, i.e. per unit length. Each set of springs at location  $i$  are distance  $h_x$ ,  $h_y$  from the centroid and  $h_{xs}$ ,  $h_{ys}$  from the shear center, as illustrated in Figure C-4.1.6-1.

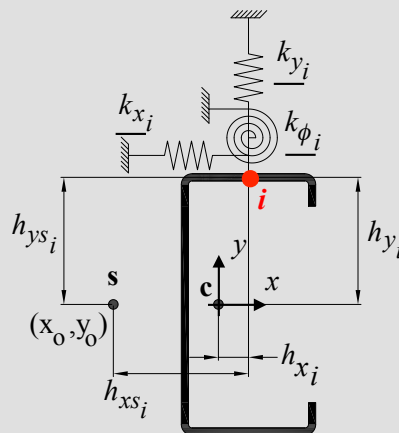


Figure C-4.1.6-1 Definition of variables for a member with foundation springs at  $i$

The stability of this section loaded at its centroid is an eigenvalue problem, where:

$$([K_e] - \lambda[K_g])\Phi = 0$$

the elastic stiffness matrix is:

$$[K_e] = \begin{bmatrix} P_{cry} + \frac{(K_{y,sp}L)^2}{m^2\pi^2} \sum_{i=1}^n k_{xi} & 0 & \frac{(K_{y,sp}L)^2}{m^2\pi^2} \sum_{i=1}^n k_{xi} h_{ysi} \\ & P_{crx} + \frac{(K_{x,sp}L)^2}{m^2\pi^2} \sum_{i=1}^n k_{yi} & -\frac{(K_{x,sp}L)^2}{m^2\pi^2} \sum_{i=1}^n k_{yi} h_{xsi} \\ sym & & \frac{I_0}{A} P_{cr\phi} + \frac{(K_{t,sp}L)^2}{m^2\pi^2} \sum_{i=1}^n k_{xi} (h_{ysi})^2 + \frac{(K_{t,sp}L)^2}{m^2\pi^2} \sum_{i=1}^n k_{yi} (h_{xsi})^2 + \frac{(K_{t,sp}L)^2}{m^2\pi^2} \sum_{i=1}^n k_{\phi i} \end{bmatrix}$$

where

$$P_{crx} = \frac{m^2\pi^2 EI_x}{(K_x L)^2}$$

$$P_{cry} = \frac{m^2\pi^2 EI_y}{(K_y L)^2}$$

$$P_{cr\phi} = \frac{A}{I_o} \left( GJ + \frac{m^2\pi^2 EC_w}{(K_t L)^2} \right)$$

and the geometric stiffness matrix is:

$$[K_g] = P \begin{bmatrix} 1 & 0 & y_o \\ & 1 & -x_o \\ sym & & \frac{I_o}{A} \end{bmatrix}$$

Solving the eigen problem results in three eigenvalues (roots to the characteristic equation), the minimum of which is the critical eigenvalue:

$$\lambda_{cr} = \min(\lambda_1, \lambda_2, \lambda_3)$$

which allows the elastic buckling load and stress to be determined:

$$P_{cr} = \lambda_{cr} P$$

$$F_e = P_{cr} / A$$

where:

$A$  = cross-sectional area of the stud

$C_w$  = Warping constant of stud

$E$  = Young's modulus of steel

$h_{xi}$  =  $x$ -distance from centroid to spring  $i$

$h_{xs}$  =  $x$ -distanced from shear center to spring  $i$

$h_{yi}$  =  $y$ -distance from centroid to spring  $i$

$h_{ysi}$  =  $y$ -distance from shear center to spring  $i$

$I_o$  = polar moment of inertia of stud ( $I_o = I_o + I_y + A(x_o^2 + y_o^2)$ )

$I_x$  = Moment of inertia about  $x$ -axis of stud

$I_y$  = Moment of inertia about  $y$ -axis of stud



$J$  = St. Venant Torsional Constant of stud

$K_x$  = effective length about  $x$ -axis (for fixed-fixed,  $m=1$   $K_x=0.5$ ,  $m=2$   $K_x=0.7$ )

$K_y$  = effective length about  $y$ -axis (for fixed-fixed,  $m=1$   $K_y=0.5$ ,  $m=2$   $K_y=0.7$ )

$K_t$  = effective length in torsion about shear center (for fixed-fixed,  $m=1$   $K_t=0.5$ ,  $m=2$   $K_t=0.7$ )

$K_{x,sp}$  = effective length for the spring foundation about  $x$ -axis (for fixed-fixed  $K_{x,sp} = \sqrt{3} / 2 = 0.866$ )

$K_{y,sp}$  = effective length for the spring foundation about  $y$ -axis (for fixed-fixed  $K_{y,sp} = \sqrt{3} / 2 = 0.866$ )

$K_{t,sp}$  = effective length for the spring foundation about shear center (for fixed-fixed  $K_{t,sp} = \sqrt{3} / 2 = 0.866$ )

$k_x$  = foundation lateral fastener-sheathing stiffness in  $x$

$k_y$  = foundation lateral fastener-sheathing stiffness in  $y$

$k_\phi$  = foundation rotational fastener-sheathing stiffness in the  $x$ - $y$  plane

$L$  = stud length

$m$  = number of buckling half-waves along the length

$P$  = axial reference load in buckling analysis

$x_o$  =  $x$  distance from centroid to shear center

$y_o$  =  $y$  distance from centroid to shear center

$\lambda_j$  = eigenvalues for the buckling modes ( $j=1, 2, 3$ )

$\Phi$  = eigenvector of the buckling mode

## **Draft Ballot 9: Add new section to C3.1.2.3 for Lateral-Torsional Buckling with Sheathing**

*Note:* Similar to columns, beams also need a trigger for sheathing-braced members in AISI S100. Note, no analytical solution is currently readily available, so computational solutions must be employed for finding  $F_e$ .

### **C3.1 Bending**

..

#### **C3.1.2 Lateral-Torsional Buckling Strength [Resistance]**

..

[The following section is entirely new]

##### **C3.1.2.3 Sections with sheathing attached to the flanges**

The elastic buckling stress  $F_e$ , for a section with sheathing attached to the member shall be determined by rational elastic buckling analysis.

*Commentary:* The lateral-torsional buckling stress of a member with sheathing attached is often significantly greater than the bare section. The fastener-sheathing restraint may be modeled as a series of springs, see AISI COFS X.1, Y.1, Z.1 and AISI S990, and 991 for further details. Numerical methods for rational elastic buckling analysis of a section with sheathing attached to the flanges are covered in detail in the Commentary to Appendix 1, Section 1.1.2. See Section 1.1.2.1.3 for specific guidance on finite strip modeling. An analytical rational elastic buckling analysis for lateral-torsional buckling similar to that provided in the commentary of Section C4.1.6 is mechanically possible, but expressions have not been formally derived at this time.

## Draft Ballot 10: Clean up Sheathing-Braced Design Charging Language in S100

*Note:* Modifications to D4 in AISI S100 are needed to make it clear how sheathing braced design can now work. It is not clear where the best place to state this language is, this ballot provides a placeholder to remind the committee that at some point D4 will need to be cleaned up, in some fashion, to make sheathing-braced design parallel to all-steel design in AISI S100.

### D4 Cold-Formed Steel Light-Frame Construction

The design and installation of *structural members* utilized in cold-formed steel repetitive framing applications where the specified minimum base steel *thickness* is not greater than 0.1180 in. (2.997 mm) shall be in accordance with the AISI S200 and the following, as applicable:

- (a) Framing for floor and roof systems in buildings shall be designed in accordance with AISI S210 or solely in accordance with this *Specification*.
- (b) Wall studs shall be designed in accordance with AISI S211, or solely in accordance with this *Specification* either on the basis of an all-steel system in accordance with Section D4.1 or on the basis of a sheathing-braced system in accordance with Section D4.2~~on the basis of sheathing braced design in accordance with an appropriate theory, tests, or *rational engineering analysis*~~. Both solid and perforated *webs* are permitted. Both ends of the stud shall be connected to restrain rotation about the longitudinal stud axis and horizontal displacement perpendicular to the stud axis.
- (c) Headers, shall be designed in accordance with AISI S212 or solely in accordance with this *Specification*.
- (d) Light-framed *shear walls*, diagonal strap bracing (that is part of a structural wall) and *diaphragms* to resist wind, seismic and other in-plane lateral *loads* shall be designed in accordance with AISI S213.
- (e) Trusses shall be designed in accordance with AISI S214.

#### D4.1 All-Steel Design of Wall Stud Assemblies

Wall stud assemblies using an all-steel design shall be designed neglecting the structural contribution of the attached sheathings and shall comply with the requirements of Chapter C. For compression members with circular or non-circular *web* perforations, the effective section properties shall be determined in accordance with Section B2.2.

#### D4.2 Sheathing Braced Design of Wall Stud Assemblies

Wall stud assemblies using a sheathing braced design philosophy shall be designed per this Specification, including Appendix 1, with the contribution from the sheathing bracing accounted for in distortional buckling ( $k_\phi$  in C3.1.4 and C4.2, or  $P_{crd}$  and  $M_{crd}$  in Appendix 1) and in global buckling (C4.1.6 for axial, C3.1.2.3 for major-axis bending, or  $P_{cre}$  and  $M_{cre}$  in Appendix 1).

## Draft Ballot 11: Fastener (Bearing and Pull-through) Demands [Required Loads]

*Note:* Once member limit states are checked, fastener limit states need to be considered. In axial only testing of studs member limit states controlled. In axial + bending tests fastener limit states controlled for gypsum or partially sheathed with gypsum cases. This ballot deals with the demand side, i.e., what are the required forces on the fastener-sheathing system.

### F.D.1 Bearing and Pull-Through Demands at Connections in Sheathing-Braced Members

The required demand in *bearing* ( $F_{r-br}$ ) for a connection supplying sheathing bracing is the sum of the required demands from direct torsional bracing in bending and axial stability bracing, as provided in this section.

The required demand in *pull-through* ( $F_{r-pt}$ ) for a connection supplying sheathing bracing is the sum of the required demands from direct torsional bracing in bending and axial stability bracing as provided in this section.

*Commentary:* The two dominant connection failure modes observed in testing on sheathing-braced members are bearing and pull-through (Peterman and Schafer 2013). These failure modes are triggered in response to the fastener-sheathing system resisting lateral and torsional deformations. Demands from axial stability bracing (Vieira and Schafer 2013) are typically less than those developed in resisting the direct torsion that develops in bending. However, total demand on the connection should be checked, and is the summation of the axial and bending requirements.

Peterman, K.D., Schafer, B.W. “Sheathed Cold-Formed Steel Studs Under Axial and Lateral Load.” Submitted to *Journal of Structural Engineering* (Submitted 2 January 2013).

Vieira Jr., L.C.M., Schafer, B.W. (2013). “Behavior and Design of Sheathed Cold-Formed Steel Stud Walls under Compression.” ASCE, *Journal of Structural Engineering* (DOI: 10.1061/(ASCE)ST.1943-541X.0000731). *In Press*

#### F.D.1.1 Required Demands to Resist Direct Torsion in Bending in Sheathing-Braced Members

The required torsion ( $T_r$ ) at a fastener location that develops due to transverse loads on a sheathing-braced stud (member) shall be determined as follows:

$T_r$  = Summation of demands from point and distributed loads:

Point load:

$$T_r = 0.4H_r e \text{ for fastener closest to point load} \quad (\text{Eq. F.D.1-1})$$

$$T_r = 0.3H_r e \text{ for the two fasteners adjacent to the fastener closest to point load} \quad (\text{Eq. F.D.1-2})$$

Distributed load:

$$T_r = w_r d_f e \text{ for each fastener} \quad (\text{Eq. F.D.1-3})$$

where:

$H_r$  = transverse point load

$w_r$  = transverse distributed load

$d_f$  = fastener spacing

$e$  = distance from the shear center to the termination of the flange flat

*Commentary:* In bending the connection demands developed to provide torsional bracing generally exceed those developed to provide stability bracing; therefore, only torsional bracing demands are considered in bending. The forces developed at the connection are a function of the torsional stiffness of the member and the torsional stiffness of the fastener-sheathing system. A stiffness analysis may be employed to precisely determine the torsion carried in the member vs. that carried by the fastener-sheathing system. The distributions assumed in the *Specification* represent typical values for a member sheathed on both sides, as provided in Peterman and Schafer (2013). Demands from point loads and transverse loads should be summed.

The pull-through and bearing demands that develop at the fastener-sheathing connections shall be determined as follows:

(a) Similar Sheathing on both flanges

Pull-through

$$F_{r-pt} = \frac{T_r}{(b/2)} \frac{k_\phi}{2k_\phi + 2k_x(h^2/4)} \quad (\text{Eq. F.D.1-4})$$

Bearing

$$F_{r-br} = T_r(h/2) \frac{k_x}{2k_\phi + 2k_x(h^2/4)} \quad (\text{Eq. F.D.1-5})$$

(b) Dis-similar sheathing on the two flanges

$$\theta_r = T_r / [k_{\phi 1} + k_{x1}(h^2/4) + k_{\phi 2} + k_{x2}(h^2/4)] \quad (\text{Eq. F.D.1-6})$$

Side 1/Flange 1

Pull-through

$$F_{r-pt1} = k_{\phi 1} \theta_r / (b/2) \quad (\text{Eq. F.D.1-7})$$

Bearing

$$F_{r-br1} = k_{x1}(h/2)\theta_r \quad (\text{Eq. F.D.1-8})$$

Side 2/Flange 2

Pull-through

$$F_{r-pt2} = k_{\phi 2} \theta_r / (b/2) \quad (\text{Eq. F.D.1-9})$$

Bearing

$$F_{r-br2} = k_{x2}(h/2)\theta_r \quad (\text{Eq. F.D.1-10})$$

where:

$h$  = out-to-out depth of the stud (member)

$b$  = out-to-out width of the stud (member) flange

$k_x$  = lateral stiffness of the fastener-sheathing assembly per AISI COFS X.1, subscript refers to flange 1 or 2 in members with dis-similar sheathing.

$k_\phi$  = rotational stiffness of the fastener-sheathing assembly per AISI COFS Z.1, subscript refers to flange 1 or 2 in members with dis-similar sheathing

*Commentary:* The expressions assume that bearing and pull-through mechanisms both combine to provide torsional resistance for the fastener-sheathing system as shown in Figure C-F.D.1.1-1 and developed in Peterman and Schafer (2013). The relative stiffness of the mechanisms is utilized to determine how the demands distribute.

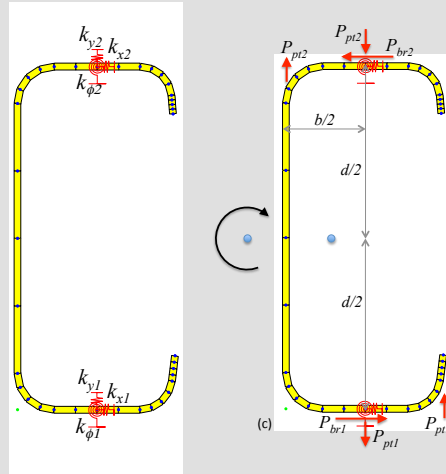


Figure C-F.D.1.1-1 Sheathing-based springs and torsion free-body diagram

The Specification assumes the member is singly symmetric with depth  $h$ , and the fasteners are placed at mid-width of the flange ( $b/2$ ). For the more general case, of two fasteners connected at arbitrary locations similar to the AISI-S100 C4.1.6 Commentary, then the following more general expressions may be employed:

$$\theta_r = T_r / [k_{\phi 1} + k_{x1}h_{ys1}^2 + k_{\phi 2} + k_{x2}h_{ys2}^2] \quad (\text{Eq. C-F.D.1-1})$$

$$F_{r-pt1} = k_{\phi 1} \theta_r / h_{xs1} \quad (\text{Eq. C-F.D.1-2})$$

$$F_{r-br1} = k_{x1} h_{ys1} \theta_r \quad (\text{Eq. C-F.D.1-3})$$

$$F_{r-pt2} = k_{\phi 2} \theta_r / h_{xs2} \quad (\text{Eq. C-F.D.1-4})$$

$$F_{r-br2} = k_{x2} h_{ys2} \theta_r \quad (\text{Eq. C-F.D.1-5})$$

## F.D.1.2 Required Demands for Axial Stability Bracing in Sheathing-Braced Members

(a) Similar Sheathing on both flanges

Pull-through

$$F_{r-pt} = \frac{0.02P_r (h/b)}{L/d_f (1+n)} \quad (\text{Eq. F.D.1-11})$$

$$n = \frac{k_x (h^2/4)}{k_{\phi}} \quad (\text{Eq. F.D.1-12})$$

Bearing

$$F_{r-br} = \frac{0.02P_r}{L/d_f} \quad (\text{Eq. F.D.1-13})$$

(b) Dis-similar sheathing on the two flanges

Side 1/Flange 1

Pull-through

$$F_{r-pt1} = \frac{0.04P_r}{L/d_f} \frac{k_{\phi 1}(h/b)}{(1+n)[k_{\phi 1} + k_{\phi 2}]} \quad (\text{Eq. F.D.1-14})$$

$$n = \frac{k_{x1}(h^2/4) + k_{x2}(h^2/4)}{k_{\phi 1} + k_{\phi 2}} \quad (\text{Eq. F.D.1-15})$$

Bearing

$$F_{r-br1} = \frac{0.04P_r}{L/d_f} \frac{k_{x1}}{k_{x1} + k_{x2}} \quad (\text{Eq. F.D.1-16})$$

Side 2/Flange 2

Pull-through

$$F_{r-pt2} = \frac{0.04P_r}{L/d_f} \frac{k_{\phi 2}(h/b)}{(1+n)[k_{\phi 1} + k_{\phi 2}]} \quad (\text{Eq. F.D.1-17})$$

Bearing

$$F_{r-br2} = \frac{0.04P_r}{L/d_f} \frac{k_{x2}}{k_{x1} + k_{x2}} \quad (\text{Eq. F.D.1-18})$$

where:

$P_r$  = Required axial force in the stud (member)

$L$  = Length of the stud (member)

$d_f$  = Distance (spacing) between fasteners along the stud length

$k_x$  = lateral stiffness of the fastener-sheathing assembly per AISI COFS X.1, subscript refers to flange 1 or 2 in members with dis-similar sheathing.

$k_{\phi}$  = rotational stiffness of the fastener-sheathing assembly per AISI COFS Z.1, subscript refers to flange 1 or 2 in members with dis-similar sheathing

*Commentary:* For stability bracing, in general, if the stiffness of the bracing system is known and an initial imperfection in the member to be braced is assumed the forces that develop in the bracing system may be determined. However the situation becomes complicated when multiple buckling modes are involved, e.g., in a sheathing-braced stud wall, the sheathing supplies bracing resistance against local, distortional, and global (weak-axis flexure, and strong-axis flexural-torsional buckling). Vieira and Schafer (2013) provide an explicit method for determining the bracing force in combined global modes (flexure and flexural-torsional) and demonstrate how to integrate knowledge of the exact buckling mode shape and imperfections to predict forces developed at fasteners in a sheathing-braced design. The method is an extension of the stability solution provided in the Commentary to C-4.1.6, see Vieira (2011) for a design example. Although the method is verified against detailed shell finite element analysis, the expressions and final methodology are complicated. Explicitly determining the bracing demands as a function of imperfection and initial stiffness in every mode is not amenable to design.

Examination of the total force developed in sheathing-braced studs under axial load in Vieira (2011) demonstrates that even when considering the additional forces that develop due to the full combination of possible buckling modes the total force at peak load remains less than 4% of the applied force. Further, the force distribution across the stud is approximately regular, therefore a simple approach for the fastener

forces was considered. For weak-axis flexural buckling the expressions are straightforward, the lateral stiffness of the two flanges resists the applied bracing demand:

$$F_r = 0.04P_r / (L / d_f) = (k_{x1} + k_{x2})\Delta_r \quad (\text{Eq. C-F.D.1-6})$$

for one fastener (e.g. on side 1):

$$F_{r-br1} = k_{x1}\Delta_r \quad (\text{Eq. C-F.D.1-7})$$

after substitution this results in:

$$F_{r-br1} = \frac{0.04P_r}{L / d_f} \frac{k_{x1}}{k_{x1} + k_{x2}}, \quad (\text{Eq. C-F.D.1-8})$$

and, for the case of similar sheathing (on the two flanges):

$$F_{r-br1} = \frac{0.02P_r}{L / d_f} \quad (\text{Eq. C-F.D.1-9})$$

The situation is decidedly more complex when torsion is involved in the buckling mode being resisted. In the absence of an exact mode shape, consider pure torsion as a worst case demand for torsional buckling, in this case the basic method explained in the commentary to C-F.D.1.1 applies. It is assumed that 2%P developed in both flanges is adequate, therefore:

$$T_r = 0.02P_r h / (L / d_f) \quad (\text{Eq. C-F.D.1-10})$$

this may be substituted into Eq. F.D.1.1-6 and 7 to provide the pull-through demand for side 1:

$$F_{r-pt1} = \frac{0.04P_r}{L / d_f} \frac{k_{\phi1}(h / b)}{k_{\phi1} + k_{x1}(h^2 / 4) + k_{\phi2} + k_{x2}(h^2 / 4)}, \quad (\text{Eq. C-F.D.1-11})$$

and Eq. F.D.1.1-6 and 8 to provide the bearing demand for side 1:

$$F_{r-br1} = \frac{0.04P_r}{L / d_f} \frac{k_{x1}(h^2 / 4)}{k_{\phi1} + k_{x1}(h^2 / 4) + k_{\phi2} + k_{x2}(h^2 / 4)}. \quad (\text{Eq. C-F.D.1-12})$$

If we recognize that the dominant mechanism for the resistance is the lateral stiffness we may further simplify, specifically, define:

$$n[k_{\phi1} + k_{\phi2}] = k_{x1}(h^2 / 4) + k_{x2}(h^2 / 4), \quad (\text{Eq. C-F.D.1-13})$$

where  $n$  is typically much greater than 1. Therefore, pull-through and bearing simplify to:

$$F_{r-pt1} = \frac{0.04P_r}{L / d_f} \frac{k_{\phi1}(h / b)}{(1 + n)[k_{\phi1} + k_{\phi2}]} \quad (\text{Eq. C-F.D.1-14})$$

$$F_{r-br1} = \frac{0.04P_r}{L / d_f} \frac{k_{x1}}{(1 + 1/n)[k_{x1} + k_{x2}]} \quad (\text{Eq. C-F.D.1-15})$$

As  $n$  increases the bearing expression may be conservatively simplified to:

$$F_{r-br1} = \frac{0.04P_r}{L / d_f} \frac{k_{x1}}{k_{x1} + k_{x2}}. \quad (\text{Eq. C-F.D.1-16})$$

Thus, with these simplifications resisting flexure and torsion are similar enough to warrant a simple approach to the bracing demands that is independent of the buckling mode shape.



## Draft Ballot 12: Fastener (Bearing and Pull-through) Capacity [Available Loads]

*Note:* The demands of F.D.1 must be compared against capacities. However, currently analytical expressions do not exist, and even manufacturer data can be difficult to come by.

### F.C.1 Available Strength of Member-Fastener-Sheathing in Bearing

Except where otherwise indicated, the following *safety factor* or *resistance factor* shall be used to determine the *allowable strength* or *design strength* [*factored resistance*] in accordance with the applicable design method in Section A4, A5, or A6.

$$\Omega = 3.00 \text{ (ASD)}$$

$$\phi = 0.50 \text{ (LRFD)}$$

$$= 0.40 \text{ (LSD)}$$

Alternatively, design values for a particular application are permitted to be based on tests, with the *safety factor*,  $\Omega$ , and the *resistance factor*,  $\phi$ , determined according to Chapter F.

$P_{n-br}$  = *Nominal bearing strength* [*resistance*] of member-fastener-sheathing combination as reported by manufacturer or determined by independent laboratory testing.

*Note:* The proposed lateral stiffness test method (Draft Ballot 2, AISI S990) could be extended to failure capacities as a means to determine the bearing capacity. Average experimental bearing strength ( $P_{br}$ ) from lateral stiffness tests reported in Vieira and Schafer (2012) are 2570 N [578 lbf] for a #8 connecting a nominal 68 mil stud to 11mm [7/16 in.] OSB (24/16 rated, exposure 1), and 380 N [86 lbf] for a #6 connecting a nominal 68 mils stud to in 12.7 mm [1/2in.] gypsum.

It is possible that NDS or APA has a rational method for determining bearing strength. Dowel bearing strength in Chapter 11 of NDS appears potentially applicable. Such a method, with appropriate modification, would be beneficial for rational application without testing.

To the authors knowledge manufacturers do not currently provide this  $P_{n-br}$  data.

### F.C.1 Available Strength of Member-Fastener-Sheathing in Pull-through

Except where otherwise indicated, the following *safety factor* or *resistance factor* shall be used to determine the *allowable strength* or *design strength* [*factored resistance*] in accordance with the applicable design method in Section A4, A5, or A6.

$$\Omega = 3.00 \text{ (ASD)}$$

$$\phi = 0.50 \text{ (LRFD)}$$

$$= 0.40 \text{ (LSD)}$$

Alternatively, design values for a particular application are permitted to be based on tests, with the *safety factor*,  $\Omega$ , and the *resistance factor*,  $\phi$ , determined according to Chapter F.

$P_{n-pt}$  = *Nominal pull-through strength* [*resistance*] of member-fastener-sheathing combination as reported by manufacturer or determined by independent laboratory testing.

*Note:* The proposed rotational stiffness test method (Draft Ballot 5, AISI S991) could be extended

to failure capacities as a means to determine the pull-through capacity. Average experimental pull-through strength ( $P_{pt}$ ) from rotational stiffness tests reported in Vieira (2011) and summarized for failure capacities in Peterman and Schafer (2013) are 1944 N [437 lbf] for a #8 connecting a nominal 68 mil stud to 11mm [7/16 in.] OSB (24/16 rated, exposure 1), and 178 N [40 lbf] for a #6 connecting a nominal 68 mils stud to in 12.7 mm [1/2in.] gypsum.

It is possible that NDS or APA has a rational method for determining pull-through strength. The author did not find such a method under a cursory review of NDS. Withdrawal is discussed in Chapter 11 of NDS, but the pull-through mechanism seems specific to cold-formed steel in that the fastener anchors in the steel so completely that pulling the head through the sheathing is actually a weaker mode. If a large washer or other modifications were made to the head of the fastener, eventually the withdrawal from the steel would limit strength, but in testing to date pull-through has been the observed limit state. An analysis based method for pull-through would be beneficial for rational application without testing.

To the authors knowledge manufacturers do not currently provide this  $P_{n-pt}$  data.

In 2012 preliminary efforts were made by the author to generate isolated pull-through data using a simple testing rig, this information can be shared with the committee and manufacturers interested in supplying this data.

## Draft Ballot 13: Strength Table (Mock Up) for COFS or Design Manual

*Note:* It is recognized that the complete method, while blissfully general, is complex. Therefore it is important that derivative products exist for use. It is possible to provide tables for the fastener-sheathing restraint springs, but the real burden to use is the computational buckling analysis. To that end, once the general method is voted upon, it is proposed to create strength tables in a form similar to what is shown here to expedite use of the method. These tables are simply derivative products of the method and could be in COFS standards, AISI Design Manual, CFSEI Aids, or Manufacturer Technical Guides.

		sheathing side 1: 7/16" OSB with #8 screws						sheathing side 2: 1/2" Gypsum with #6 screws					
stud designation*	stud spacing [in.]	AXIAL CAPACITY (Pn) [kips]						BENDING CAPACITY (Mn) [kip-in.]					
		8		9		10		8		9		10	
		6	12	6	12	6	12	6	12	6	12	6	12
362S162-33 [33 ksi]	16 24												
362S162-43 [33 ksi]	16 24												
362S162-54 [33 ksi]	16 24												
362S162-68 [33 ksi]	16 24	[axial capacities here, possibly with limit state designated in some form, note, some thickness and fastener combinations not possible, so some cells may be blank in the end, or stud list decreased]						[bending capacities listed here]					
362S162-97 [33 ksi]	16 24												
362S162-54 [50 ksi]	16 24												
362S162-68 [50 ksi]	16 24												
362S162-97 [50 ksi]	16 24												
[continued]													

<- sheathing height [ft]  
<- fastener spacing [in.]

		sheathing side 1: 5/32" Structural 1 with #8 screws						sheathing side 2: 1/2" Gypsum with #6 screws					
stud designation*	stud spacing [in.]	AXIAL CAPACITY (Pn) [kips]						BENDING CAPACITY (Mn) [kip-in.]					
		8		9		10		8		9		10	
		6	12	6	12	6	12	6	12	6	12	6	12
362S162-33 [33 ksi]	16 24												
362S162-43 [33 ksi]	16 24												
362S162-54 [33 ksi]	16 24												
362S162-68 [33 ksi]	16 24	[axial capacities here, possibly with limit state designated in some form, note, some thickness and fastener combinations not possible, so some cells may be blank in the end, or stud list decreased]						[bending capacities listed here]					
362S162-97 [33 ksi]	16 24												
362S162-54 [50 ksi]	16 24												
362S162-68 [50 ksi]	16 24												
362S162-97 [50 ksi]	16 24												
[continued]													

<- sheathing height [ft]  
<- fastener spacing [in.]

\*track matches stud thickness

## **Appendix: Design Example**

# Design Example: Sheathing Braced Design of a Wall Stud

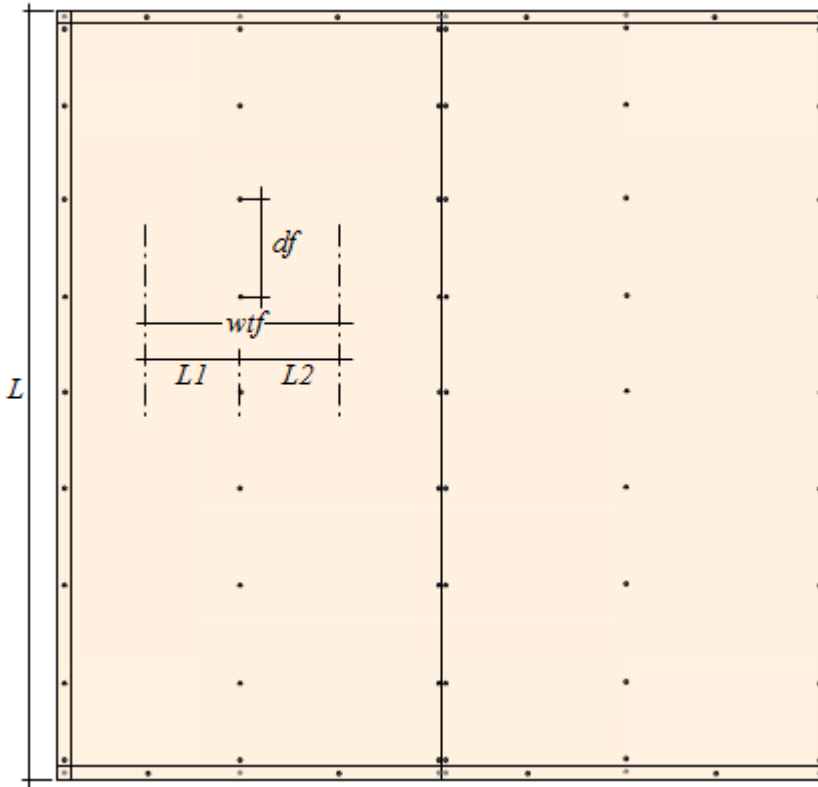
BWS, 27 January 2013

**Objective:** Determine the nominal axial and bending capacity (under a uniform distributed load) of an 8' x 8' stud wall with OSB on one face and gypsum board on the other face employing a sheathing-braced design philosophy.

**Given:**

- wall: 8' x 8' wall, studs spaced 24 in. o.c.
- studs: 362S162-68 [50ksi]
- track: 362T125-68 [50ksi]
- face 1 sheathing: 7/16 in. OSB (24/16 rated, exposure 1)
- face 1 fasteners: #8 at 12 in. o.c.
- face 2 sheathing: 1/2 in. Gypsum Board
- face 2 fasteners: #6 at 12 in. o.c.

Basic illustration of sheathing braced wall



**Basic variables:**

$L := 96 \text{ in}$

$d_f := 12 \text{ in}$

$w_{tf} := 24 \text{ in}$

$L_1 := 12 \text{ in}$

$L_2 := 12 \text{ in}$

other variables and dimensions are defined as needed in the problem below.

**ASSUME** the field stud controls the capacity, in full design all studs would have to be checked, here only the field stud dimensioned above is checked.

**Method:**

1. Find stiffness of fastener-sheathing bracing springs
2. Find elastic buckling of stud with bracing
3. Calculate member capacities
4. Check fasteners (in bearing and pull-through)

# **K<sub>X</sub>** Lateral Restraint Provided by the Fastener Sheathing System

## Face 1: 7/16 in. OSB (24/16 rated, exposure 1)

$$k_x := \frac{1}{\frac{1}{k_{xl}} + \frac{1}{k_{xd}}} \quad (\text{Eq. X.1.1 of draft ballot 1})$$

$$k_{xd} := \frac{\pi^2 G_b \cdot t_b \cdot d_f \cdot w_{tf}}{L^2} \quad (\text{Eq. X.1.2 of draft ballot 1})$$

$$t_b := 0.437 \cdot \text{in} \quad (\text{APA panel design Spec. 2004, Table 5})$$

$$G_b := \frac{83500 \cdot \frac{\text{lb}}{\text{in}}}{t_b} \quad G_b = 191.076 \cdot \text{ksi} \quad (\text{APA panel design Spec. 2004, Table 4a})$$

(NDS 2005, SDPWS-2005, Table C4.2.2A)

$$d_f = 12 \cdot \text{in} \quad w_{tf} = 24 \cdot \text{in} \quad L = 96 \cdot \text{in} \quad \text{as defined previously}$$

$$k_{xd} := \frac{\pi^2 G_b \cdot t_b \cdot d_f \cdot w_{tf}}{L^2} \quad k_{xd} = 25.753 \cdot \frac{\text{kip}}{\text{in}}$$

$k_{xl}$  may be determined by test or by formula provided. First consider the provided (conservative formula) to demonstrate how the terms work, etc.

$$k_{xl} := \frac{3 \cdot \pi \cdot E \cdot d^4 \cdot t^3}{4 \cdot t_b^2 \cdot (9 \cdot \pi \cdot d^4 + 16 \cdot t_b \cdot t^3)} \quad (\text{Eq. X.1.3 of draft ballot 1})$$

$$E := 29500 \cdot \text{ksi} \quad (\text{per AISI S100})$$

$$t := 0.0713 \cdot \text{in} \quad (\text{design stud thickness per AISI S200, or SSMA or SFIA...})$$

$$d := 0.164 \cdot \text{in} \quad (\text{per CFSEI TN-F701-12 or manufacturer})$$

$$t_b = 0.437 \cdot \text{in} \quad (\text{as defined previously})$$

$$k_{xl} := \frac{3 \cdot \pi \cdot E \cdot d^4 \cdot t^3}{4 \cdot t_b^2 \cdot (9 \cdot \pi \cdot d^4 + 16 \cdot t_b \cdot t^3)} \quad k_{xl} = 4.152 \cdot \frac{\text{kip}}{\text{in}}$$

For these details lateral stiffness tests were also conducted to determine the stiffness. These tests were conducted as proposed in draft ballot 2 and are fully detailed in Vieira and Schafer (2012) "Lateral stiffness and strength of sheathing braced cold-formed steel stud walls." from this work we have

$$k_{xl} := 7.08 \cdot \frac{\text{kip}}{\text{in}} \quad \text{here one can see the advantage of conducting the testing, for this example we will use this experimental value going forward.}$$

## **$k_x$** Lateral Restraint Provided by the Fastener Sheathing System

Face 1: 7/16 in. OSB (24/16 rated, exposure 1) **(CONTINUED)**

$$k_{x1} := \frac{1}{\frac{1}{k_{x1}} + \frac{1}{k_{xd}}} \quad k_{x1} = 5.553 \cdot \frac{\text{kip}}{\text{in}}$$

Note for FSM or other analysis we use a foundation stiffness not a spring stiffness. In publications and proposed codes this is designated with an underbar. Here, since such notation is not available in Mathcad it is denoted with the subscript "fnd"

$$k_{x1\_fnd} := \frac{k_{x1}}{d_f} \quad k_{x1\_fnd} = 0.463 \cdot \frac{\frac{\text{kip}}{\text{in}}}{\text{in}}$$

# **K<sub>X</sub>** Lateral Restraint Provided by the Fastener Sheathing System

## Face 2: 1/2 in. Gypsum Board

$$k_{xd} := \frac{\pi^2 G_b \cdot t_b \cdot d_f \cdot w_{tf}}{L^2} \quad (\text{Eq. X.1.2 of draft ballot 1})$$

$$t_b := 0.5 \cdot \text{in} \quad (\text{cite to other nominal thickness, not known, use specified thickness})$$

$$G_b := \frac{40000 \cdot \frac{\text{lb}}{\text{in}}}{t_b} \quad G_b = 80 \cdot \text{ksi} \quad (\text{NDS 2005, SDPWS-2005, Table C4.2.2B})$$

$$d_f = 12 \cdot \text{in} \quad w_{tf} = 24 \cdot \text{in} \quad L = 96 \cdot \text{in} \quad \text{as defined previously}$$

$$k_{xd} := \frac{\pi^2 G_b \cdot t_b \cdot d_f \cdot w_{tf}}{L^2} \quad k_{xd} = 12.337 \cdot \frac{\text{kip}}{\text{in}}$$

$$k_{xl} := \frac{3 \cdot \pi \cdot E \cdot d^4 \cdot t^3}{4 \cdot t_b^2 \cdot (9 \cdot \pi \cdot d^4 + 16 \cdot t_b \cdot t^3)} \quad (\text{Eq X.1.3 of draft ballot 1})$$

$$E := 29500 \cdot \text{ksi} \quad t := 0.0713 \cdot \text{in} \quad t_b = 0.5 \cdot \text{in} \quad (\text{as defined previously})$$

$$d := 0.138 \cdot \text{in} \quad (\#6, \text{ per CFSEI TN-F701-12 or manufacturer})$$

$$k_{xl} := \frac{3 \cdot \pi \cdot E \cdot d^4 \cdot t^3}{4 \cdot t_b^2 \cdot (9 \cdot \pi \cdot d^4 + 16 \cdot t_b \cdot t^3)} \quad k_{xl} = 2.779 \cdot \frac{\text{kip}}{\text{in}}$$

Tests conducted in Vieira and Schafer (2012) provided an average

$$k_{xl} := 2.43 \cdot \frac{\text{kip}}{\text{in}} \quad \text{similar to the design formula. again, the test data is preferred and is thus used here going forward. (Note, variability is high in test data for Gypsum based values.)}$$

$$k_{x2} := \frac{1}{\frac{1}{k_{xl}} + \frac{1}{k_{xd}}} \quad k_{x2} = 2.03 \cdot \frac{\text{kip}}{\text{in}}$$

Note for FSM or other analysis we use a foundation stiffness not a spring stiffness in publications and proposed codes this is designated with an underbar. Here, since such notation is not available in Mathcad it is denoted with the subscript "fnd"

$$k_{x2\_fnd} := \frac{k_{x2}}{d_f} \quad k_{x2\_fnd} = 0.169 \cdot \frac{\text{kip}}{\text{in}}$$



# **K<sub>y</sub>** Vertical Restraint Provided by the Fastener Sheathing System

## Face 1: 7/16 in. OSB (24/16 rated, exposure 1)

$$k_{y1} := \frac{EI_w \cdot \pi^4 \cdot d_f}{L^4} \quad (\text{Eq. Y.1.1 of draft ballot 3})$$

$$d_f = 12 \cdot \text{in} \quad L = 96 \cdot \text{in} \quad (\text{as previously defined})$$

$$EI_w := 78000 \cdot \frac{\text{lb} \cdot \text{in}^2}{\text{ft}} \cdot w_{tf} \quad EI_w = 156 \cdot \text{kip} \cdot \text{in}^2 \quad (\text{per APA panel design spec. 2004, Table 4a, stress parallel to strength axis})$$

$$k_{y1} := \frac{EI_w \cdot \pi^4 \cdot d_f}{L^4} \quad k_{y1} = 2.147 \times 10^{-3} \cdot \frac{\text{kip}}{\text{in}} \quad d_f = 12 \cdot \text{in}$$

$$k_{y1\_fnd} := \frac{k_{y1}}{d_f} \quad k_{y1\_fnd} = 1.789 \times 10^{-4} \cdot \frac{\text{kip}}{\text{in}}$$

(note, this is a lower bound value for non-composite action. additional guidance is provided in draft ballot 3 if partially composite action is accounted for in the bracing resistance. Often, even the non-composite action may be enough to restrict the strong-axis flexural portion of flexural-torsional buckling adequately.)

## Face 2: 1/2 in. Gypsum Board

$$k_{y2} := \frac{EI_w \cdot \pi^4 \cdot d_f}{L^4} \quad (\text{Eq. Y.1.1 of draft ballot 3})$$

$$d_f = 12 \cdot \text{in} \quad L = 96 \cdot \text{in} \quad (\text{as previously defined})$$

$$EI_w := 1500 \cdot \frac{\text{lb} \cdot \text{in}^2}{\text{in}} \cdot w_{tf} \quad EI_w = 36 \cdot \text{kip} \cdot \text{in}^2 \quad (\text{per GA-235-10, minimum effective stiffness provided})$$

$$k_{y2} := \frac{EI_w \cdot \pi^4 \cdot d_f}{L^4} \quad k_{y2} = 4.954 \times 10^{-4} \cdot \frac{\text{kip}}{\text{in}} \quad d_f = 12 \cdot \text{in}$$

$$k_{y2\_fnd} := \frac{k_{y2}}{d_f} \quad k_{y2\_fnd} = 4.129 \times 10^{-5} \cdot \frac{\text{kip}}{\text{in}}$$

# $k_{\phi}$ Rotational Restraint Provided by the Fastener Sheathing System

## Face 1: 7/16 in. OSB (24/16 rated, exposure 1)

$$k_{\phi} := k_{\phi\_fnd} \cdot d_f \quad (\text{Eq. Z.1-1 of draft ballot 4})$$

$$k_{\phi\_fnd} := \frac{1}{\frac{1}{k_{\phi w\_fnd}} + \frac{1}{k_{\phi c\_fnd}}} \quad (\text{Eq. Z.1-2 of draft ballot 4})$$

$$k_{\phi w\_fnd} := \frac{EI_w}{L_1} + \frac{EI_w}{L_2} \quad (\text{Eq. Z.1-3 of draft ballot 4})$$

$$EI_w := 16000 \cdot \frac{\text{lbf} \cdot \text{in}^2}{\text{ft}} \quad (\text{stress perp. to strength axis, per Table Z.1-1 of draft ballot 4, or per APA panel design spec.})$$

$$L_1 := \frac{w_{tf}}{2} \quad L_1 = 12 \cdot \text{in} \quad L_2 := \frac{w_{tf}}{2} \quad L_2 = 12 \cdot \text{in}$$

$$k_{\phi w\_fnd} := \frac{EI_w}{L_1} + \frac{EI_w}{L_2} \quad k_{\phi w\_fnd} = 0.222 \cdot \frac{\text{kip} \cdot \text{in}}{\text{rad}}$$

$$k_{\phi c\_fnd} := 123 \cdot \frac{\text{lbf} \cdot \text{in}}{\text{rad}} \quad (\text{per Table Z.1-2 of draft ballot 4})$$

$$k_{\phi 1\_fnd} := \frac{1}{\frac{1}{k_{\phi w\_fnd}} + \frac{1}{k_{\phi c\_fnd}}} \quad k_{\phi 1\_fnd} = 0.079 \cdot \frac{\text{kip} \cdot \text{in}}{\text{rad}}$$

$$k_{\phi 1} := k_{\phi 1\_fnd} \cdot d_f \quad k_{\phi 1} = 0.95 \cdot \frac{\text{kip} \cdot \text{in}}{\text{rad}}$$

Alternatively the rotational stiffness may be determined by test using the method of draft ballot 5. Test results on this configuration are reported in Vieira and Schafer (2012) and Vieira's thesis (2011) in Table 3.1.

$$k_{\phi 1\_fnd} := 70.3 \cdot \frac{\text{lbf} \cdot \text{in}}{\text{rad}} \quad k_{\phi 1\_fnd} = 0.07 \cdot \frac{\text{kip} \cdot \text{in}}{\text{rad}} \quad (\text{average tested value})$$

$$k_{\phi 1} := k_{\phi 1\_fnd} \cdot d_f \quad k_{\phi 1} = 0.844 \cdot \frac{\text{kip} \cdot \text{in}}{\text{rad}} \quad (\text{slightly less than the value predicted by equations, but considered more accurate, so employed herein}).$$

# $k_{\phi}$ Rotational Restraint Provided by the Fastener Sheathing System

## Face 2: 1/2 in. Gypsum Board

$$k_{\phi} := k_{\phi\_fnd} \cdot d_f \quad (\text{Eq. Z.1-1 of draft ballot 4})$$

$$k_{\phi\_fnd} := \frac{1}{\frac{1}{k_{\phi w\_fnd}} + \frac{1}{k_{\phi c\_fnd}}} \quad (\text{Eq. Z.1-2 of draft ballot 4})$$

$$k_{\phi w\_fnd} := \frac{EI_w}{L_1} + \frac{EI_w}{L_2} \quad (\text{Eq. Z.1-3 of draft ballot 4})$$

$$EI_w := 1500 \cdot \frac{\text{lbf} \cdot \text{in}^2}{\text{in}} \quad (\text{per Table Z.1-1 of draft ballot 4, or per GA-235-10})$$

$$L_1 := \frac{w_{tf}}{2} \quad L_1 = 12 \cdot \text{in} \quad L_2 := \frac{w_{tf}}{2} \quad L_2 = 12 \cdot \text{in}$$

$$k_{\phi w\_fnd} := \frac{EI_w}{L_1} + \frac{EI_w}{L_2} \quad k_{\phi w\_fnd} = 0.25 \cdot \frac{\text{kip} \cdot \text{in}}{\text{rad}}$$

$$k_{\phi c\_fnd} := 123 \cdot \frac{\text{lbf} \cdot \text{in}}{\text{rad}} \quad (\text{per Table Z.1-2 of draft ballot 4})$$

$$k_{\phi 2\_fnd} := \frac{1}{\frac{1}{k_{\phi w\_fnd}} + \frac{1}{k_{\phi c\_fnd}}} \quad k_{\phi 2\_fnd} = 0.082 \cdot \frac{\text{kip} \cdot \text{in}}{\text{rad}}$$

$$k_{\phi 2} := k_{\phi 2\_fnd} \cdot d_f \quad k_{\phi 2} = 0.989 \cdot \frac{\text{kip} \cdot \text{in}}{\text{rad}}$$

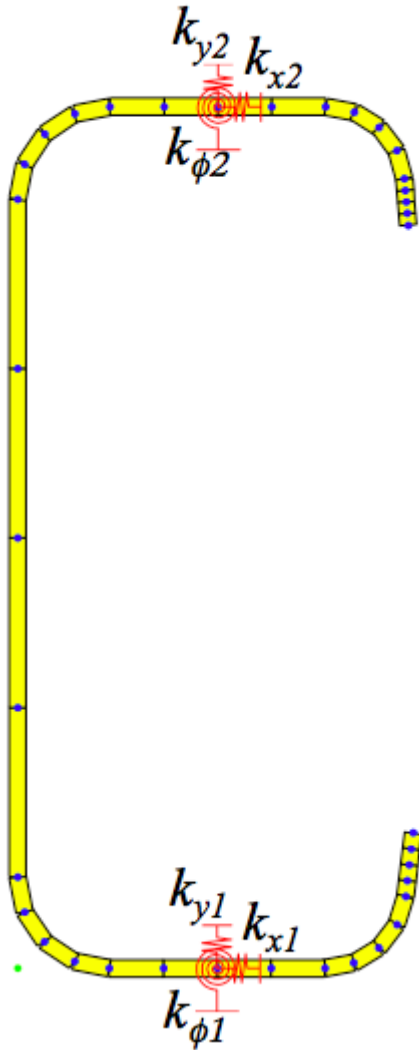
Alternatively the rotational stiffness may be determined by test using the method of draft ballot 5. Test results on this configuration are reported in Vieira and Schafer (2012) and Vieira's thesis (2011) in Table 3.1.

$$k_{\phi 2\_fnd} := 70.8 \cdot \frac{\text{lbf} \cdot \text{in}}{\text{rad}} \quad k_{\phi 2\_fnd} = 0.071 \cdot \frac{\text{kip} \cdot \text{in}}{\text{rad}} \quad (\text{average tested value})$$

$$k_{\phi 2} := k_{\phi 2\_fnd} \cdot d_f \quad k_{\phi 2} = 0.85 \cdot \frac{\text{kip} \cdot \text{in}}{\text{rad}} \quad (\text{slightly less than the value predicted by equations, but considered more accurate, so employed herein}).$$

Note, elastic  $k_{\phi}$  for gypsum and OSB are essentially the same. As detailed in draft ballot 4 and the related research, the thickness of the stud (in which the fastener is anchored into) is the most influential variable in determining  $k_{\phi}$ .

## Summary of Sheathing-Braced Stiffness



### Face 2: 1/2 in. Gypsum Board

$$k_{x2} = 2.03 \cdot \frac{\text{kip}}{\text{in}} \quad k_{x2\_fnd} = 0.169 \cdot \frac{\text{kip}}{\text{in}}$$

$$k_{y2} = 4.954 \times 10^{-4} \cdot \frac{\text{kip}}{\text{in}} \quad k_{y2\_fnd} = 4.129 \times 10^{-5} \cdot \frac{\text{kip}}{\text{in}}$$

$$k_{\phi 2} = 0.85 \cdot \frac{\text{kip} \cdot \text{in}}{\text{rad}} \quad k_{\phi 2\_fnd} = 0.071 \cdot \frac{\text{kip} \cdot \text{in}}{\text{rad}}$$

### Face 1: 7/16 in. OSB

$$k_{x1} = 5.553 \cdot \frac{\text{kip}}{\text{in}} \quad k_{x1\_fnd} = 0.463 \cdot \frac{\text{kip}}{\text{in}}$$

$$k_{y1} = 2.147 \times 10^{-3} \cdot \frac{\text{kip}}{\text{in}} \quad k_{y1\_fnd} = 1.789 \times 10^{-4} \cdot \frac{\text{kip}}{\text{in}}$$

$$k_{\phi 1} = 0.844 \cdot \frac{\text{kip} \cdot \text{in}}{\text{rad}} \quad k_{\phi 1\_fnd} = 0.07 \cdot \frac{\text{kip} \cdot \text{in}}{\text{rad}}$$

## Summary of Elastic Buckling Analysis

Elastic buckling analysis of the 362S162-68 [50ksi] with the sheathing-based springs is completed in CUF5M version 4. **Complete details of the analysis are available in an Appendix to this report.** The results from the analysis are summarized here:

### AXIAL RESULTS

$$A_g := 0.524 \cdot \text{in}^2$$

$$F_y := 50 \cdot \text{ksi}$$

$$P_y := A_g \cdot F_y \quad P_y = 26.2 \cdot \text{kip}$$

$$P_{\text{crl}} := 1.207 \cdot P_y \quad P_{\text{crl}} = 31.623 \cdot \text{kip} \quad (\text{local})$$

$$P_{\text{crd}} := 1.579 \cdot P_y \quad P_{\text{crd}} = 41.37 \cdot \text{kip} \quad (\text{distortional})$$

$$P_{\text{cre}} := 2.88 \cdot P_y \quad P_{\text{cre}} = 75.456 \cdot \text{kip} \quad (\text{global})$$

### MAJOR-AXIS BENDING RESULTS

$$S_g := 0.590 \cdot \text{in}^3$$

$$F_y = 50 \cdot \text{ksi}$$

$$M_y := S_g \cdot F_y \quad M_y = 29.5 \cdot \text{kip} \cdot \text{in} \quad (\text{local})$$

$$M_{\text{crl}} := 5.08 \cdot M_y \quad M_{\text{crl}} = 3.806 \text{ m} \cdot \text{kip} \quad (\text{distortional})$$

$$M_{\text{crd}} := 2.84 \cdot M_y \quad M_{\text{crd}} = 2.128 \text{ m} \cdot \text{kip} \quad (\text{global})$$

note,  $M_{\text{crd}}$  is reported for constant moment, we can increase slightly to account for moment gradient following C3.1.4  $\beta$  expression, but the boost is quite small and ignored here.

$$M_{\text{cre}} := 5.26 \cdot M_y \quad M_{\text{cre}} = 3.941 \text{ m} \cdot \text{kip}$$

note  $M_{\text{cre}}$  is reported for constant moment, to account for a uniform load we can introduce  $C_b$ , it is clear in this case that the elastic buckling moment is already so high that  $C_b$  is not necessary; however, since  $C_b$  is so commonly used, for completeness.

$$C_b := 1.32 \quad \text{for a uniform load on a simply supported span}$$

$$M_{\text{cre}} := C_b \cdot M_{\text{cre}} \quad M_{\text{cre}} = 204.824 \cdot \text{kip} \cdot \text{in} \quad \frac{M_{\text{cre}}}{M_y} = 6.943$$

## Axial member capacity per Direct Strength Method (AISI-S100 App 1)

### Global buckling check per DSM 1.2.1.1

$$\lambda_c := \sqrt{\frac{P_y}{P_{cre}}} \quad \lambda_c = 0.589 \quad \text{note } P_y = 26.2 \cdot \text{kip} \quad P_{cre} = 75.456 \cdot \text{kip} \quad (\text{Eq. 1.2.1-3})$$

$$P_{ne} := \begin{cases} 0.658 \lambda_c^2 \cdot P_y & \text{if } \lambda_c \leq 1.5 \end{cases} \quad (\text{Eq. 1.2.1-1})$$

$$\begin{cases} \frac{0.877}{\lambda_c^2} \cdot P_y & \text{if } \lambda_c > 1.5 \end{cases} \quad (\text{Eq. 1.2.1-2})$$

$$P_{ne} = 22.7 \cdot \text{kip}$$

### Local buckling check per DSM 1.2.1.2

$$\lambda_1 := \sqrt{\frac{P_{ne}}{P_{crl}}} \quad \lambda_1 = 0.846 \quad (\text{Eq. 1.2.1-7})$$

$$P_{nl} := \begin{cases} P_{ne} & \text{if } \lambda_1 \leq 0.776 \end{cases} \quad (\text{Eq. 1.2.1-5})$$

$$\left[ \left[ 1 - 0.15 \cdot \left( \frac{P_{crl}}{P_{ne}} \right)^{0.4} \right] \left[ \left( \frac{P_{crl}}{P_{ne}} \right)^{0.4} \right] \cdot P_{ne} \right] \quad \text{if } \lambda_1 > 0.776 \quad (\text{Eq. 1.2.1-6})$$

$$P_{nl} = 21.5 \cdot \text{kip}$$

### Distortional buckling check per DSM 1.2.1.3

$$\lambda_d := \sqrt{\frac{P_y}{P_{crd}}} \quad \lambda_d = 0.796 \quad (\text{Eq. 1.2.1-10})$$

$$P_{nd} := \begin{cases} P_y & \text{if } \lambda_d \leq 0.561 \end{cases} \quad (\text{Eq. 1.2.1-8})$$

$$\left[ \left[ 1 - 0.25 \cdot \left( \frac{P_{crd}}{P_y} \right)^{0.6} \right] \left[ \left( \frac{P_{crd}}{P_y} \right)^{0.6} \right] \cdot P_y \right] \quad \text{if } \lambda_d > 0.561 \quad (\text{Eq. 1.2.1-9})$$

$$P_{nd} = 23.1 \cdot \text{kip}$$

### Predicted nominal compressive strength per DSM 1.2

$$P_n := \min((P_{ne} \ P_{nl} \ P_{nd})) \quad P_n = 21.5 \cdot \text{kip}$$

Available axial capacity  $\Omega_c := 1.80$   $\phi_c := 0.85$  note, section is prequalified.

$$\frac{P_n}{\Omega_c} = 11.917 \cdot \text{kip} \quad \phi_c \cdot P_n = 18.234 \cdot \text{kip}$$

## Axial member capacity per main Specification (AISI-S100)

### (NEW) C4.1.6 Sections with sheathing attached to flanges (draft ballot 8)

The elastic buckling stress  $F_e$  is to be determined by rational elastic buckling analysis, per the earlier provided CUFSM results this is known:

$$F_e := \frac{P_{cre}}{A_g} \quad F_e = 144 \cdot \text{ksi}$$

#### C4.1 Nominal compressive strength

$$\lambda_c := \sqrt{\frac{F_y}{F_e}} \quad \lambda_c = 0.589 \quad \text{note } F_y = 50 \cdot \text{ksi} \quad F_e = 144 \cdot \text{ksi} \quad (\text{Eq. C4.1-4})$$

$$F_n := \begin{cases} 0.658 \lambda_c^2 \cdot F_y & \text{if } \lambda_c \leq 1.5 \\ \frac{0.877}{\lambda_c^2} \cdot F_y & \text{if } \lambda_c > 1.5 \end{cases} \quad (\text{Eq. C4.1-2})$$

$$F_n = 43.2 \cdot \text{ksi} \quad (\text{Eq. C4.1-3})$$

$$F_n = 43.2 \cdot \text{ksi}$$

Determine effective area per Chapter B at  $F_n$ . This step is not detailed here in the interest of space.

$$A_e := 0.482 \cdot \text{in}^2 \quad \text{calculated in CFS v7, by changing } F_y \text{ to } F_n = 43.2 \text{ ksi.}$$

$$P_{nC4.1} := A_e \cdot F_n \quad P_{nC4.1} = 20.84 \cdot \text{kip}$$

#### C4.2 Nominal distortional buckling strength

$$F_d := \frac{P_{crd}}{A_g} = 78.95 \cdot \text{ksi} \quad \text{using provisions of C4.2(b), or equations in C4.2(a) may be utilized. Also, see AISI Design Manual, or CFSEI Tech Notes for tabulated values.}$$

returning back to the main part of C4.2

$$P_{crd} := A_g \cdot F_d \quad P_{crd} = 41.37 \cdot \text{kip} \quad (\text{Eq. C4.2-5})$$

$$\lambda_d := \sqrt{\frac{P_y}{P_{crd}}} \quad \lambda_d = 0.796 \quad (\text{Eq. C4.2-3})$$

$$P_{ndC4.2} := \begin{cases} P_y & \text{if } \lambda_d \leq 0.561 \\ \left[ \left[ 1 - 0.25 \cdot \left( \frac{P_{crd}}{P_y} \right)^{0.6} \right] \left[ \left( \frac{P_{crd}}{P_y} \right)^{0.6} \right] \cdot P_y \right] & \text{if } \lambda_d > 0.561 \end{cases} \quad (\text{Eq. C4.2-1})$$

$$P_{ndC4.2} = 23.1 \cdot \text{kip} \quad (\text{identical provisions to DSM}) \quad (\text{Eq. C4.2-2})$$

#### Predicted nominal compressive strength per C4

$$P_{nC4} := \min((P_{nC4.1} \quad P_{ndC4.2})) \quad P_{nC4} = 20.8 \cdot \text{kip} \quad \Omega_c := 1.80 \quad \phi_c := 0.85$$

$$\text{Available axial capacity} \quad \frac{P_{nC4}}{\Omega_c} = 11.578 \cdot \text{kip} \quad \phi_c \cdot P_{nC4} = 17.714 \cdot \text{kip}$$

## Major-axis member bending capacity per Direct Strength Method

### Lateral-torsional buckling check per DSM 1.2.2.1.1

$$\frac{M_{cre}}{M_y} = 6.943 \text{ per Eq. 1.2.2-3} \quad M_{ne} := M_y \quad M_{ne} = 29.5 \cdot \text{kip} \cdot \text{in}$$

because  $M_{cre}/M_y$  is  $> 2.78$  inelastic LTB could also be considered per 1.2.2.1.1.1.2. here it is not included, but certainly some capacity is available through inelastic reserve.

### Local buckling check per DSM 1.2.2.1.2

$$\lambda_1 := \sqrt{\frac{M_{ne}}{M_{cr1}}} \quad \lambda_1 = 0.444 \quad \text{section will see no reduction..} \quad (\text{Eq. 1.2.2-9})$$

$$M_{nl} := \begin{cases} M_{ne} & \text{if } \lambda_1 \leq 0.776 \\ \left[ \left[ 1 - 0.15 \cdot \left( \frac{M_{cr1}}{M_{ne}} \right)^{0.4} \right] \left( \frac{M_{cr1}}{M_{ne}} \right)^{0.4} \right] \cdot M_{ne} & \text{if } \lambda_1 > 0.776 \end{cases} \quad (\text{Eq. 1.2.2-7})$$

$$M_{nl} = 29.5 \cdot \text{kip} \cdot \text{in} \quad (\text{Eq. 1.2.2-8})$$

### Distortional buckling check per DSM 1.2.2.1.3

$$\lambda_d := \sqrt{\frac{M_y}{M_{crd}}} \quad \lambda_d = 0.593 \quad \text{section will see no reduction..} \quad (\text{Eq. 1.2.2-19})$$

$$M_{nd} := \begin{cases} M_y & \text{if } \lambda_d \leq 0.673 \\ \left[ \left[ 1 - 0.22 \cdot \left( \frac{M_{crd}}{M_y} \right)^{0.5} \right] \left( \frac{M_{crd}}{M_y} \right)^{0.5} \right] \cdot M_y & \text{if } \lambda_d > 0.673 \end{cases} \quad (\text{Eq. 1.2.2-17})$$

$$M_{nd} = 29.5 \cdot \text{kip} \cdot \text{in} \quad (\text{Eq. 1.2.1-18})$$

### Predicted nominal compressive strength per DSM 1.2.2

$$M_n := \min((M_{ne} \ M_{nl} \ M_{nd})) \quad M_n = 29.5 \cdot \text{kip} \cdot \text{in} \quad \text{i.e. sheathing creates a fully braced beam behavior.}$$

$$\text{Available bending capacity} \quad \Omega_b := 1.67 \quad \phi_b := 0.90 \quad \text{note, section is prequalified}$$

$$\frac{M_n}{\Omega_b} = 17.665 \cdot \text{kip} \cdot \text{in} \quad \phi_b \cdot M_n = 26.55 \cdot \text{kip} \cdot \text{in}$$



## Major-axis member bending capacity per main Spec. (AISI-S100)

### C3.1.2 Lateral-torsional buckling strength

#### (NEW) C3.1.2.3 Sections with sheathing attached to the flanges

$F_e$  is to be determined by rational elastic buckling analysis. In this case the previously conducted CUFSM analysis provides the results

$$F_e := \frac{M_{cre}}{S_g} \quad F_e = 347.16 \cdot \text{ksi}$$

returning to the body of C3.1.2..

$$\frac{F_e}{F_y} = 6.943 \quad \text{per C3.1.2.1 no LTB} \quad F_n := F_y \quad F_n = 50 \cdot \text{ksi}$$

the effective modulus shall be determined at  $F_n$ , in this case from SSMA or SFIA tables.. ( $F_n = F_y$ )

$$S_e := 0.579 \cdot \text{in}^3$$

$$M_{nC3.1.2} := S_e \cdot F_y \quad M_{nC3.1.2} = 28.95 \cdot \text{kip} \cdot \text{in} \quad (\text{Eq. C3.1.1-1})$$

### C3.1.4 Distortional buckling strength

The elastic distortional buckling stress may be found using the expressions of C3.1.4(a) or elastic buckling analysis of C3.1.4(b). Since elastic buckling analysis is available this is used here. Thus, in the end the DSM and main Spec. provisions for distortional buckling are the same.

$$\lambda_d := \sqrt{\frac{M_y}{M_{crd}}} \quad \lambda_d = 0.593 \quad (\text{Eq. 1.2.2-19})$$

$$M_{ndC3.1.4} := \begin{cases} M_y & \text{if } \lambda_d \leq 0.673 \\ \left[ \left[ 1 - 0.22 \cdot \left( \frac{M_{crd}}{M_y} \right)^{0.5} \right] \left( \frac{M_{crd}}{M_y} \right)^{0.5} \right] \cdot M_y & \text{if } \lambda_d > 0.673 \end{cases} \quad (\text{Eq. 1.2.2-17})$$

$$(\text{Eq. 1.2.1-18})$$

$$M_{ndC3.1.4} = 29.5 \cdot \text{kip} \cdot \text{in}$$

### Predicted nominal compressive strength per DSM 1.2

$$M_{nC3.1} := \min((M_{nC3.1.2} \quad M_{ndC3.1.4})) \quad M_{nC3.1} = 28.9 \cdot \text{kip} \cdot \text{in}$$

$$\text{Available bending capacity} \quad \Omega_b := 1.67 \quad \phi_b := 0.90$$

$$\frac{M_{nC3.1}}{\Omega_b} = 17.335 \cdot \text{kip} \cdot \text{in} \quad \phi_b \cdot M_{nC3.1} = 26.055 \cdot \text{kip} \cdot \text{in}$$

## Summary of predicted member capacity

### Main Specification

$$P_{nC4} = 20.84 \cdot \text{kip}$$

$$\phi_c \cdot P_{nC4} = 17.714 \cdot \text{kip}$$

$$M_{nC3.1} = 28.95 \cdot \text{kip} \cdot \text{in}$$

$$\phi_b \cdot M_{nC3.1} = 26.055 \cdot \text{kip} \cdot \text{in}$$

stud distributed load

$$w_{nC3.1} := \frac{M_{nC3.1} \cdot 8}{L^2}$$

$$w_{nC3.1} = 301.563 \cdot \frac{\text{lbf}}{\text{ft}}$$

$$\phi_b \cdot w_{nC3.1} = 271.406 \cdot \frac{\text{lbf}}{\text{ft}}$$

wall pressure

$$p_{nC3.1} := \frac{w_{nC3.1}}{w_{tf}}$$

$$p_{nC3.1} = 150.781 \cdot \text{psf}$$

$$\phi_b \cdot p_{nC3.1} = 135.703 \cdot \text{psf}$$

$$\phi M := \begin{pmatrix} 0 \\ \phi_b \cdot M_{nC3.1} \end{pmatrix} \quad \phi P := \begin{pmatrix} \phi_c \cdot P_{nC4} \\ 0 \end{pmatrix}$$

### DSM Appendix 1 of Specification

$$P_n = 21.451 \cdot \text{kip}$$

$$\phi_c \cdot P_n = 18.234 \cdot \text{kip}$$

$$M_n = 29.5 \cdot \text{kip} \cdot \text{in}$$

$$\phi_b \cdot M_n = 26.55 \cdot \text{kip} \cdot \text{in}$$

stud distributed load

$$w_n := \frac{M_n \cdot 8}{L^2}$$

$$w_n = 307.292 \cdot \frac{\text{lbf}}{\text{ft}}$$

$$\phi_b \cdot w_n = 276.563 \cdot \frac{\text{lbf}}{\text{ft}}$$

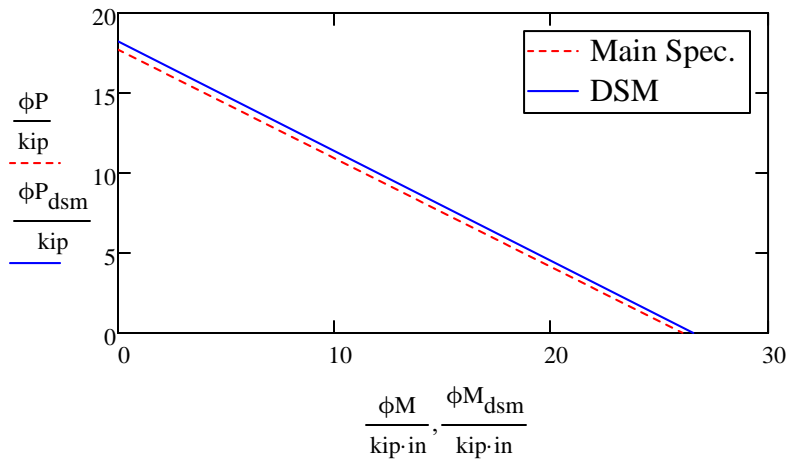
wall pressure

$$p_n := \frac{w_n}{w_{tf}}$$

$$p_n = 153.646 \cdot \text{psf}$$

$$\phi_b \cdot p_n = 138.281 \cdot \text{psf}$$

$$\phi M_{dsm} := \begin{pmatrix} 0 \\ \phi_b \cdot M_n \end{pmatrix} \quad \phi P_{dsm} := \begin{pmatrix} \phi_c \cdot P_n \\ 0 \end{pmatrix}$$



## Check Fasteners - Fastener Demands in Bending

Fastener demands in pull-through (pt) and bearing (br) are a function of the required axial force (Pr) and moment (Mr). First, consider the case of bending only, and consider the maximum possible Mr, i.e. Mr = full available capacity.

$$M_r := \phi_b \cdot M_n \quad M_r = 26.55 \cdot \text{kip} \cdot \text{in}$$

$$w_r := \frac{8 \cdot M_r}{L^2} \quad w_r = 0.023 \cdot \frac{\text{kip}}{\text{in}}$$

### F.D.1.1 Required Forces to Resist Direct Torsion in Bending (per draft ballot 11)

first find the eccentricity, i.e., distance from the shear center (s.c) to the end of the flange flat.

$m := 0.765 \cdot \text{in}$  per SSMA or SFIA table, dist. from s.c. to centerline of web

$r_{\text{inner}} := 0.1070 \cdot \text{in}$  again per SSMA or SFIA table.  $t = 0.071 \cdot \text{in}$

$r_{\text{outer}} := r_{\text{inner}} + t$

$e := m - \frac{t}{2} + r_{\text{outer}} \quad e = 0.908 \cdot \text{in}$

now the torsion demand, tributary to a fastener, that must be resisted

$$T_r := w_r \cdot d_f \cdot e \quad T_r = 0.251 \cdot \text{kip} \cdot \text{in} \quad (\text{Eq. F.D.1-3})$$

$h := 3.62 \cdot \text{in}$  (out-to-out depth of the stud)  $b := 1.62 \cdot \text{in}$  (flange width)

$$\theta_r := T_r \cdot \left( k_{\phi 1} + k_{x1} \cdot \frac{h^2}{4} + k_{\phi 2} + k_{x2} \cdot \frac{h^2}{4} \right)^{-1} \quad (\text{Eq. F.D.1-6})$$

Side 1 / Flange 1 (#8 in 7/16 in. OSB)

pull-through:

$$F_{rM\_pt1} := \frac{k_{\phi 1} \cdot \theta_r}{\frac{b}{2}} \quad F_{rM\_pt1} = 9.852 \cdot \text{lbf} \quad (\text{Eq. F.D.1-7})$$

bearing:

$$F_{rM\_br1} := k_{x1} \cdot \frac{h}{2} \cdot \theta_r \quad F_{rM\_br1} = 95.079 \cdot \text{lbf} \quad (\text{Eq. F.D.1-8})$$

Side 2 / Flange 2 (#6 in 1/2in. Gypsum)

pull-through:

$$F_{rM\_pt2} := \frac{k_{\phi 2} \cdot \theta_r}{\frac{b}{2}} \quad F_{rM\_pt2} = 9.922 \cdot \text{lbf} \quad (\text{Eq. F.D.1-9})$$

bearing:

$$F_{rM\_br2} := k_{x2} \cdot \frac{h}{2} \cdot \theta_r \quad F_{rM\_br2} = 34.758 \cdot \text{lbf} \quad (\text{Eq. F.D.1-10})$$

## Fastener Demands under Axial Load

Consider axial load only at its maximum possible required force.

$$P_r := \phi_c \cdot P_n \quad P_r = 18.234 \cdot \text{kip}$$

### F.D.1.2 Required Demands for Axial Stability Bracing (per draft ballot 11)

per F.D.1.2(b) for dissimilar sheathing

Side 1 / Flange 1 (#8 in 7/16 in. OSB)

pull-through

$$n := \frac{k_{x1} \cdot \left(\frac{h^2}{4}\right) + k_{x2} \cdot \left(\frac{h^2}{4}\right)}{k_{\phi1} + k_{\phi2}} \quad n = 14.673 \quad (\text{Eq. F.D.1-15})$$

note, n is a measure of what modes resist twisting of the stud, the higher the n the more that the bearing mode resists the twist of the stud, only the rotational springs directly engage the pull-through mechanism.

$$F_{rP\_pt1} := \frac{0.04 \cdot P_r}{\frac{L}{d_f}} \cdot \frac{k_{\phi1} \cdot \frac{h}{b}}{(1+n) \cdot (k_{\phi1} + k_{\phi2})} \quad F_{rP\_pt1} = 6.476 \cdot \text{lbf} \quad (\text{Eq. F.D.1-14})$$

bearing

$$F_{rP\_br1} := \frac{0.04 \cdot P_r}{\frac{L}{d_f}} \cdot \frac{k_{x1}}{k_{x1} + k_{x2}} \quad F_{rP\_br1} = 66.762 \cdot \text{lbf} \quad (\text{Eq. F.D.1-16})$$

Side 2 / Flange 2 (#6 in 1/2in. Gypsum)

pull-through

$$F_{rP\_pt2} := \frac{0.04 \cdot P_r}{\frac{L}{d_f}} \cdot \frac{k_{\phi2} \cdot \frac{h}{b}}{(1+n) \cdot (k_{\phi1} + k_{\phi2})} \quad F_{rP\_pt2} = 6.522 \cdot \text{lbf} \quad (\text{Eq. F.D.1-17})$$

bearing

$$F_{rP\_br2} := \frac{0.04 \cdot P_r}{\frac{L}{d_f}} \cdot \frac{k_{x2}}{k_{x1} + k_{x2}} \quad F_{rP\_br2} = 24.406 \cdot \text{lbf} \quad (\text{Eq. F.D.1-18})$$

## Available Fastener Capacity and Strength Check

### F.C.1 Available Strength of Member-Fastener-Sheathing in Bearing (draft ballot 12)

$$\text{side 1, \#8 in 7/16 in. OSB} \quad P_{n\_br1} := 578 \cdot \text{lbf} \quad \phi_{br} := 0.5 \quad \phi_{br} \cdot P_{n\_br1} = 289 \cdot \text{lbf}$$

$$\text{side 2, \#6 in 1/2 in. Gyp} \quad P_{n\_br2} := 86 \cdot \text{lbf} \quad \phi_{br} \cdot P_{n\_br2} = 43 \cdot \text{lbf}$$

These nominal capacities are based on tests conducted by the author. The test setup is the same as that of draft ballot 2 for determining  $k_x$  springs. See commentary and notes to draft ballot 12 for additional ideas on how to determine these capacities in other cases. Currently, to the authors knowledge, manufacturers do not regularly supply this data.

### F.C.2 Available Strength of Member-Fastener-Sheathing in Pull-through (draft ballot 12)

$$\text{side 1, \#8 in 7/16 in. OSB} \quad P_{n\_pt1} := 437 \cdot \text{lbf} \quad \phi_{br} := 0.5 \quad \phi_{br} \cdot P_{n\_pt1} = 218.5 \cdot \text{lbf}$$

$$\text{side 2, \#6 in 1/2 in. Gyp} \quad P_{n\_pt2} := 40 \cdot \text{lbf} \quad \phi_{br} \cdot P_{n\_pt2} = 20 \cdot \text{lbf}$$

These nominal capacities are based on tests conducted by the author. The test setup is the same as that of draft ballot 5 for determining  $k_\phi$  springs. See commentary and notes to draft ballot 12 for additional ideas on how to determine these capacities in other cases. Currently, to the authors knowledge, manufacturers do not regularly supply this data. In addition, this mode of failure may be unique to cold-formed steel as in wood construction withdrawal typically controls (it seems).

### Strength Check - Axial Loads

Side 1, 7/16 in. OSB with #8's

$$\text{Bearing} \quad F_{rP\_br1} = 66.762 \cdot \text{lbf} < \phi_{br} \cdot P_{n\_br1} = 289 \cdot \text{lbf} \quad \text{OK}$$

$$\text{Pull-through} \quad F_{rP\_pt1} = 6.476 \cdot \text{lbf} < \phi_{br} \cdot P_{n\_pt1} = 218.5 \cdot \text{lbf} \quad \text{OK}$$

Side 2. 1/2 in. Gyp with #6's

$$\text{Bearing} \quad F_{rP\_br2} = 24.406 \cdot \text{lbf} < \phi_{br} \cdot P_{n\_br2} = 43 \cdot \text{lbf} \quad \text{OK}$$

$$\text{Pull-through} \quad F_{rP\_pt2} = 6.522 \cdot \text{lbf} < \phi_{br} \cdot P_{n\_pt2} = 20 \cdot \text{lbf} \quad \text{OK}$$

### Strength Check - Bending

Side 1, 7/16 in. OSB with #8's

$$\text{Bearing} \quad F_{rM\_br1} = 95.079 \cdot \text{lbf} < \phi_{br} \cdot P_{n\_br1} = 289 \cdot \text{lbf} \quad \text{OK}$$

$$\text{Pull-through} \quad F_{rM\_pt1} = 9.852 \cdot \text{lbf} < \phi_{br} \cdot P_{n\_pt1} = 218.5 \cdot \text{lbf} \quad \text{OK}$$

Side 2. 1/2 in. Gyp with #6's

$$\text{Bearing} \quad F_{rM\_br2} = 34.758 \cdot \text{lbf} < \phi_{br} \cdot P_{n\_br2} = 43 \cdot \text{lbf} \quad \text{OK}$$

$$\text{Pull-through} \quad F_{rM\_pt2} = 9.922 \cdot \text{lbf} < \phi_{br} \cdot P_{n\_pt2} = 20 \cdot \text{lbf} \quad \text{OK}$$

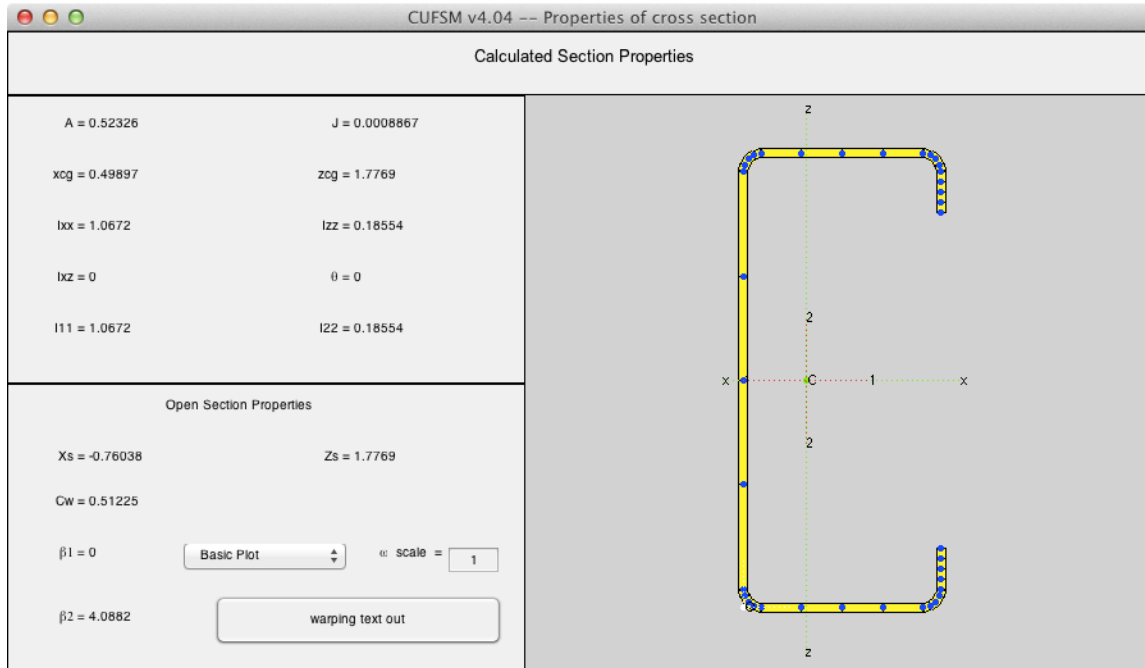
### **ALL FASTENERS OK FOR MAXIMUM REQUIRED DEMANDS**

Note, gypsum board is near its maximum capacity in bearing, and even pull-through is close to capacity; thus one can expect with standard details Gyp board may sometimes limit the capacity of the stud from developing its full available member capacity.

## Appendix: CUFSM Elastic Buckling Analysis for Design Example

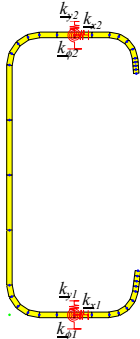
Elastic buckling analysis of a nominal 362S162-68 [50ksi] with 7/16 in. OSB fastened with #8s @ 12 in. o.c. on one face and 1/2 in. gypsum board fastened with #6s @ 12 in. o.c. on the other face. Analysis conducted in CUFSM version 4. [www.ce.jhu.edu/cufsm](http://www.ce.jhu.edu/cufsm)

The bare model of the cross-section is built and shown here:



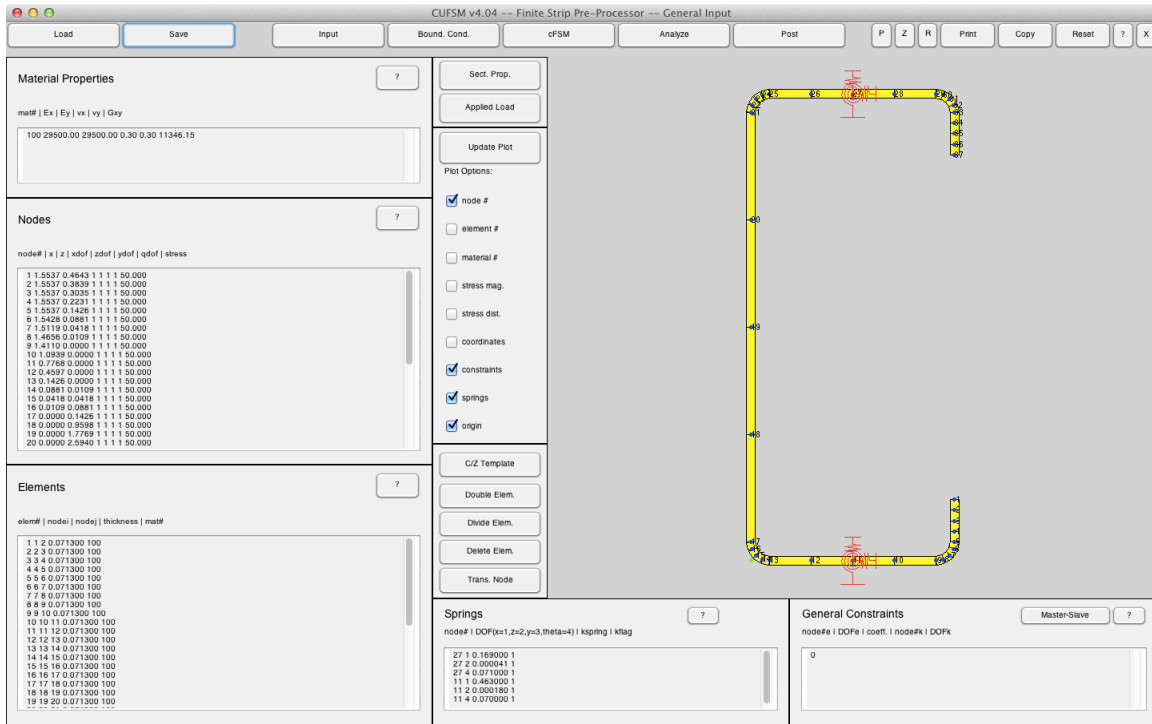
note, to check accuracy of the inputted geometry the  $A = 0.523 \text{ in}^2$  and  $I = 1.067 \text{ in}^4$  above, this may be compared with SFIA tables  $A = 0.524 \text{ in}^2$  and  $I = 1.069 \text{ in}^4$ . The geometry is accurate.

From the work reported in the design example the sheathing are modeled as foundation springs with the following values:

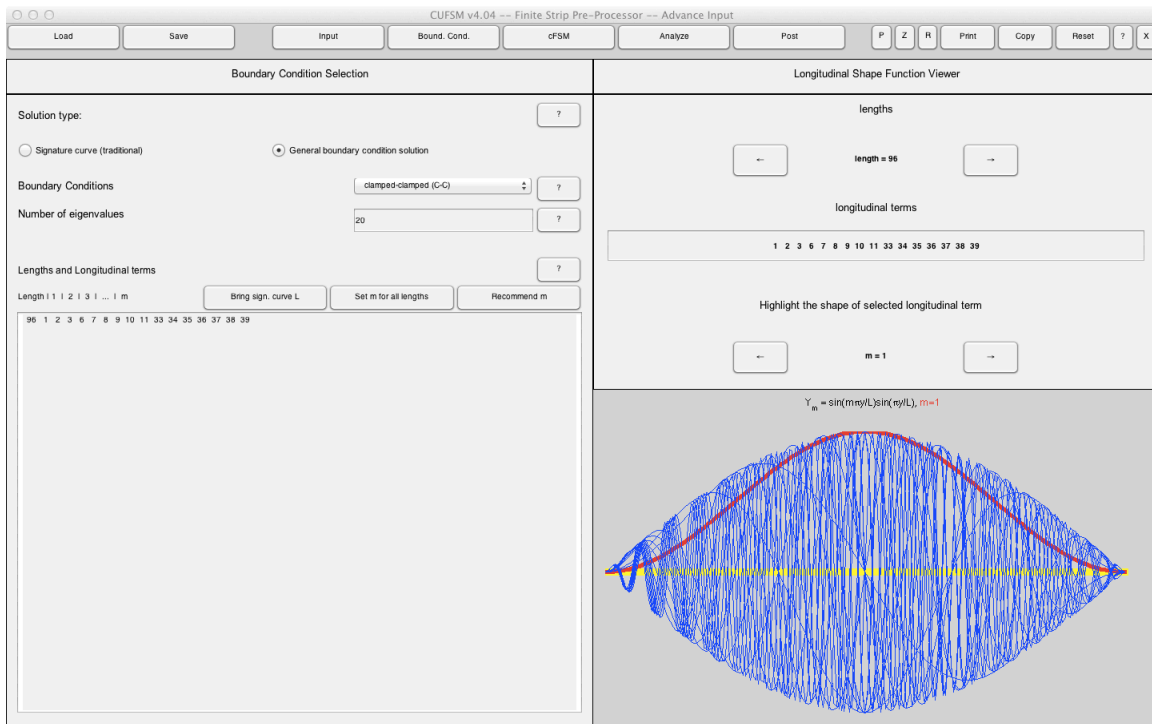
	<p>Face 2, 1/2 in. Gyp  <math>k_{x2} = 0.169 \text{ kip/in. / in.}</math>  <math>k_{y2} = 0.000041 \text{ kip/in. / in.}</math>  <math>k_{r2} = 0.071 \text{ kip-in./rad / in.}</math></p> <p>Face 1, 7/16 in. OSB  <math>k_{x1} = 0.463 \text{ kip/in. / in.}</math>  <math>k_{y1} = 0.00018 \text{ kip/in. / in.}</math>  <math>k_{r1} = 0.07 \text{ kip-in./rad / in.}</math></p>
---	--

Note, per proposed commentary to AISI Appendix 1, DSM, use of a foundation spring is accurate at this fastener spacing. See draft ballot 6 for additional commentary and references.

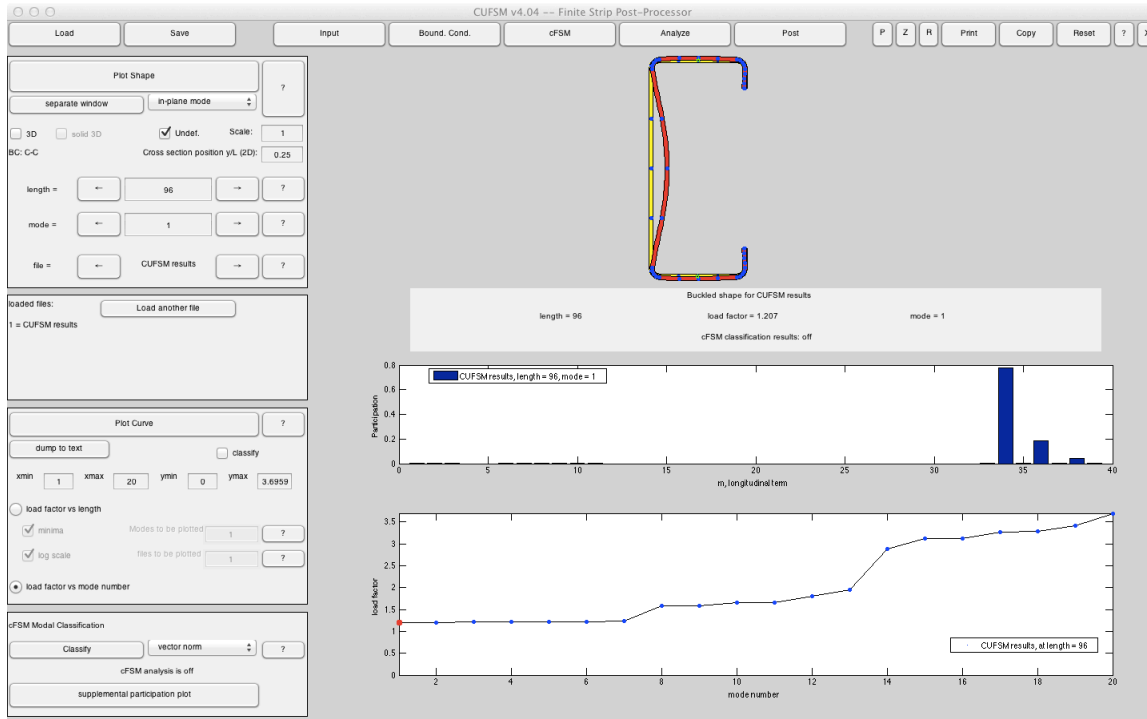
These foundation springs are introduced into the model as shown in the small Springs box below, and visually by the addition of springs depicted on the model cross-section.



**For the axial stability** the member is loaded with a reference load equal to the squash load (note the applied stress = 50 ksi on all nodes in the previous screen). **Clamped-clamped boundary conditions...** The slide below shows the longitudinal terms used in the model. The analysis is not a signature curve analysis, rather like FE the analysis is conducted at the physical length (96 in.) and the modes examined.

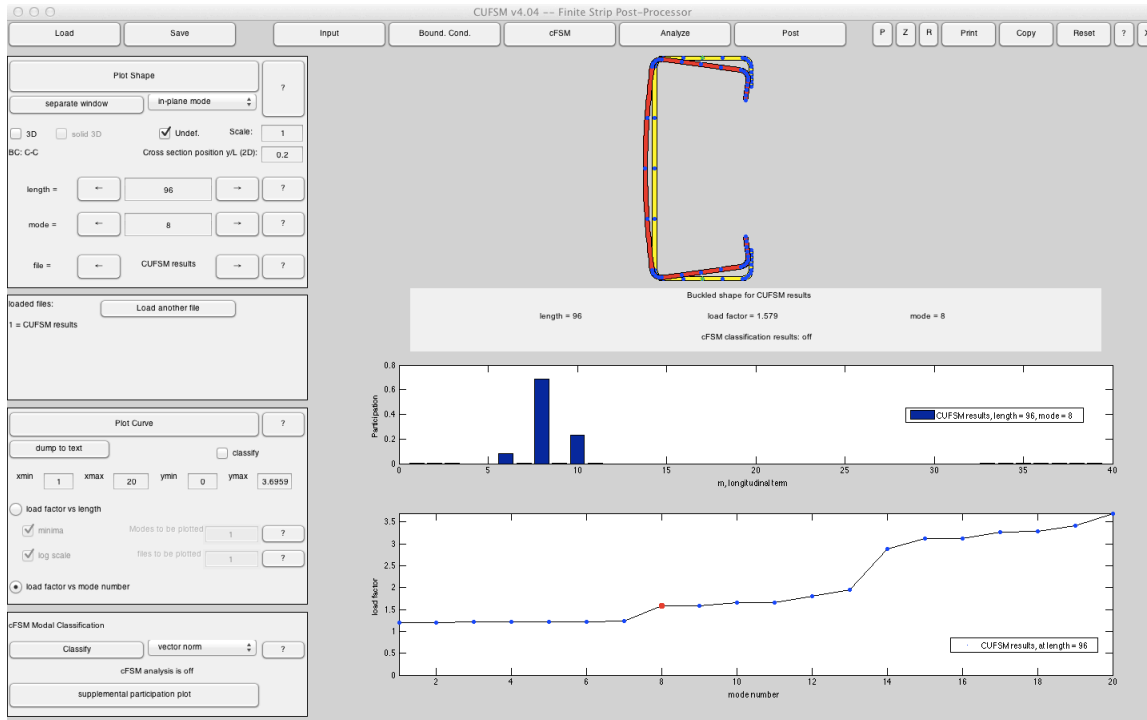


**Model results  $P_{cr}/P_y = 1.207$ .** In the screen below the top figure shows the buckled shape at  $x=0.25L$  along the length, second figure shows that  $m=34$  half-waves is the dominant number of half-waves along the 96 in. length (clearly local with a typical half-wave of  $96/34=2.82$  in.), bottom figure shows additional results (first 20 modes provided). Note this model includes all springs, strictly the springs should be removed for the local buckling value; however in this case the elastic local buckling load is 1.2069 with all springs removed as the web is dominating local buckling so either model acceptable.

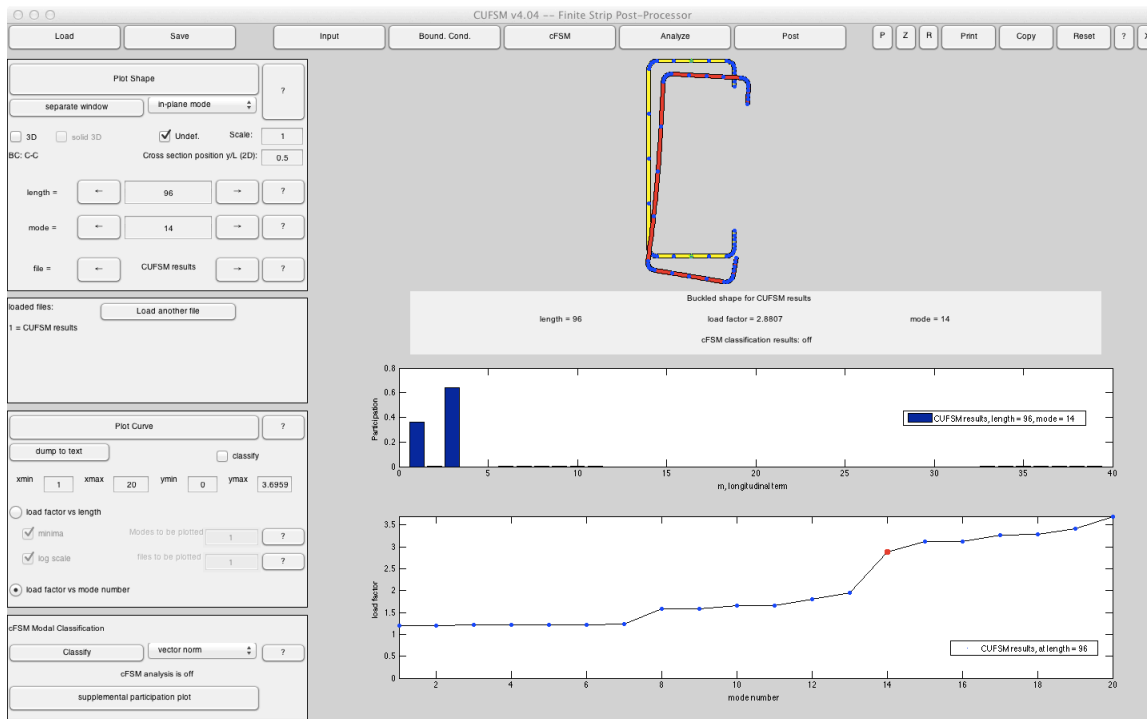




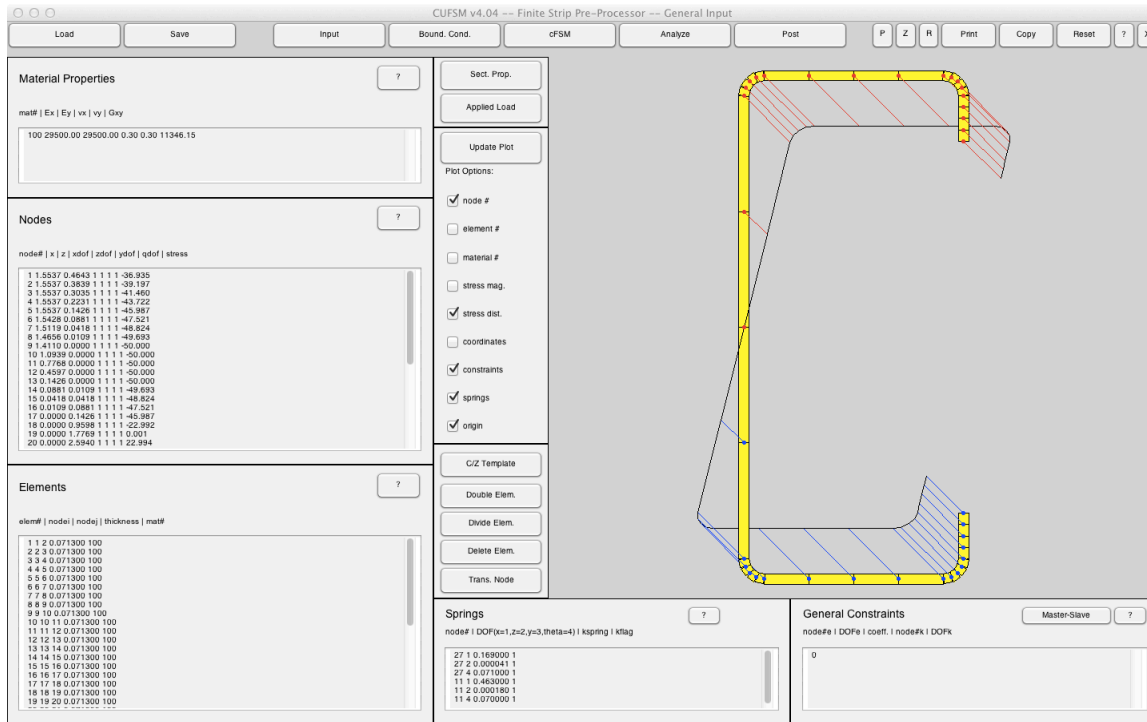
**Model results  $P_{crd}/P_y = 1.579$ .** In the screen below the top figure shows the buckled shape at  $x=0.2L$  along the length, second figure shows that  $m=8$  half-waves is the dominant number of half-waves along the 96 in. length (clearly distortional with a typical half-wave of  $96/8=12$  in.), bottom figure shows additional results (first 20 modes provided).



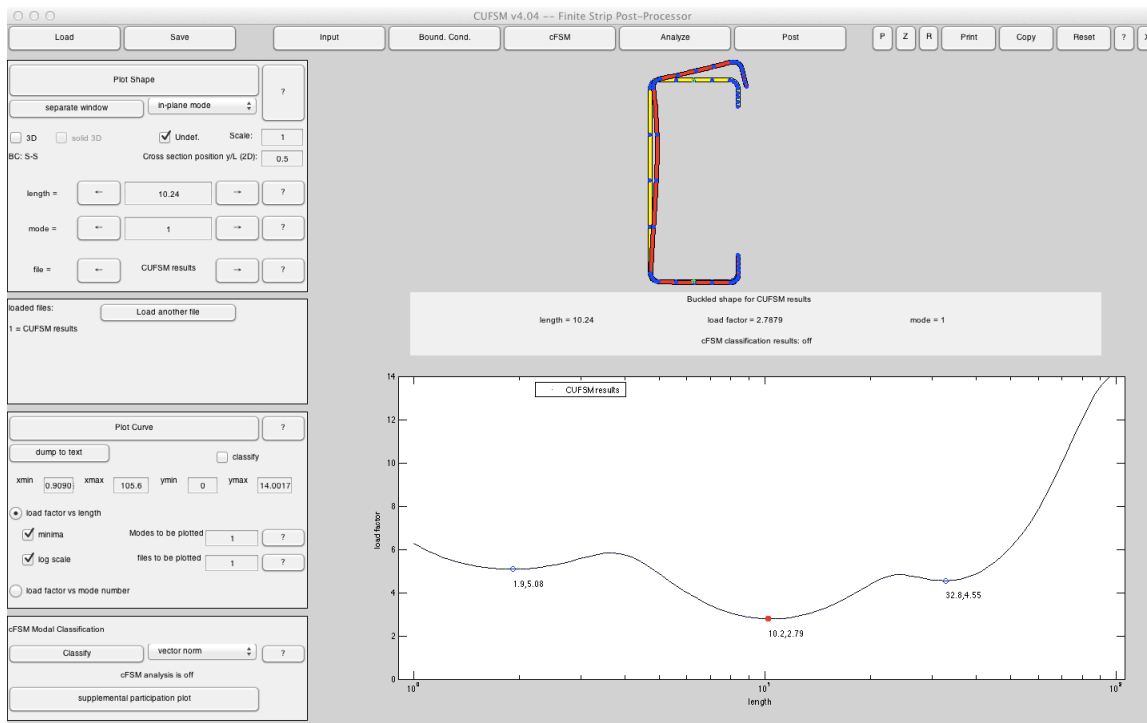
**Model results  $P_{cre}/P_y = 2.88$ .** In the screen below the top figure shows the buckled shape at  $x=0.5L$  along the length, second figure shows that  $m=1,3$  half-waves dominante, i.e. global mode is found.



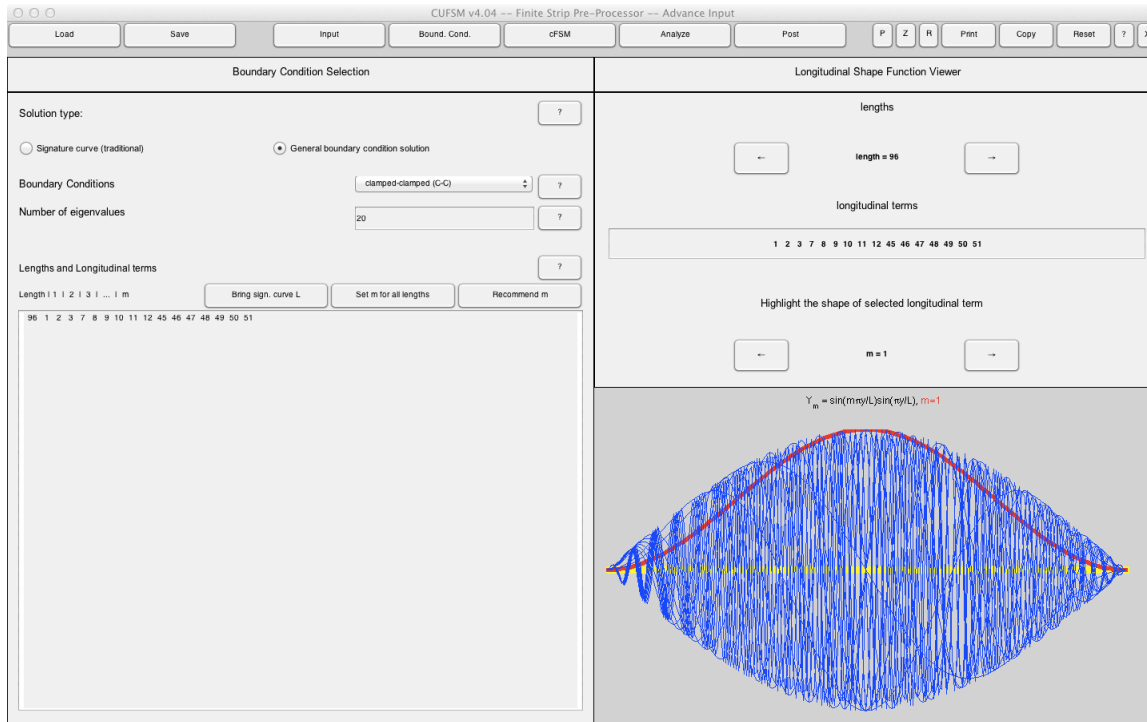
For bending stability analysis, we apply the reference  $M_y$  stress (for restrained bending). Placing the weaker (gypsum sheathed) flange in compression as the worst case bending demand.



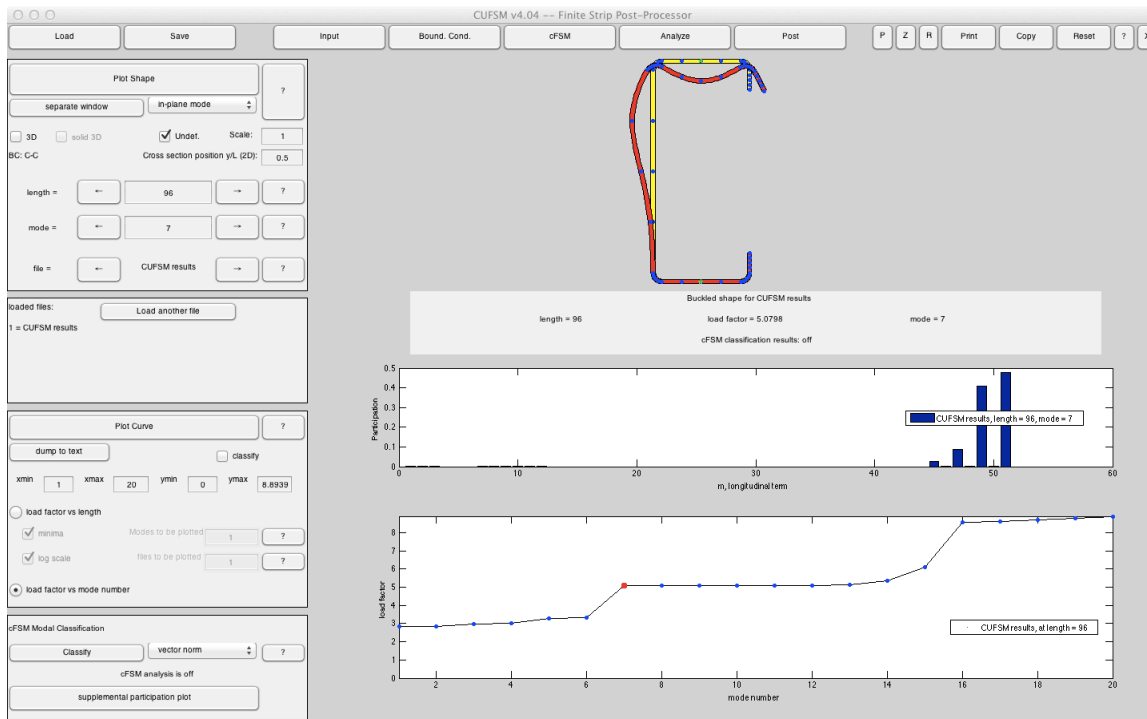
Also, we use pinned-pinned ends, so we can perform a classical signature curve analysis if desired. Results are shown below with distortional highlighted.  $M_{cr}/M_y=5.08$ ,  $M_{crd}/M_y=2.79$ ,  $M_{cre}/M_y=4.55$ . Note, the presence of springs means a minimum exists for global.



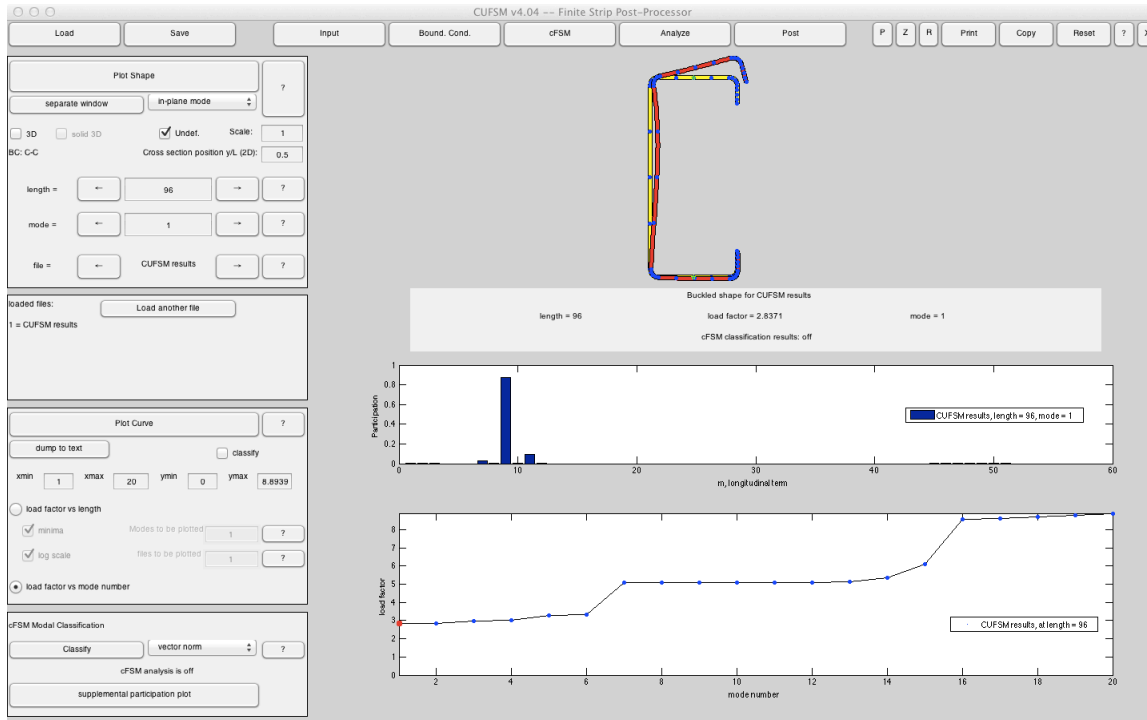
We can be more precise if desired, and perform the analysis even for pinned-pinned at the actual physical length, similar to the compression analysis under clamped-clamped. Selected  $m$  terms are shown:



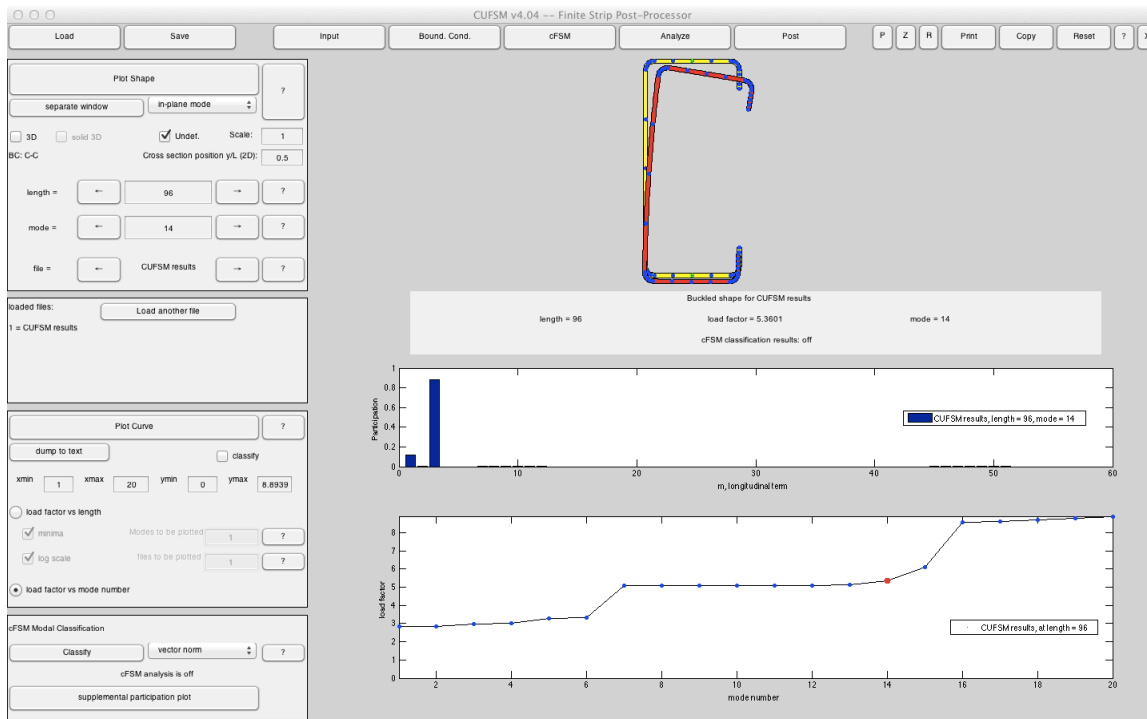
**Model results  $M_{cr}/M_y = 5.08$ .** Note,  $m=51$  half-waves is the dominant number of half-waves along the 96 in. length (clearly local with a typical half-wave of  $96/51=1.88$  in. same as signature curve). Also note, for this high of  $M_{cr}$  the section will not have a local buckling reduction.



**Model results  $M_{crd}/M_y = 2.84$ .** Note,  $m=9$  half-waves is dominant. Results are slightly higher than signature curve ( $M_{crd}/M_y = 2.79$ ), which does not take into account end effects (i.e. when the model length is not an integer number of half-waves). Signature curve is always the most conservative if minima employed. Also note, for this high of  $M_{crd}$  the section will not have a distortional buckling reduction.



**Model results  $M_{cre}/M_y = 5.26$ .** Note,  $m=3$  half-waves is dominant, but  $m=1$  also contributes at this physical length. Results are higher than signature curve ( $M_{cre}/M_y = 4.55$ ) similar to distortional case. Also note, for this high of  $M_{cre}$  the section will not have a global buckling reduction.



## Appendix: Project Monitoring Task Group Responses

The Project Monitoring Task Group (PMTG) met in April 2012 to discuss the closeout materials provided for this project at that time. Namely this email from 21 March 2012:

**From:** Benjamin Schafer <schafer@jhu.edu>  
**Date:** March 21, 2012 1:30:20 PM EDT  
**To:** Jay Larson <JLarson@steel.org>  
**Cc:** Debbie Lantry <dlantry1@jhu.edu>  
**Subject:** project closeout for AISI Sheathing Braced Design of Wall Studs

Jay

As we discussed it is time to formally close out the Sheathing Braced Design of Wall Studs project.

I have organized and updated the project webpage so that it may provide you all closeout materials and provide a permanent repository for those interested in this work.

Specifically, in terms of a "final report", please find at

<http://www.ce.jhu.edu/bschafer/sheathedwalls>

at the top of the page these two summary documents:

- Vieira Jr., L.C.M. (2011) Behavior and design of cold-formed steel stud walls under axial compression, Department of Civil Engineering, Ph.D. Dissertation, Johns Hopkins University.
- Peterman, K.D.P. (2012) Experiments on the stability of sheathed cold-formed steel stud under axial load and bending, M.S. Essay, Department of Civil Engineering, Johns Hopkins University.

These two dissertations are the summary of all work completed. The page provides significant ancillary materials as well, but these two are the permanent and necessary final documentation. I will update the page as additional conference papers and journal articles are completed.

Further, I am well aware that now is the time to produce the ballots related to this work and I have begun that process as well. This work should keep us busy in COFS for some time.

If you need anything else with respect to close out of this project please let me know.

Sincerely,  
Ben Schafer

Benjamin W. Schafer  
Swirnow Family Faculty Scholar  
Professor and Chair  
Department of Civil Engineering  
Johns Hopkins University  
[www.ce.jhu.edu/bschafer](http://www.ce.jhu.edu/bschafer)  
[schafer@jhu.edu](mailto:schafer@jhu.edu) 410.516.6265

The PMTG determined in April 2012 that the provided materials were insufficient for closing out the project. They provided a series of questions in a 14 April 2012 email to the PI: Ben Schafer. These questions were answered by the PI on 24 April 2012 and the PMTG and PI met on 1 May 2012 to discuss the answers.

It was determined at the 1 May 2012 meeting that a final report should be prepared, in addition to the 21 March 2012 email and that the answers to the PMTG questions should be cleaned up and included as an Appendix in that report. This is that appendix.

In the following

[...] indicates extraneous material that was removed.

Black Courier text is the PI's initial response

**Black Times New Roman** text is additional response provided in the preparation of this report

Blue Courier Text is the PMTG's original questions.

**From:** Benjamin Schafer <schafer@jhu.edu>  
**Date:** April 24, 2012 6:21:03 PM EDT  
**Additional Comments added 14 January 2013**  
**To:** Jay Larson <jlarson@steel.org>  
**Subject: Re: Sheathing Braced Design of Wall Studs**

Just so we start off on the right foot for our meeting I provided some short responses to the basic questions below. I look forward to meeting with the PMTG.

On Apr 23, 2012, at 10:23 PM, Jay Larson wrote:

All –

We have scheduled the GoToMeeting® to discuss PMTG feedback on the project closeout

[...]

A summary of PMTG feedback is in the email below.

Thank you.

Jay W. Larson, P.E., F. ASCE  
Managing Director, Construction Technical  
American Iron and Steel Institute  
3425 Drighton Court  
Bethlehem, PA 18020-1335  
tel: 610.691.6334

**From:** Jay Larson  
**Sent:** Saturday, April 14, 2012 9:42 AM  
**To:** Ben Schafer (schafer@jhu.edu)  
**Cc:** Nabil Rahman (nabil@steelnetwork.com)  
**Subject:** Sheathing Braced Design of Wall Studs

Dear Ben –

As discussed on the phone on April 5th, the Project Monitoring Task Group (PMTG) met via GoToMeeting® on April 4th to discuss the project closeout. We felt that a GoToMeeting® with you would be in order to discuss PMTG feedback. To facilitate the discussion the members of the PMTG submitted comments, which are compiled below.

Generally, the PMTG would like to see a concise final report that summarizes the primary test and analysis information, conclusions and the proposed design methods from the two theses (20-25 pages). Specifically, we would like to discuss the following:

- Content of the final report; such as:

- specific recommendations

Understood

**Provided in this report.**

- brief outline of the proposed ballots that are going to be submitted to COFS

Understood

**Provided in this report.**

- design example(s) (either in the summary or with the ballots).

Understood

**Provided in this report.**

- Specific recommendations, such as:

- need for more information about how the role of wall length (or wall aspect ratio) will be addressed in the proposed design methods

This aspect is already embedded in the method w.r.t stud spacing and tributary area of sheet when determining spring stiffness. Brace force accumulation is less well handled. I look forward to discussing this with the PMTG so I fully understand this comment.

..try to address this at least in a design example

..accumulation? not a problem up to our 5 stud wall

..intuition of the group does not concern ourselves with the accum.

**Wall length and wall aspect ratio are intrinsic to the method, specifically when determining the bracing restraint provided by the fastener-sheathing system to the studs. This issue is included in the method.**

- need for a chart for the proposed design method for Axial + Bending similar to the one presented for Axial only in the 2011 thesis

Understood.

**Full design method provided in this report.**

- Calibration concerns; such as:

- whether the 362S162-68 used for most of the testing is sufficient for calibration (results in less LB, DB and fastener tilt than thinner and deeper members)

Definitely worth discussing, but I am confident that we have validated an overall approach and not simply the idea that local buckling always controls. To be discussed further.

..Ben asserts we are ok based on member design practice

**The method provided in the report is general and checks all relevant limit states. The PI is confident that extension to other wall studs is appropriate since the approach is a direct extension of already-in-place methods for member design.**

- whether inelastic reserve and composite effect of sheathing should be accounted for when studying test/predicted data

Very tricky issue, I look forward to discussing. I do not know that we will resolve this, but we can be very clear on what we did. Dominant composite action WAS removed by isolating the loading into the studs. This was shown in the early work and can be reinforced in the final writeup.

..ky spring includes potential composite action (bending only)

..what about the axial force that bleeds into the sheathing?

..Ben's argument is that the location of the failure mechanism limits the comp. action

..group would like more discussion on this point

..What about bending + axial?? Ben to think about this.

..Useful to explain that our predictions "fall where they should" as a conservative estimate should be pointed out for people to understand this.

**The design method proposed herein assumes non-composite action unless one tests. If one tests, then partial composite action is allowed in terms of bracing, but not strength. Strength is always limited to the member strength, but bracing may include composite action if tests are used to determine ky. This seems like a fair compromise to the PI.**

**As far as inelastic reserve, additional fastener (bracing) strength checks may be required to allow the section to develop higher bending capacities. Currently the strength is limited to  $M_y$ .**

- how the 2a fastener statistical treatment would be integrated into the overall calibration ( $\phi = 0.85$  required for the 2a effect alone)

To be discussed. We have not integrated this work into our design method yet.

..my argument is that this is not a unique fabrication issue

..Ben to look at fabrication factor or other possible avenues for integrating this into the design method?

**The PI does not intend to include this factor uniquely in the method. The work on 2a addressed elastic buckling and the effect is much smaller for ultimate strength. Further work on reliability is needed, but the primary issue here is the reliability of the sheathing materials.**

• Other uncertainties; such as:

- the composite sheathing effect, if any

let's discuss.

**The design method proposed herein assumes non-composite action unless one tests. If one tests, then partial composite action is allowed in terms of bracing, but not strength. Strength is always limited to the member strength, but bracing may include composite action if tests are used to**



**determine ky. This seems like a fair compromise to the PI.**

- whether the composite effect goes away with load cycle conditioning  
let's discuss, we may only be able to point this out, our work in this project is not covering this in depth, but CFS-NEES work can be helpful in this regard.

..ky spring is the main issue here

..how to handle the testing? How to handle drywall?

..Ben's proposal here would be non-composite by calculation, and testing if you want greater brace stiffness... final report needs to address the test method.

- whether the wall tests are for flexure only and are pinned ends required

We will need to discuss this further so I fully understand.

..in the end we are satisfied that the ends acted as pinned. Should be highlighted in the final report

..what to do about axial fixed-fixed, flexure pinned-pinned

..should axial stay fixed-fixed? Final design method approach?

..mention this flexibility in final report

**The final report and paper on the columns under combined axial and bending assumed axial fixed-fixed (w.r.t warping) and bending pinned-pinned (w.r.t major-axis bending) and showed the best agreement with observed behavior and strength. This is recommended as the assumptions in this case.**

- whether the fastener torsion demand for uniformly distributed load instead of point load is more representative of the design case

Sure, sure. Here we are stretching our results and have not studied the uniform case. No doubt uniform case is more forgiving. We may not be able to say a great deal more on this particular aspect within this project.

..Some additional known analysis needed.

**This issue is fully addressed in**

Peterman, K.D., Schafer, B.W. "Sheathed Cold-Formed Steel Studs Under Axial and Lateral Load." Submitted to *Journal of Structural Engineering* (Submitted 2 January 2013).

**A method is provided for extension to uniformly distributed load cases.**

• Drywall reliability issues both for axial and flexure (moisture, load cycling and installation error issues)

Only studied in part in this project

..Ben has no obvious resolution

..phi factor?

..mention where we have landed and leave it beyond the scope of the report?

..let people see the data so they understand gyp board + and -

..unresolved issue at this point, load case dependent? Other design approaches? Possible rational avenues

**No resolution, the current approach is to provide the information in the design method and let engineers decide if they want to rely on gypsum board in their designs.**

**Appendix: Vieira Jr., L.C.M., Schafer, B.W. (2013). “Behavior and Design of Sheathed Cold-Formed Steel Stud Walls under Compression.” ASCE, *Journal of Structural Engineering* (DOI: 10.1061/(ASCE)ST.1943-541X.0000731). *In Press***

# 1                    **Behavior and Design of Sheathed Cold-Formed Steel** 2                    **Stud Walls under Compression**

3                    L.C.M. Vieira Jr., Ph.D.<sup>1</sup> and B.W. Schafer, Ph.D., P.E., A.M. ASCE<sup>2</sup>

## 4                    **Abstract**

5                    The objective of this paper is to provide a robust design method for walls framed from cold-  
6                    formed steel (CFS) stud and track that utilize traditional sheathing materials as the primary  
7                    means of bracing against compressive load. Existing design methods are unable to handle dis-  
8                    similar sheathing attached to the CFS stud flanges (e.g., oriented strand board (OSB) on the  
9                    exterior face and gypsum board on the interior face) and provide no clarity on the impact of key  
10                    properties including sheathing shear rigidity and stud spacing. A series of tests on axially loaded  
11                    sheathed single studs and sheathed full walls utilizing OSB, gypsum board, or an unsheathed  
12                    face (and combinations thereof) are performed to elucidate the basic behavior and limit states.  
13                    The stiffness that the fastener-sheathing system supplies to the stud as bracing is characterized  
14                    analytically and experimentally. The characterization clarifies how both local fastener  
15                    deformations and global sheathing deformations contribute to sheathing bracing. The impact of  
16                    sheathing on elastic stability of the stud in local, distortional, and global buckling modes is  
17                    provided. Both computational and analytical methods for stability determination including  
18                    bracing stiffness from sheathing are detailed. A simple extension to current design methods that  
19                    utilizes the enhanced elastic stability provided by sheathing bracing is proposed for member  
20                    strength prediction. The design method is shown to agree well with the performed tests,  
21                    providing consistent predictions for the limit state and the strength for walls with sheathing,  
22                    including sheathing on one-side only, and dis-similar sheathing on the two stud flanges.

23                    **Keywords:** cold-formed steel, sheathed wall stud

---

<sup>1</sup> Faculty, Dept. of Mechanical, Civil & Environmental Eng., University of New Haven, 300 Boston Post Road, West Haven, CT, USA, 06516, Tel.: +1.410.608.2549, email: luizvieirajr@gmail.com <Corresponding author>

<sup>2</sup> Professor and Chair, Department of Civil Engineering, Johns Hopkins University, 3400 N. Charles St., Baltimore, MD, USA, 21218, Tel.: +1.410.516.6265, email: schaffer@jhu.edu

## 24 **1 INTRODUCTION**

25 Load bearing cold-formed steel (CFS) framed buildings utilize one of two design philosophies  
26 for bracing of the CFS studs in walls – all-steel, or sheathing-braced. The all-steel design  
27 philosophy (Figure 1a) uses discrete steel bridging to brace the stud walls. The sheathing-braced  
28 design philosophy (Figure 1b) may or may not utilize bridging for construction loads, but for  
29 design loads relies on sheathing: oriented strand board (OSB), plywood, or gypsum board to  
30 brace the stud. Since sheathing is nearly always present, accounting for the sheathing in the  
31 structural performance provides significant potential economies; however, accurate and reliable  
32 prediction of the strength of sheathing-braced stud walls can be challenging.

33 Recently, the first author completed a multi-year study of sheathing-braced CFS stud walls in  
34 axial compression Vieira (2011) and this work is summarized herein. Specifically, this paper  
35 provides a brief review of the theory and design approaches for the strength of sheathing-braced  
36 studs (Section 2); a summary of recent tests on sheathing-braced studs including single stud  
37 (Figure 1c) tests and full wall (Figure 1b) tests (Section 3), a summary of recent tests and  
38 analytical formulae characterizing the stiffness that fastener-sheathing systems (Figure 1d,e)  
39 supply to brace studs (Section 4), an assessment of the elastic stability of studs braced by  
40 sheathing that utilizes the determined fastener-sheathing stiffness (Section 5), member strength  
41 predictions based on the stability assessment (Section 6), and comparisons to tests as well as a  
42 discussion of fastener demands and future work (Section 7).

## 43 2 BACKGROUND

44 Formal design of sheathing-braced CFS studs in the AISI Specification has progressed  
45 through three periods: 1962-1980, the local stiffness approach (AISI 1962); 1980-2004 the  
46 diaphragm stiffness approach (AISI 1980); and, 2004-present a variation on the local stiffness  
47 approach focused on an unbraced length equal to twice the fastener spacing (AISI-S100 2007,  
48 AISI-S211 2007). The limitations and inherent contradictions in the existing design approaches  
49 are an important pre-text for the multi-year study summarized here; detailed examination is  
50 provided in Schafer et al. (2008) and supplemented in Vieira (2011), only summary information  
51 is provided here.

52 The local stiffness approach which was pioneered by Winter and his students (Green, et al.  
53 1947, Winter 1960) had two key features: (1) the stability of the stud walls in axial compression  
54 included local translational springs ( $k_x$  springs, see Figure 1e) to account for the bracing provided  
55 by the fasteners, and (2)  $k_x$  was determined by direct experiments on small-scale stud-fastener-  
56 sheathing assemblies. The design implementation in AISI (1962) was prescriptive in nature, the  
57 weak-axis flexural buckling of the stud ( $P_{cry}$ ) with the springs ( $k_x$ ) included had to be greater than  
58 or equal to the column squash load ( $P_y$ ), the weak-axis buckling of the stud over an unbraced  
59 length equal to twice the fastener spacing (i.e.,  $L=2a$ ) had to be greater than or equal to the  
60 strong-axis flexural buckling load ( $P_{crx}$ ), and the fasteners had to be designed for approximately  
61 2% of the axial demand. The local stiffness approach ignored flexural-torsional buckling and  
62 ignored distortional buckling. Further, the design rules implemented were rather arbitrary and the  
63 method was abandoned in 1980.

64 The diaphragm stiffness approach developed by Simaan and Peköz (1976) was adopted by  
65 the AISI Specification in 1980 and used until 2004. In this approach the bracing provided by the

66 fastener-sheathing system is treated in a more global manner – the local fastener stiffness is  
67 ignored (or more accurately experimentally smeared into the shear stiffness of the diaphragm)  
68 and instead the energy developed due to the in-plane shear deformation of the diaphragm as the  
69 studs deforms is included in an overall energy solution to determine the sheathing-braced  
70 buckling load. The method accounted for flexural-torsional buckling and theoretically could  
71 account for dis-similar sheathing on the two faces of the stud, though the procedure was not  
72 explicitly provided in AISI (1980). In addition, the method provides for a discrete check on the  
73 shear strain of the sheathing (though failures generally occur at fastener locations not due to  
74 basic material failure in the sheathing). The method is complex in its use, yields counter-intuitive  
75 solutions with regard to stud spacing, and did not agree well with more recent testing (Schafer, et  
76 al. 2008, Miller and Pekoz 1993, Trestain 2002). The method was abandoned in 2004.

77 A return to a variation on the local stiffness approach occurred in the 2004 interim update to  
78 the AISI Specification (see AISI-S100 2007, AISI-S211 2007). Bracing stiffness characterization  
79 is abandoned; instead, it is assumed that the stud should only be checked for an unbraced length  
80 equal to twice the fastener spacing (i.e.  $L=2a$ ) and the fasteners should be checked for 2% of the  
81 axial demand – both checks utilized from 1962-1980 in the AISI Specification. Use of the  
82 method is restricted to similar sheathing on the two stud flanges. The global buckling check at  
83  $L=2a$  includes flexural-torsional buckling. The method has the advantage of extreme simplicity,  
84 but critically ignores the influence that the stiffness of the fastener-sheathing system has on the  
85 stability solution. It is assumed, regardless of fastener type, sheathing type, and stud spacing the  
86 design strength is the same. The approach has limited applicability and provides no overall  
87 philosophy for extension to stud walls with dis-similar sheathing on the two stud flanges.

### 88 **3 TESTS ON SHEATHING-BRACED CFS STUDS**

89 Testing of axially loaded CFS studs with different combinations of sheathing attached to  
90 the stud flanges was completed. The work consisted of two test series: (a) single studs with short  
91 segments of track and attached sheathing (Figure 1c) tested at lengths from 0.6 m to 2.4 m (2 ft  
92 to 8 ft), and (b) stud walls (Figure 1b) 2.4 m x 2.4 m (8 ft x 8 ft) consisting of five equally spaced  
93 studs with track and sheathing. The sheathing attached to the flanges included various  
94 combinations of OSB, gypsum board (abbreviated Gyp herein) and/or no sheathing (termed  
95 BARE herein) attached to the stud flanges.

96 A total of 26 sheathed single stud tests were completed and are reported in Vieira et al.  
97 (2011). A key finding from the single stud tests is that if sheathing is attached to both stud  
98 flanges, even dis-similar sheathing (e.g., OSB and Gyp), the stud fails in a limit state dominated  
99 by local buckling of the stud web. For one-sided sheathing (OSB-BARE, or Gyp-BARE), or no  
100 sheathing (BARE-BARE) the behavior is more complicated and distortional and (restrained)  
101 flexural-torsional buckling is observed, depending on the unbraced length. It was also found that  
102 the sheathing must be prevented from direct bearing on the loading platens. If bearing of the  
103 sheathing is allowed composite action develops that increases the stud capacity by as much as  
104 20% over a stud with identical sheathing details, but not allowed to bear.

105 A total of 12 sheathed full wall tests were also completed, have not been previously  
106 reported, and are summarized here.

#### 107 **3.1 Full wall specimen details and instrumentation**

108 The 2.4 m x 2.4 m (8 ft x 8 ft) stud walls consist of 5 equally spaced studs, track, and  
109 sheathing fastened to the flanges, as depicted in Figure 1. The studs employed throughout are  
110 362S162-68's (50 ksi) per U.S. industry standard nomenclature (AISI-S200 2007, SSMA 2001).

111 Therefore, the nominal web height is 92 mm (3.62 in.), the nominal flange width is 41 mm (1.62  
112 in.), and the nominal thickness is 1.73 mm (0.068 in.). These members also have a nominal lip  
113 length of 13 mm (0.5 in.) and an inside corner radius of 2.72 mm (0.1070 in.). The nominal track  
114 employed is a 362T125-68 (similar nomenclature). As-measured dimensions, geometric  
115 imperfections, and measured material properties for the stud and track are provided in Vieira  
116 (2011). Two types of sheathing are employed: OSB (11.1 mm, (7/16 in.), rated 24/16, exposure  
117 1) and Gypsum (12.7 mm, (1/2 in.) Sheetrock Regular). Number 6 screws (Simpson DWF #6 x  
118 41.3 mm (1 5/8 in.)) were used to connect to the Gypsum boards and number 8 screws (Simpson  
119 PPSD #8 x 49.2 mm (1 15/16 in.)) to connect to the OSB boards. The sheathing is connected to  
120 the studs and tracks every 152 mm (6 in.) along the edges, and to the studs every 305 mm (12  
121 in.) in the field, as depicted in Figure 1.

122 As shown in Figure 3a the walls are tested under axial compression in the multi-degree of  
123 freedom (MDOF) testing rig in the Thin-walled Structures Laboratory at Johns Hopkins  
124 University. The testing rig is utilized only for axial testing here, the specimen (the wall) is  
125 connected to the upper (actuated) load beam and lower fixed beam of the rig through 12.7mm (1/2  
126 in.) bolts through the track at every stud location. In addition, 12.7mm (1/2 in.) plates are used at  
127 each stud location to insure the sheathing cannot bear against the loading beams. Full details of  
128 the rig and testing are available (Vieira 2011).

129 In addition to the internal actuator LVDTs and load cells, simple linear position  
130 transducers (PTs) are used extensively to record the deformations of the stud. PT triplets (Figure  
131 3b,f) are utilized along the height of the field studs in the interior of the wall to capture flexure,  
132 twist, and local deformations (the difference between the exterior and interior sensor). In some  
133 cases (given limited numbers of sensors and channels, see Figure 3c) the center PT is removed,



134 thus allowing only global flexure and twist to be captured. In other cases, particularly near the  
135 ends where global deformations are limited by the boundary conditions, but local buckling may  
136 still occur, only the center PT is utilized (see Figure 3d,i). Global lateral deformation of the  
137 axially compressed wall is also recorded (typically by PT 11).

### 138 **3.2 General results and discussion**

139 The observed specimen strength is summarized in Table 1 and typical axial load vs. axial  
140 displacement is provided in Figure 2. Note, the last column of Table 1 also includes the results  
141 from the single stud tests for the same height as the wall tests detailed here. Sheathing is an  
142 effective way to increase wall strength: the attachment of sheathing can increase the axial  
143 strength of the wall by as much as 91% (compare BARE-BARE to OSB-OSB). From the  
144 standpoint of strength, sheathing is always beneficial. The ascending order of values for peak  
145 load is BARE-BARE, OSB-BARE, Gyp-Gyp, OSB-Gyp and OSB-OSB. As shown in Figure 2,  
146 axial stiffness is largely unaffected by the sheathing (evidence of the success in avoiding direct  
147 composite action and direct bearing of the sheathing in the testing), but peak strength, and post-  
148 peak behavior are significantly influenced. Walls with sheathing on both sides are all dominated  
149 by local buckling limit states (Figure 3d,e,g,h) and exhibit at least some stable post-peak  
150 behavior. Variation in peak strength across the specimens sheathed on both sides is 12%. The  
151 walls with sheathing on only one side (OSB-BARE) exhibit a significant strength increase above  
152 walls without sheathing (16%), but the post-peak response is catastrophic and the wall remains  
153 unable to carry essentially any axial load (the lateral sensor rig arrested the complete collapse of  
154 these walls). More detailed examination of the tested performance for each sheathing  
155 configuration follows.

156        **3.3 Results for an unsheathed wall**

157            A wall tested without sheathing (i.e. BARE-BARE) is essentially a test of five  
158 independent studs. Both weak-axis flexure and flexural-torsional buckling are observed in the  
159 same wall (these two global modes have similar buckling loads for a 2.4 m (8 ft) long 362S162-  
160 68 stud). The wall tests provide a capacity 14% lower than a single stud with track (as  
161 summarized in Table 1). Although the tested strength is known to exhibit scatter, it is postulated  
162 that an important source for the lower result for the walls is that the wall fails when the weakest  
163 of the five studs in the wall fails, as without sheathing, redistribution is nearly impossible.

164            The end conditions of the stud-to-track are of great interest as they are highly influential  
165 for global buckling. The observed performance, under the tested conditions (i.e. perfect bearing  
166 against steel plates in the presence of axial load) is that of a member with fixed end conditions. It  
167 is observed that the axial load present is large enough to fully seat the stud (note the change in  
168 stiffness in Figure 2 after the stud seats) and provide warping and bending fixity to the member  
169 ends. This issue is examined further in Section 4 and is consistent with the experiments and  
170 modeling from the single stud tests reported in Vieira et al. (2011).

171        **3.4 Sheathing on one-side only**

172            Walls tested with OSB sheathing on one-side only (OSB-Bare, see Figure 3a) suffer from  
173 restrained axis flexural-torsional buckling and post-peak behavior with no reserve. As Figure 4  
174 indicates for the 1-OSB-BARE test, the twist, i.e. the difference between PT7 and 9, increases  
175 dramatically as failure is approached. Variation in the load response of the OSB-BARE tests was  
176 relatively high (see Table 1). In test 6-OSB-BARE, which had the highest peak load of the OSB-  
177 BARE tests, what occurred during the test was that one of the studs started to twist towards the  
178 flange side instead of towards the lip side (the usual side that buckles). After the other studs all

179 buckled towards the lip side the stud had to reverse its initial twist before finally twisting to the  
180 lip side and failing along with the rest of the wall. Thus, providing a physical demonstration of  
181 the imperfection sensitivity of this failure mode.

182 The most important feature of the OSB-BARE wall tests was the pronounced lack of  
183 post-buckling reserve. The failures were dramatic, in sharp contrast even to the single column  
184 tests with the same sheathing configuration. The load-displacement response of Figure 2 does not  
185 do justice to the violent nature of the observed collapse, even in displacement controlled loading.  
186 Given the nature of this collapse the common practice of using strap on the BARE side may not  
187 be sufficient to restrict this mode (i.e., blocking or sheathing may be necessary).

### 188 **3.5 Similar sheathing on both sides**

189 The walls with gypsum sheathed on both sides (Gyp-Gyp) or OSB sheathing on both  
190 sides (OSB-OSB) failed in a limit state dominated by local buckling. For the gypsum sheathed  
191 walls the local buckling (Figure 3d) causes significant damage in the gypsum (Figure 3e). After  
192 local buckling, distortional buckling is present in some of the gypsum-sheathed tests as Figure 3i  
193 shows for the 7-Gyp-Gyp test after failure. The distinction between local buckling and  
194 distortional buckling can be quite subtle and the preceding discussion relies primarily on the  
195 (half-) wavelength of the observed deformations.

196 Local buckling in an OSB sheathed specimen (test 9-OSB-OSB) is shown in Figure 3g  
197 after the test and after removing one side of the sheathing. Failure occurred at the member ends:  
198 top in 9-OSB-OSB, bottom in 5-OSB-OSB. The PTs captured the amplification of displacements  
199 during local buckling. For example for the 5-OSB-OSB test Figure 5 shows the measurement  
200 location and reading from all PTs and for PTs 8,9, and 10 (mounted as depicted in Figure 3d or i)

201 as the axial displacement increases these PTs undergo the large displacements associated with  
202 the local buckling failure.

203         The OSB-OSB tests carried 12% more load than the Gyp-Gyp tests even though the studs  
204 fail in the same local buckling limit state dominated by web deformations near the member ends.  
205 As demonstrated further in Section 4 since the sheathing, which is connected to the flanges, has  
206 little to no influence on the local buckling of these studs the additional capacity must derive from  
207 the sheathing itself carrying a modest amount of axial load (and the stiffer, stronger OSB  
208 sheathing carrying more than gypsum board). This occurs despite the fact that the sheathing is  
209 not allowed to directly bear on the loading or support beams and instead must transfer its axial  
210 load to the track via fasteners in shear back to the stud.

### 211         **3.6 Dis-similar sheathing on the two sides**

212         Walls with dis-similar sheathing, OSB on one side and Gypsum on the other (OSB-Gyp)  
213 present an interesting response: limit state (local buckling), strength (Table 1) and axial load-  
214 displacement (Figure 2) is essentially the same for all tests, but deformations observed in the  
215 post-peak behavior vary. Test 3-OSB-Gyp failed in local buckling (Figure 6d), but in the post-  
216 peak regime also exhibited flexural-torsional buckling (stud S14, Figure 7c). Test 10-OSB-Gyp  
217 also failed in local buckling; however, post peak one stud was also observed to fail in distortional  
218 buckling (Figure 3i). Test 8-OSB-Gyp failed in local buckling alone. OSB and gypsum board  
219 restrain the stud with different stiffness and strength, this leads to fastener tearing (bearing  
220 failures) in the Gypsum board (Figure 6b,c) as the stud twists about the more restrained OSB  
221 face. Though the imbalance in sheathing stiffness creates this demand, the observed limit state  
222 remains local buckling and the observed strength is consistent with walls with similarly sheathed  
223 studs.

### 224 **3.7 Comparison between wall tests and single stud tests**

225 The observed limit states in the single stud tests of (Vieira, et al. 2011) are the same as  
226 for the wall tests reported here. However, as indicated in Table 1, the peak load is usually  
227 slightly lower in the complete wall tests (except for the OSB-Bare tests). Postulated reasons for  
228 the slight decrease in the full-scale wall tests, when compared with the single columns tests: (a)  
229 the tributary area of the board designated to each stud in the wall as engaged for sheathing  
230 resistance is modestly less than in the single column tests, (b) bracing forces in the sheathing  
231 accumulate and may have a modestly detrimental influence, (c) when the weakest of the 5 studs  
232 in the wall fail the forces must be carried by the other studs, thus strength may be more of a  
233 weakest link strength as opposed to an idealized redistribution of a fully parallel system.

234 For the OSB-Bare case the failure is in flexural-torsional buckling and the full wall  
235 actually has a higher observed per stud mean strength than the single column, this may be due to  
236 the increased torsional resistance at the ends of the studs in a full wall, but the variability is  
237 significant and the failure mode in the full walls and one-sided sheathed single studs is similar.

## 238 **4 FASTENER-SHEATHING STIFFNESS**

239 The bracing forces that are supplied to a sheathed stud occur at the fastener locations.  
240 Thus, Winter's basic idea of a stud braced by springs (Figure 1d) still provides the conceptually  
241 correct beginning. However, many types of springs exist (not just those restricting lateral  
242 translation, see Figure 1e) and perhaps more importantly, the springs represent a fastener-  
243 sheathing system and not just local fastener stiffness. A contribution of the work of Vieira  
244 (Vieira 2011), summarized here, is the marriage of local and diaphragm stiffness in the  
245 determination of the fastener-sheathing stiffness and the formalization of experimental and  
246 simplified analytical methods for determining this stiffness.

247           Theoretically, the fastener-sheathing system supplies three translation and three rotational  
248 springs at every fastener location bracing the stud. Practically, a more limited set of springs in  
249 the plane of the cross-section, as shown in Figure 1e, consisting of lateral translation ( $k_x$ ) which  
250 is in the plane of the sheathing, “vertical” translation ( $k_y$ ) which is out of the plane of the  
251 sheathing, and rotational stiffness ( $k_\phi$ ) which is in the plane of the cross-section are the most  
252 important. The  $k_x$  springs restrain against buckling modes associated with weak-axis flexure and  
253 torsion, while  $k_\phi$  springs restrains flange distortion (distortional buckling), and  $k_y$  springs restrain  
254 strong-axis flexure and account for flexural composite action. The translational spring along the  
255 length ( $k_z$ ) is neglected because the fastener-sheathing system is not allowed to provide an  
256 independent vertical load path. The rotational spring about the fastener ( $k_{\phi y}$ ) is neglected since the  
257 fasteners are largely free to twist in the sheathing. The out-of-plane rotational spring about the x-  
258 axis ( $k_{\phi x}$ ) may be approximated as the same as  $k_\phi$  (the mechanisms are similar) but is generally  
259 neglected because restriction of in-plane (cross-section) deformations are of the most importance.

#### 260           **4.1 Lateral translational stiffness ( $k_x$ )**

261           Resistance to lateral translation at the fastener location from the fastener-sheathing system  
262 consists of two parts: local resistance as the fastener tilts and bears into the sheathing, and  
263 diaphragm resistance as the stud undergoes bending which is resisted by shear in the diaphragm  
264 equilibrated by differential lateral forces at the fasteners. These two mechanisms are fully  
265 detailed in Vieira and Schafer (2012); in particular, it is shown that they act in series and thus the  
266 lateral translational stiffness  $k_x$  is determined by combining the local translational stiffness ( $k_{xl}$ )  
267 and diaphragm translational stiffness ( $k_{xd}$ ) via:

$$k_x = 1 / (1 / k_{xl} + 1 / k_{xd}) \quad (1)$$

268 The local translational stiffness ( $k_{x\ell}$ ) was the focus of Winter's pioneering work (Green, et al.  
 269 1947, Winter 1960) and the most direct means to determine  $k_{x\ell}$  is by test. Figure 8 shows a  
 270 simple test of two horizontal studs connected by sheathing fastened to the flanges where the  
 271 studs are pulled apart (perpendicular to the long axis of the stud). This test was preferred by  
 272 Winter and by the authors, but other valid methods exist (Fiorino, et al. 2007, Okasha 2004,  
 273 Chen, et al. 2006). The observed bearing response in the simple fastener test is similar to the wall  
 274 tests, as shown in Figure 8b and c.

275 Alternatively,  $k_{x\ell}$  may be approximated by a lower bound formula:

$$k_{x\ell} = \frac{3Ed^4t^3\pi}{4t_{board}^2(9d^4\pi + 16t_{board}t^3)} \quad (2)$$

276 where:  $E$  = Young's modulus of the steel stud,  $d$  = fastener diameter,  $t$  = flange thickness, and  
 277  $t_{board}$  = board or sheathing thickness. The expression assumes that a tributary width of the stud  
 278 flange and the fastener form a frame, that in bending resist the lateral movement of a force  
 279 applied at the fastener head (a distance  $t_{board}$  from the flange). Though approximate, and only  
 280 accounting for the sheathing in terms of its thickness, the expression is found to provide a useful  
 281 lower bound (Vieira and Schafer 2012).

282 The lateral diaphragm resistance developed at the fasteners as the studs attempt to bend in a  
 283 single half sine wave about the weak-axis,  $k_{xd}$ , is:

$$k_{xd} = \frac{\pi^2 G t_{board} d_f w_{tf}}{L^2} \quad (3)$$

284 where:  $G$  = shear modulus of the sheathing, and may be found through testing by ASTM-D2719-  
 285 89 (ASTM 2002a), or utilizing tabulated values from NDS (NDS 2005),  $w_{tf}$  = fastener tributary  
 286 width,  $d_f$  = distance between fasteners, and  $L$  = sheathing height. Derivation and validation of the  
 287 expression is available (Vieira and Schafer 2012).

288 The marriage of the local and diaphragm stiffness is critical to the method's robustness. The  
 289 local stiffness accounts for the stud ( $E$ ,  $t$ ) the fastener ( $d$ ) and its length ( $t_{board}$  is the fastener  
 290 length in bending) while the diaphragm stiffness brings in the critical issues of sheathing shear  
 291 stiffness ( $G$ ) and stud spacing ( $w_{if}$ ). If the diaphragm is stiff enough sheathing shear rigidity and  
 292 stud spacing are irrelevant and only local mechanisms dominate, but if the sheathing is weak in  
 293 shear, as shown analytically and experimentally in Vieira and Schafer (2012), the opposite  
 294 occurs. Thus, as an example, even for the same stud the importance of stud spacing may be great  
 295 for one type of sheathing and irrelevant for another. This explains the sometime contradictory  
 296 existing results regarding stud spacing and unites the fundamentals of the local approach used in  
 297 the AISI Specification from 1962-1980 and the diaphragm approach from 1980-2004.

298 **4.2 Out of plane translational stiffness ( $k_y$ )**

299 Translational stiffness  $k_y$ , restricts deformations out of the plane of the sheathing, and is  
 300 typically ignored in derivations related to sheathing bracing. However, in flexural-torsional  
 301 buckling of studs the flexure is in the strong-axis and even small resistance to vertical (out-of-  
 302 plane) movement can be influential. If composite action is ignored then  $k_y$  is the stiffness from  
 303 bending of the sheathing about its own axis. For a stud bending about its strong axis in a single  
 304 half sine wave sheathing bent in the same mode will contribute:

$$k_y = \frac{(EI)_w \pi^4 d_f}{L^4} \quad (4)$$

305 where:  $(EI)_w$  = sheathing rigidity per APA-D510C (APA-D510C 2008) for OSB and plywood  
 306 sheathing, and GA-235-10 (GA-235-10 2010) for gypsum sheathing,  $d_f$  = distance between  
 307 fasteners, and  $L$  = sheathing height. For fully composite action  $(EI)_{wc}$  replaces  $(EI)_w$  in Eq. (4):

$$(EI)_{wc} = (EI)_w + E_w w_{if} t_{board} \left( \frac{1}{2} h + \frac{1}{2} t_{board} \right)^2 \quad (5)$$



308 where  $E_w$  may be back-calculated from the tabled  $(EI)_w$  as

$$E_w = 12(EI)_w / w_{tf} t_{board}^3 \quad (6)$$

309  $w_{tf}$  = tributary width of the fastener,  $t_{board}$  = thickness of the board, and  $h$  = out-to-out depth of  
310 the stud.

311 Determination of partial composite action (the most realistic situation) requires testing. For  
312 non-structural stud walls it is common practice to determine the stiffness of the composite wall  
313 system via ASTM-E72 (ASTM 2002b) tests, a similar test is recommended here. The strong-axis  
314 bending rigidity of the composite stud-sheathing system ( $(EI)_{system}$ ) may be found from the  
315 results of ASTM-E72 tests in one of the two loading alternatives:

$$(EI)_{system} = \frac{11HL^3}{384\delta} \text{ (two point loads) or } = \frac{5wL^4}{384\delta} \text{ (uniform load)} \quad (7)$$

316 where:  $H$  = concentrated load applied perpendicular to the wall,  $L$  = height of the wall,  $w$  =  
317 uniform load perpendicular to the wall, and  $\delta$  = maximum measured displacement for the  
318 respective loading case ( $H$  or  $w$ ). The stiffness of the stud must be removed from the system  
319 stiffness to determine  $k_y$ , also recognizing that sheathing is on two sides (i.e.  $k_y$  is on the two  
320 flanges) the sheathing bending rigidity  $(EI)_{wpc}$  that should be used in Eq. (4) for partially  
321 composite action is:

$$(EI)_{wpc} = \frac{1}{2} \left[ (EI)_{system} - (EI)_{stud} \right] \quad (8)$$

### 322 **4.3 Rotational Stiffness ( $k_\phi$ )**

323 Rotational stiffness restricts cross-section torsion and flange rotation/distortion. For  
324 sheathing on both flanges the  $k_x$  pair is more effective in resisting torsion than  $k_y$ , so in practical  
325 cases the importance of  $k_x$  is in restricting flange rotation associated with distortional buckling.  
326 The rotational stiffness develops as the flange attempts to rotate against the sheathing and a

327 moment couple consisting of contact at the stud flange/web juncture and pull-through at the  
 328 fastener location develops. This mechanism is fully explored in Schafer et al. (2010) along with  
 329 experiments utilizing an augmented version of AISI-TS-1 (2002) and a simple analytical  
 330 formulation that in 2011 was adopted in AISI-S210 in a tabular form. The rotational stiffness is  
 331 separated (similar to lateral stiffness) into two components the local fastener (connector)  
 332 foundation stiffness  $\underline{k}_{fc}$  and the sheathing stiffness  $\underline{k}_{sw}$ , and the two are combined as springs in  
 333 series:

$$\underline{k}_{fc} = 0.00035Et^2 + 75 \text{ (note: } E \text{ in lbf/in}^2, t \text{ in in.)} \quad (9)$$

$$\underline{k}_{sw} = (EI)_w / d_f \quad (10)$$

$$\underline{k}_s = 1 / (1/\underline{k}_{fc} + 1/\underline{k}_{sw}) \quad (11)$$

334 where:  $E$  = Young's modulus of the steel stud,  $t$  = flange thickness,  $d_f$  = distance between  
 335 fasteners, and  $(EI)_w$  = sheathing rigidity per APA-D510C (APA-D510C 2008) for OSB and  
 336 plywood sheathing, and GA-235-10 (GA-235-10 2010) for gypsum sheathing. Note, for  $(EI)_w$  the  
 337 appropriate sheathing orientation must be selected: horizontal for  $\underline{k}_{sw}$  and vertical for  $k_y$ . In  
 338 addition, if the discrete rotational stiffness at the fastener is desired, i.e.,  $k_s$  then  $\underline{k}_s$  is simply  
 339 multiplied times the fastener tributary length along the stud, i.e.  $d_f$ .

#### 340 **4.4 Fastener-sheathing stiffness for tested members**

341 The fastener-sheathing stiffness  $k_x$ ,  $k_y$  and  $k_s$  was determined for the details consistent with  
 342 the sheathed stud and wall testing of Section 3. For  $k_x$  the small scale experimental values as  
 343 detailed in Vieira and Schafer (2012) are selected for  $k_{x/s}$ , and  $k_{xd}$  and  $k_x$  are determined per Eq. 3  
 344 and 1 respectively. For  $k_y$  non-composite and composite limits based on Eq.'s 4 and 5 are used,  
 345 and for  $\underline{k}_s$  Eq.'s 9-11 are used. In addition, the discrete springs  $k_x$  and  $k_y$  are smeared into  
 346 foundation stiffnesses (divided by fastener tributary length of the stud) which is denoted with an

347 underbar, i.e.  $\underline{k}_x$ ,  $\underline{k}_y$ , The rotational stiffness of Eq. 11 is a foundation stiffness. Summary results  
348 and key assumptions are provided in Table 2 and complete details and further discussion are  
349 available in Vieira (2011).

## 350 **5 ELASTIC STABILITY**

351 The elastic stability of a CFS stud is significantly altered by the presence of sheathing. An  
352 unsheathed CFS stud such as the 362S162-68 studied in detail here has a classical finite strip  
353 signature curve (Schafer and Adany 2006) and the three typical stability modes: local,  
354 distortional, and global buckling as provided in Figure 9. The global buckling mode is either  
355 weak-axis flexural buckling, or flexural-torsional buckling – both are at similar elastic buckling  
356 loads. At practical lengths flexural-torsional buckling is the minimum (slightly lower than weak-  
357 axis flexure), while at extreme lengths (greater than 3 m) weak-axis flexural buckling is the  
358 minimum. If spring foundations are introduced into the finite strip model to account for the  
359 sheathing (per Section 4, numerical values in Table 2) then the influence of the sheathing may be  
360 observed to alter the signature curve. Note, comparison between shell finite element models with  
361 discrete springs and FSM models with smeared (foundation) springs indicate satisfactory  
362 accuracy for the smeared spring model up to fastener spacing as large as 203 mm (8 in.) in the  
363 studied cases (Iourio and Schafer 2008).

364 For the case of one-sided sheathing (OSB-Bare, Figure 10a) local buckling is largely  
365 unchanged, distortional buckling is slightly elevated, and global buckling is (a) elevated, (b)  
366 exhibits minima, (c) is dominated by restrained axis flexural-torsional buckling, and (d) shows  
367 significant sensitivity to the magnitude of  $\underline{k}_y$  (i.e. the level of composite action in strong-axis  
368 flexure). The elevated elastic global buckling values provide an increase in strength. The global  
369 minimum (just like minima for local and distortional buckling) indicate that the half-wavelength

370 at which the particular (restrained axis flexural-torsional) global mode will repeat itself along the  
371 length (increases to the right of a minima for the same mode should be ignored). The dominance  
372 of flexural-torsional buckling is to be expected given the highly unsymmetric nature of the  
373 sheathing restraint. The sensitivity to  $k_y$  indicates the important role that the coupling of torsion  
374 and strong-axis flexure play in flexural-torsional buckling.

375 For the case of two-sided OSB sheathing (OSB-OSB, Figure 10b) local buckling is largely  
376 unchanged, distortional buckling is modestly elevated, and global buckling is (a) significantly  
377 elevated, (b) exhibits minima, and (c) shows sensitivity to the magnitude of  $k_y$  only when  
378 significant composite action is present. Comparison of the global stability with and without the  
379 non-composite (lower bound)  $k_y$  shows little change; indicating that the lateral stiffness ( $k_x$ )  
380 supplied to the two flanges provides the primary resistance needed against both flexural-torsional  
381 and weak-axis flexural buckling at practical lengths. If no  $k_y$  is present at extreme lengths strong-  
382 axis flexure controls. If  $k_y$  is present a restrained flexural-torsional mode with a global minimum  
383 results – and this restrained mode is dependent on the magnitude of  $k_y$ . At the fully composite  
384 limit global buckling is restrained (elastic global buckling values are extremely high). Note, if  
385 testing for partially composite action is not completed then the lower bound non-composite  
386 action for  $k_y$  should be employed in design predictions.

387 An important aspect of the elastic stability not provided in the finite strip signature curves of  
388 Figure 9 and Figure 10 is the impact of end boundary conditions. As detailed in Vieira et al.  
389 (2011) and discussed in Section 3.2 a fully seated stud bearing against a level steel plate (as in  
390 the testing conducted herein) develops bending and warping fixed end conditions. The finite strip  
391 signature curve is for pinned end conditions. It is possible to extend the finite strip method to  
392 general end conditions (Li and Schafer 2010a), but as a result the meaning of the signature curve

393 is lost and analysis is only useful at physical lengths (similar to a finite element method analysis  
394 of a member discretized as shell elements). Specific guidance on finding the elastic buckling  
395 loads for a sheathed stud follow.

### 396 **5.1 Local Buckling ( $P_{cr\ell}$ )**

397 Sheathing does not affect local buckling. The sheathing restrains the flange, but local  
398 buckling is largely driven by the web. Theoretically,  $\underline{k}_x$  and  $\underline{k}_\circ$  (if located at the exact mid-width  
399 of the flange) have no influence on local buckling, only  $\underline{k}_y$ . The out-of-plane stiffness,  $\underline{k}_y$ , is  
400 derived consistent with global bending resistance and not localized resistance. For local buckling  
401 predictions it is recommended to ignore the sheathing. Due to the short wavelength of the  
402 buckling mode, end conditions also have little influence on local buckling. Thus, a conventional  
403 finite strip signature curve result completed on the bare stud (or similar shell finite element  
404 model) is adequate for finding the local elastic buckling load,  $P_{cr\ell}$ . For industry standard studs  
405  $P_{cr\ell}$  has been tabled (Li and Schafer 2011); and practical modeling guidance and analytical hand  
406 solutions (if desired) are available (Schafer 2006).

### 407 **5.2 Distortional Buckling ( $P_{crd}$ )**

408 Sheathing provides beneficial rotational restraint against distortional buckling, and  $\underline{k}_\circ$  as  
409 discussed in Section 4.3 should be included when determining the elastic distortional buckling  
410 load ( $P_{crd}$ ). For studs with deep webs (and narrow flanges) the additional restraint supplied by  $\underline{k}_x$   
411 may be influential – its inclusion is optional, but if included requires the use of computational  
412 stability solutions. Stiffness  $\underline{k}_y$  should not be included when determining distortional buckling. In  
413 distortional buckling  $\underline{k}_y$  would be engaged, but as derived,  $\underline{k}_y$ 's deformations are consistent with  
414 strong-axis stud flexure, not rotation of the flange. Further,  $\underline{k}_\circ$  already accounts for the moment  
415 couple that develops between  $\underline{k}_y$  at the fastener and bearing between the flange and sheathing.

416 End conditions have influence on distortional buckling at practical lengths. General end  
417 conditions may be treated in the finite strip solution (Li and Schafer 2010a), in shell finite  
418 element models, or by using a correction factor ( $D_{boost}$  in (Moen 2008)) for fixed-fixed end  
419 conditions on a simply-supported model. In some cases the distortional buckling mode can be  
420 difficult to identify in a finite strip model, in such cases the constrained FSM is recommended  
421 (Li and Schafer 2010a, 2010b).

422 For industry standard studs, tables are provided to aid in the determination of  $\underline{k}_\phi$  and  $P_{crd}$   
423 along with full design examples of the available analytical hand solutions (Li and Schafer 2011,  
424 Schafer 2008) including the  $P_{crd}$  solutions adopted in AISI-S100 (2007).

### 425 **5.3 Global Buckling ( $P_{cre}$ )**

426 Sheathing greatly influences the global buckling load ( $P_{cre}$ ). For determining  $P_{cre}$  inclusion of  
427 all available fastener-sheathing springs ( $\underline{k}_x, \underline{k}_y, \underline{k}_\phi$ ) is recommended, but  $\underline{k}_x$  is critical as it provides  
428 the primary fastener-sheathing restraint for both weak-axis flexure and torsion (when present on  
429 both flanges). Experimental determination of  $k_{x\ell}$  may well be warranted for maximum efficiency;  
430 otherwise the lower bound solution of Eq. (2) combined with Eq.'s (3) and (1) may be used to  
431 determine  $\underline{k}_x$ . Flexural composite action can be beneficial and if tests are available can be utilized  
432 as detailed in Section 4.2; otherwise, the non composite value for  $\underline{k}_y$  (Eq. 4) should be used.

433 End conditions (in the testing conducted here fixed ends are appropriate) should be  
434 accounted for in determining  $P_{cre}$ . To include the impact of fixed end conditions (and the bracing  
435 springs) the recently developed finite strip model for general end conditions (Li and Schafer  
436 2010a) or shell finite element models may be utilized. Alternatively, classical analytical solutions  
437 with appropriate effective length factors may be employed. An analytical solution for global  
438 buckling of an unsymmetric section with multiple springs is not generally available. Timoshenko

439 (1961) provides the necessary fundamentals, but not the details for this particular case. A  
440 solution is provided for  $P_{cre}$  in the Appendix, including the appropriate effective length factors  
441  $K_x$ ,  $K_y$ , and  $K_t$  for the member buckling terms and  $K_{x\_spring}$ ,  $K_{y\_spring}$ , and  $K_{t\_spring}$  for the spring  
442 terms (see Appendix and Figure 11).

443 Comparison of the classical (Appendix) solution for  $P_{cre}$  to numerical solutions using FSM  
444 for general end boundary conditions, i.e. (Li and Schafer 2010a) are provided in Figure 11. For  
445 simply supported end boundary conditions the solutions are in exact agreement. For fixed-fixed  
446 end conditions the analytical solution is provided for a single buckling half-wave, i.e.  $m=1$  and  
447 for two buckling half-waves  $m=2$  with appropriate effective length ( $K$ ) factors. Agreement is  
448 excellent, but care must be taken to use the  $m$  solution with the lowest  $P_{cre}$ . Computational  
449 solutions are preferred by the authors, but for cases where formal analytical solutions must be  
450 provided (and ultimately programmed), the analytical solution provides the correct answer.

## 451 **6 MEMBER STRENGTH DETERMINATION**

452 The basic method proposed for strength determination is to correct the elastic buckling loads  
453 for the presence of the sheathing and then to use existing design expressions; either the Direct  
454 Strength Method (DSM) of Appendix 1 of AISI-S100, or the Effective Width Method (EWM) of  
455 the main specification of AISI-S100 to find the strength. Determining the fastener-sheathing  
456 stiffness  $\underline{k}_x$ ,  $\underline{k}_y$ ,  $\underline{k}_\phi$  per Section 4 is the first step. Finding the elastic buckling loads  $P_{cr\phi}$ ,  $P_{crd}$ ,  
457  $P_{cre}$  with appropriate inclusion of  $\underline{k}_x$ ,  $\underline{k}_y$ ,  $\underline{k}_\phi$  per Section 5 is the second step. The final step is to  
458 utilize existing design expressions to convert the elastic buckling loads (and knowing the squash  
459 load,  $P_y$ ) to predict the nominal strength  $P_n$ .

460 **6.1 DSM Approach for finding  $P_n$**

461 The Direct Strength Method requires that the engineer provide the elastic buckling loads ( $P_{cr\ell}$ ,  
 462  $P_{crd}$ ,  $P_{cre}$ ) by rational analysis. With those loads determined the predicted nominal capacity is a  
 463 direct application of the available design expressions in Appendix 1 of AISI-S100, specifically  
 464 global strength  $P_{ne}$  is found by:

$$P_{ne} = \begin{cases} 0.658\lambda_c^2 P_y & \text{for } \lambda_c \leq 1.5 \\ 0.877P_{cre} & \text{for } \lambda_c > 1.5 \end{cases} \text{ and } \lambda_c = \sqrt{P_y / P_{cre}} \quad (12)$$

465 Local-global interaction is accounted for utilizing:

$$P_{nl} = \begin{cases} P_{ne} & \text{for } \lambda_c \leq 0.766 \\ \left[ 1 - 0.15 \left( \frac{P_{cr\ell}}{P_{ne}} \right)^{0.4} \right] \left( \frac{P_{cr\ell}}{P_{ne}} \right)^{0.4} P_{ne} & \text{for } \lambda_c > 0.766 \end{cases} \text{ and } \lambda_\ell = \sqrt{P_{ne} / P_{cr\ell}} \quad (13)$$

466 Distortional buckling is found as follows

$$P_{nd} = \begin{cases} P_y & \text{for } \lambda_c \leq 0.561 \\ \left[ 1 - 0.25 \left( \frac{P_{crd}}{P_y} \right)^{0.6} \right] \left( \frac{P_{crd}}{P_y} \right)^{0.6} P_y & \text{for } \lambda_c > 0.561 \end{cases} \text{ and } \lambda_d = \sqrt{P_y / P_{crd}} \quad (14)$$

467 Finally the capacity is the minimum (note,  $P_{n\ell}$  is strictly less than or equal to  $P_{ne}$ ,  $P_{ne}$  is just an  
 468 intermediary calculation):

$$P_n = \min(P_{ne}, P_{n\ell}, P_{nd}) \quad (15)$$

469 **6.2 EWM Approach for Finding  $P_n$**

470 The main body of the AISI Specification utilizes the EWM approach for local buckling, which  
 471 leads to a modestly different implementation for the strength. To account for local-global  
 472 interaction an effective area ( $A_e$ ) utilizing the design expressions in AISI-S100 Chapter B must  
 473 be found at the long column stress  $F_n$ .



$$P_{nC4.1} = A_e F_n \quad (16)$$

$$F_n = \begin{cases} 0.658 \lambda_c^2 F_y & \text{for } \lambda_c \leq 1.5 \\ 0.877 F_e & \text{for } \lambda_c > 1.5 \end{cases} \quad \text{and } \lambda_c = \sqrt{F_y / F_e} \text{ and } F_e = P_{cre} / A_g \quad (17)$$

474 Note,  $F_n$  is identical to  $P_{ne}/A_g$  from the DSM method,  $P_{nC4.1}$  is directly comparable to  $P_{ne}$ , and the  
 475 key modification is the introduction of a long column elastic buckling stress,  $F_e$ , that accounts for  
 476 sheathing restraint (i.e.  $P_{cre}$  as per Section 5 includes the benefit of sheathing). Distortional  
 477 buckling, found in C4.2 of the main Specification of AISI-S100 is identical to the DSM method:

$$P_{nC4.2} = \begin{cases} P_y & \text{for } \lambda_c \leq 0.561 \\ \left[ 1 - 0.25 \left( \frac{P_{crd}}{P_y} \right)^{0.6} \right] \left( \frac{P_{crd}}{P_y} \right)^{0.6} P_y & \text{for } \lambda_c > 0.561 \end{cases} \quad \text{and } \lambda_d = \sqrt{P_y / P_{crd}} \quad (18)$$

478 Finally, the strength is simply the minimum of the two

$$P_n = \min(P_{n-C4.1}, P_{n-C4.2}) \quad (19)$$

## 479 7 COMPARISON WITH TESTS AND DISCUSSION

### 480 7.1 Strength Comparison

481 In this section the observed axial capacity of the 0.6 m to 1.8 m (2 ft to 6 ft) tall sheathed  
 482 single stud tests (Vieira, et al. 2011) and the 2.44 m (8 ft) tall sheathed stud and wall tests (Table  
 483 1) are compared against the predicted member strength. Consider first the comparison for  
 484 specimens sheathed on one-side only (OSB-Bare) as provided in Figure 12. The figure provides  
 485 comparison to design predictions with pinned and fixed end conditions, as well as predictions  
 486 with no sheathing, with sheathing and a lower bound non composite flexural action assumption,  
 487 and with sheathing and upper bound composite flexural action assumed. The test data most  
 488 closely follows the assumption of fixed-fixed end conditions (this was also observed of bare-bare  
 489 specimens (Vieira, et al. 2011)). In fact, up to 183 cm (72 in.), the end conditions are more

490 influential than the sheathing restraint. For longer columns the importance of the sheathing  
491 restraint grows significantly. For the fixed-fixed end conditions, the lower bound (non  
492 composite) approximation for the sheathing contribution to the major-axis bending of the stud is  
493 sufficiently accurate.

494 For the columns and walls with sheathing restraint on both sides: Gyp-Gyp, OSB-Gyp and  
495 OSB-OSB Figure 13 provides a comparison with potential design assumptions (to provide some  
496 clarity the spring values employed in the design curves are those for OSB-OSB alone, additional  
497 curves with all combinations are provided subsequently). All of the tested columns fail in local  
498 buckling, at approximately the same per stud strength. In stark contrast to the case with one-  
499 sided sheathing (OSB-Bare) having springs on both flanges dramatically decreases the impact of  
500 the end boundary conditions. Even when only considering the in-plane resistance ( $k_x$  and  $k_\phi$ )  
501 this restraint is enough to strongly restrict weak-axis bending and torsion. However, for longer  
502 lengths the major-axis bending becomes increasingly important to restrain the stud. The  
503 assumption of fixed-fixed end conditions and the noncomposite lower bound for  $k_y$  is again  
504 found to be a good predictor of the behavior. Pin-pin end conditions and only in-plane resistance  
505 (in essence the traditional model) is observed to be (a) a conservative predictor, and (b) one that  
506 reasonably follows the observed experimental trends.

507 Finally, the proposed design method (using DSM and employing fixed-fixed end conditions,  
508  $k_x$  and  $k_\phi$  in-plane restraint and the non composite  $k_y$  lower bound resistance) is compared to  
509 the tests and other currently available design methods. The test data compares well with the  
510 proposed method and the small differences between OSB-OSB, OSB-Gyp, and Gyp-Gyp are  
511 even reflected in the predicted strength, along with the relatively pronounced decrease as a  
512 function of length for the one-sided sheathing case: OSB-Bare. The strength prediction is a

513 significant improvement over (a) ignoring the sheathing and end conditions (labeled AISI-S100-  
514 07 in Figure 14), (b) the diaphragm stiffness model used from 1980-2004 (labeled AISI-S100-01  
515 in sheathing as Figure 14), and (c) the empirically simplified variation on the local stiffness  
516 approach adopted in 2004 (labeled AISI-S210-07 in Figure 14).

## 517 **7.2 Fastener Demands**

518 In all of the completed axial testing, member failure (not fastener failure) was the first  
519 observed limit state: flexural-torsional for tests without sheathing or one-sided sheathing, and  
520 local buckling for tests with sheathing on both flanges. In the post-peak collapse regime both  
521 local bearing failures in the sheathing and pull-through of the fastener through the sheathing are  
522 observed. The fastener demands due to global buckling, including those deriving from one-sided  
523 sheathing or dis-similar sheathing, may be predicted from an analytical method as provided in  
524 the Appendix. The method is dependent on the ratio of the axial load to the buckling load, the  
525 size of imperfection, and the mode shape itself. The method can readily be extended to FSM  
526 solutions as well (the FSM mode shapes and  $P_{cre}$  replace the analytical solution).

527 An extensive study of fastener demand using detailed shell finite element models of the stud,  
528 track, and sheathing, and discrete springs for the fasteners is provided in Vieira (2011). In global  
529 buckling fastener forces predicted by the analytical method agree reasonably well with the more  
530 detailed finite element model. The finite element model also provides fastener demands that  
531 develop due to local buckling and accumulation of fastener forces. These final two points  
532 warrant further study, but it is worth recalling that in the 2.4 m x 2.4 m (8 ft x 8 ft) CFS wall  
533 studied here fastener (and related) limit states did not control.

534        **7.3 Discussion**

535        Both practical and research work remains related to the design of axially loaded sheathed  
536 CFS studs. Development or augmentation of formal test standards for  $k_{x\ell}$ ,  $k_y$ , and  $k_{ec}$  are needed.  
537 Formal code-approved interfaces for the use of  $EI$  and  $G$  for gypsum board, plywood, oriented  
538 strand board and other sheathing materials are needed. The lower bound expressions provided  
539 herein for stiffness need adoption by the AISI Specification. The appropriate selection of end  
540 boundary conditions for imperfect bearing surfaces needs further study, as the analysis here  
541 shows that fixed end boundary conditions are possible against steel surfaces. Though preliminary  
542 work is complete formal methods are needed in the AISI Specification for predicting all fastener  
543 demands and for predicting capacities for various sheathing materials (particularly, bearing and  
544 pull-through). Extensions are possible, and needed, for (a) systems that use both steel bridging  
545 and sheathing to brace studs; (b) to account for brace force accumulation, and (c) for beam-  
546 columns where fastener demands to resist direction torsion can be much greater than those  
547 observed here for axial loads alone.

548        **8 CONCLUSIONS**

549        Studs of load bearing cold-formed steel framed walls may be adequately braced by sheathing.  
550        Characterization of the sheathing-bracing requires careful consideration of local fastener  
551 deformations and global sheathing deformations. This insight of the dual sources (local and  
552 global) for sheathing-bracing leads to a unification of proposed analytical and design methods  
553 which focused exclusively on either local fastener deformations (Winter's method) or global  
554 deformations (shear diaphragm method). Analytical formulae are provided for characterizing the  
555 stiffness of sheathing-bracing and may be augmented by material and small-scale fastener tests  
556 for greater accuracy as described herein. With the correct stiffness of the sheathing-bracing

557 established local, distortional, and global buckling of the sheathing-braced studs may be readily  
558 predicted; including cases of one-sided or dis-similar sheathing, in addition to studs with similar  
559 sheathing attached to the two stud flanges. Both computational and analytical methods are  
560 provided for the elastic buckling determination and specific guidance is provided for  
561 appropriately including the sheathing-bracing springs in each of the local, distortional, and global  
562 buckling modes. It is proposed to use the sheathing-braced elastic buckling values in design, and  
563 both Direct Strength and Effective Width procedures for doing so are detailed. A series of full-  
564 scale tests on 2.4 m x 2.4 m (8 ft x 8 ft) cold-formed steel framed walls with combinations of  
565 oriented strand board, gypsum board, and no sheathing were tested to failure in axial  
566 compression. All tests with sheathing attached to both stud flanges (oriented strand board,  
567 gypsum, or a combination of the two) failed in local buckling. Tests with sheathing on one side  
568 only, failed in a dramatic restrained-axis flexural-torsional buckling mode. Comparison of the  
569 tested capacities with the proposed design method demonstrates good agreement across the  
570 member lengths and sheathing conditions studied. Further, the proposed method is a significant  
571 improvement over existing and past Specification methods. Work remains to simplify the  
572 fastener demand predictions, explicitly incorporate brace force accumulation, and extend the  
573 approach to allow for discrete bridging and sheathing-bracing to both be included in the design –  
574 a highly desired feature for practice.

## 575 **9 ACKNOWLEDGMENTS**

576 For all their help in the lab acknowledgments are extended to Senior Instrument Designer  
577 Nickolay Logvinovsky and undergraduate researchers: Hannah Blum, Mo Alkyasi, Lauren  
578 Thompson, Linda Wan and Maggie Wildnauer. For providing materials and equipment thanks  
579 are also extended to the Steel Stud Manufacturers Association and Simpson Strong Tie. Finally,  
580 the American Iron and Steel Institute and the Steel Stud Manufactures Association are  
581 acknowledged for funding the research. Any opinions, findings, and conclusions or  
582 recommendations expressed in this material are those of the authors only and do not necessarily  
583 reflect the views of the sponsors, or material suppliers.

584

## 585 **10 REFERENCES**

- 586 [1] Vieira, L. C. M. J. (2011). "Behavior and Design of Sheathed Cold-Formed Steel Stud Walls  
587 under Compression." Doctor of Philosophy, Johns Hopkins University, Baltimore.
- 588 [2] AISI (1962). "Light Gage Cold-Formed Steel Design Manual." *American Iron and Steel*  
589 *Institute*.
- 590 [3] AISI (1980). "Light Gage Cold-Formed Steel Design Manual." *American Iron and Steel*  
591 *Institute*.
- 592 [4] AISI-S100 (2007). "North American Specification for the Design of Cold-Formed Steel  
593 Structural Members." *American Iron and Steel Institute*.
- 594 [5] AISI-S211 (2007). "North American Specification for the Design of Cold-Formed Steel  
595 Structural Members." *American Iron and Steel Institute*.
- 596 [6] Schafer, B. W., Iourio, O., and Vieira Jr, L. C. M. (2008). "Notes on AISI Design Methods  
597 for Sheathing Braced Design of Wall Studs in Compression." *A supplemental report for AISI-*  
598 *COFS Project on Sheathing Braced Design of Wall Studs*, The Johns Hopkins University,  
599 Baltimore.
- 600 [7] Green, G. G., Winter, G., and Cuykendall, T. R. (1947). "Light Gage Steel Columns in Wall-  
601 braced Panels." *Cornell University Engineering Experiment Station*, 35, 1-50.
- 602 [8] Winter, G. (1960). "Lateral Bracing of Beams and Columns." *Journal of the Structural*  
603 *Division*.
- 604 [9] Simaan, A., and Pekoz, T. B. (1976). "Diaphragm Braced Members and Design of Wall  
605 Studs." *ASCE J Struct Div*, 102(1), 77-92.
- 606 [10] Miller, T. H., and Pekoz, T. (1993). "Behavior of cold-formed wall stud-assemblies."  
607 *Journal of structural engineering New York, N.Y.*, 119(2), 641-651.
- 608 [11] Trestain, T. (2002). "AISI Cold-Formed Steel Framing Design Guide CF02-1." American  
609 Iron and Steel Institute, Washigton D.C.

610 [12] Vieira, L. C. M. J., Shifferaw, Y., and Schafer, B. W. (2011). "Experiments on sheathed  
611 cold-formed steel studs in compression." *Journal of Constructional Steel Research*.

612 [13] AISI-S200 (2007). "North American Standard for Cold-Formed Steel Framing - General  
613 Provisions." *American Iron and Steel Institute*, AISI-S200-07.

614 [14] SSMA (2001). "Product Technical Information, ICBO ER-4943P." S. S. M. Association, ed.

615 [15] Vieira, L. C. M. J., and Schafer, B. W. (2012). "Lateral Stiffness and Strength of Sheathing  
616 Braced Cold-Formed Steel Stud Walls." *Engineering Structures*(Accepted for Publication).

617 [16] Fiorino, L., Della Corte, G., and Landolfo, R. (2007). "Experimental tests on typical screw  
618 connections for cold-formed steel housing." *Engineering Structures*, 29(8), 1761-1773.

619 [17] Okasha, A. F. (2004). "Okasha, A.F., Performance of Steel Frame/Wood Sheathing Screw  
620 Connections  
621 Subjected to Monotonic and Cyclic Loading, 2004, McGill University." M.S., McGill  
622 University, Montreal.

623 [18] Chen, C. Y., Okasha, A. F., and Rogers, C. A. (2006). "Analytical Predictions Of Strength  
624 and Deflection Of Light Gauge Steel Frame/Wood Panel Shear Walls." *Advances in Engineering  
625 Structures, Mechanics & Construction*, 381-391.

626 [19] ASTM (2002a). "Standard Test Method for Structural Panels in Shear Through-the-  
627 Thickness." *ASTM D2719-89*, American Society for Testing and Materials, West Conshohocken,  
628 PA.

629 [20] NDS (2005). "National Design Specification (NDS) for Wood Construction, ANSI/AF&PA  
630 NDS." A. F. a. P. Association, ed. Washington, DC.

631 [21] APA-D510C (2008). "Panel Design Specification." A.-T. e. W. Association, ed. Tacoma,  
632 Washington, USA.

633 [22] GA-235-10 (2010). "Gypsum Board Typical Mechanical and Physical Properties." Gypsum  
634 Association, Hyattsville, MD, USA.

635 [23] ASTM (2002b). "Standard Test Methods of Conducting Strength Tests of Panels for  
636 Building Construction." *E 72-98*, American Society for Testing and Materials, West  
637 Conshohocken, PA.

638 [24] Schafer, B. W., Vieira Jr, L. C. M., Sangre, R. H., and Guan, Y. (2010). "Rotational  
639 Restraint and Distortional Buckling in Cold-Formed Steel Framing Systems." *Revista Sul-  
640 Americana de Engenharia Estrutural (South American Journal of Structural Engineering)*, 7(1),  
641 71-90.

642 [25] AISI-TS-1-02 (2002). "Rotational-Lateral Stiffness Test Method for Beam-to-Panel  
643 Assemblies." *AISI Cold-Formed Steel Design Manual*.

644 [26] Schafer, B. W., and Adany, S. "Buckling analysis of cold-formed steel members using  
645 CUFSM: Conventional and constrained finite strip methods." *Proc., Eighteenth International  
646 Specialty Conference on Cold-Formed Steel Structures: Recent Research and Developments in  
647 Cold-Formed Steel Design and Construction*, 39-54.

648 [27] Iourio, O., and Schafer, B. W. (2008). "FE modeling of elastic buckling of stud walls."  
649 *research report to American Iron and Steel Institute*, Johns Hopkins University, Baltimore, MD,  
650 42.

651 [28] Li, Z., and Schafer, B. W. "Buckling analysis of cold-formed steel members with general  
652 boundary conditions using CUFSM: conventional and constrained finite strip methods." *Proc.,  
653 Twentieth International Specialty Conference on Cold-Formed Steel Structures*.

654 [29] Li, Z., and Schafer, B. W. (2011). "Local and Distortional Elastic Buckling Loads and  
655 Moments for SSMA Stud Sections." *Cold-Formed Steel Engineers Institute*, 5.

656 [30] Schafer, B. W. (2006). "Direct Strength Method Design Guide." American Iron and Steel  
657 Institute, Washington, D.C., 171.

658 [31] Moen, C. D. (2008). "Direct strength design for cold-formed steel members with  
659 perforations." Ph.D., Johns Hopkins University, Baltimore, MD USA.

660 [32] Li, Z., and Schafer, B. W. (2010b). "Application of the finite strip method in cold-formed  
661 steel member design." *Journal of Constructional Steel Research*, 66(8-9), 971-980.

662 [33] Schafer, B. W. (2008). "Design Aids and Examples for Distortional Buckling." *Tech Note*,  
663 Cold-Formed Steel Engineers Institute, 22.

664 [34] Timoshenko, S. P., Gere, James M. (1961). *Theory of Elastic Stability*, McGraw-Hill, New  
665 York.

666 [35] Zeinoddini, V. M., and Schafer, B. W. (2011). "Global Imperfections and Dimensional  
667 Variations in Cold-Formed Steel Members." *International Journal of Structural Stability and*  
668 *Dynamics*, (Accepted 2011).

669  
670



671 **11 GLOSSARY OF VARIABLES**

672 See Figure 15 for axis definition

673

674  $k_{x\ell}$  = local (fastener) translational stiffness in  $x$

675  $k_{xd}$  = lateral diaphragm stiffness in  $x$

676  $k_x$  = discrete lateral fastener-sheathing stiffness in  $x$

677  $k_{fx}$  = foundation lateral fastener-sheathing stiffness in  $x$

678  $k_y$  = discrete lateral fastener-sheathing stiffness in  $y$

679  $k_{fy}$  = foundation lateral fastener-sheathing stiffness in  $y$

680  $k_{rc}$  = local rotational fastener (connector) stiffness in the  $x$ - $y$  plane

681  $k_{rw}$  = sheathing rotational stiffness in the  $x$ - $y$  plane

682  $k_r$  = discrete rotational fastener-sheathing stiffness in the  $x$ - $y$  plane

683  $k_{rf}$  = foundation rotational fastener-sheathing stiffness in the  $x$ - $y$  plane

684  $h_{xi}$  =  $x$ -distance from centroid to spring  $i$

685  $h_{yi}$  =  $y$ -distance from centroid to spring  $i$

686  $h_{xs}$  =  $x$ -distance from shear center to spring  $i$

687  $h_{ysi}$  =  $y$ -distance from shear center to spring  $i$

688  $I_o$  = polar moment of inertia of stud ( $I_o = I_x + I_y + A(x_o^2 + y_o^2)$ )

689  $A$  = cross-sectional area of the stud

690  $E$  = Young's modulus of steel

691  $E_w$  = Young's modulus of sheathing

692  $G$  = Shear modulus of sheathing

693  $J$  = St. Venant Torsional Constant of stud

694  $I_x$  = Moment of inertia about  $x$ -axis of stud

695  $I_y$  = Moment of inertia about  $y$ -axis of stud

696  $C_w$  = Warping constant of stud

697  $x_o$  =  $x$  distance from centroid to shear center

698  $y_o$  =  $y$  distance from centroid to shear center

699  $K_x$  = effective length about  $x$ -axis

700  $K_y$  = effective length about  $y$ -axis

701  $K_t$  = effective length in torsion about shear center

702  $K_{x,spring}$  = effective length for the spring foundation about  $x$ -axis

703  $K_{y,spring}$  = effective length for the spring foundation about  $y$ -axis

704  $K_{t,spring}$  = effective length in torsion for the spring foundation about shear center

705  $d$  = fastener diameter

706  $t$  = flange thickness

707  $t_{board}$  = board or sheathing thickness

708  $w_{tf}$  = fastener tributary width

709  $d_f$  = distance between fasteners

710  $L$  = sheathing height

711  $(EI)_w$  = sheathing rigidity per APA-D510C (APA-D510C 2008) for OSB and plywood sheathing,

712 and GA-235-10 (GA-235-10 2010) for gypsum sheathing (for fully composite action  $(EI)_{wc}$

713 replaces  $(EI)_w$ )

714  $(EI)_{wpc}$  = sheathing bending rigidity for partially composite action

715  $(EI)_{system}$  = strong-axis bending rigidity of the composite stud-sheathing system found from the  
 716 results of ASTM-E72 tests  
 717  $h$  = out-to-out depth of the stud  
 718  $H$  = concentrated load applied perpendicular to the wall for composite action testing  
 719  $L$  = stud length or height of the wall  
 720  $w$  = uniform load perpendicular to the wall for composite action testing  
 721  $\delta$  = maximum measured displacement at mid-height for the respective loading case ( $H$  or  $w$ )  
 722  $P$  = axial reference load in buckling analysis  
 723  $P_{cr\ell}$  = local elastic buckling load  
 724  $P_{crd}$  = distortional elastic buckling load  
 725  $P_{cre}$  = global elastic buckling load  
 726  $P_y$  = squash load  
 727  $P_n$  = nominal strength  
 728  $P_{ne}$  = global strength  
 729  $P_{n\ell}$  = local strength  
 730  $P_{nd}$  = distortional strength  
 731  $P_{crx}$  = global elastic buckling load in  $x$   
 732  $P_{cry}$  = global elastic buckling load in  $y$   
 733  $P_{cr\phi}$  = torsional elastic buckling load about shear center  
 734  $\lambda_c$  = column non-dimensional slenderness  
 735  $A_e$  = effective area  
 736  $P_{nC4.1}$  = local buckling strength, found in C4.1 of the main Specification of AISI-S100  
 737  $P_{nC4.2}$  = distortional buckling strength, found in C4.2 of the main Specification of AISI-S100  
 738  $F_n$  = nominal stress (long column) =  $P_{ne}/A_g$   
 739  $K_e$  = elastic stiffness matrix  
 740  $\lambda$  = eigenvalue  
 741  $K_g$  = geometric stiffness matrix  
 742  $\Phi$  = eigenvector  
 743  $P_{crj}$  = buckling loads for the buckling modes ( $j=1, 2, 3$ )  
 744  $\lambda_j$  = eigenvalues for the buckling modes ( $j=1, 2, 3$ )  
 745  $u_{crj}$  = eigenvector in the  $x$  direction for the buckling modes ( $j=1, 2, 3$ )  
 746  $v_{crj}$  = eigenvector in the  $y$  direction for the buckling modes ( $j=1, 2, 3$ )  
 747  $\phi_{crj}$  = eigenvector on the plane  $x$ - $y$  for the buckling modes ( $j=1, 2, 3$ )  
 748  $u_\lambda$  = buckling mode shape along the length in the  $x$  direction  
 749  $v_\lambda$  = buckling mode shape along the length in the  $y$  direction  
 750  $\phi_\lambda$  = buckling mode shape along the length in the  $x$ - $y$  plane  
 751  $u_0$  = mid-height bow  
 752  $v_0$  = mid-height camber  
 753  $\phi_0$  = mid-height twist  
 754  $u_{imp}$  = initial imperfection shape along the length in the  $x$  direction  
 755  $v_{imp}$  = initial imperfection shape along the length in the  $y$  direction  
 756  $\phi_{imp}$  = initial imperfection shape along the length in the  $x$ - $y$  plane  
 757  $\beta_j$  = amplification of deflection for any buckling mode ( $j=1, 2, 3$ )  
 758  $\delta_{xi}$  = amplification of the deformation in the  $x$  direction at fastener location  $i$  at the mid-height  
 759  $\delta_{yi}$  = amplification of the deformation in the  $y$  direction at fastener location  $i$  at the mid-height

- 760  $\phi_{xyi}$  = amplification of the twist in the  $x$ - $y$  plane at fastener location  $i$  at the mid-height  
761  $u_i$  = deformation along the length in the  $x$  direction at fastener location  $i$   
762  $v_i$  = deformation along the length in the  $y$  direction at fastener location  $i$   
763  $\phi_i$  = twist along the length in the plane  $x$ - $y$  at fastener location  $i$

764 **12 APPENDIX: GLOBAL BUCKLING AND FASTENER DEMANDS**

765 The following provides an extension to Timoshenko (1961) Article 5.6. Consider the stability  
 766 of an axially loaded member with an arbitrary number of  $k_{xi}$ ,  $k_{yi}$ ,  $k_{\phi i}$  foundation springs attached at  
 767 location  $i$  in the cross-section as depicted in Figure 15. The axial stability is an eigen problem:

$$(K_e - \lambda K_g) \Phi = 0 \tag{A1}$$

768 where the elastic stiffness including the contribution from the foundation springs is:

769

$$K_e = \begin{bmatrix} P_{cry} + \frac{(K_{y,spring}L)^2}{m^2\pi^2} \sum_{i=1}^n k_{xi} & 0 & \frac{(K_{y,spring}L)^2}{m^2\pi^2} \sum_{i=1}^n k_{xi} h_{ysi} \\ P_{crx} + \frac{(K_{x,spring}L)^2}{m^2\pi^2} \sum_{i=1}^n k_{yi} & -\frac{(K_{x,spring}L)^2}{m^2\pi^2} \sum_{i=1}^n k_{yi} h_{xsi} & \\ sym & \frac{I_0}{A} P_{cr\phi} + \frac{(K_{t,spring}L)^2}{m^2\pi^2} \sum_{i=1}^n k_{xi} (h_{ysi})^2 + \frac{(K_{t,spring}L)^2}{m^2\pi^2} \sum_{i=1}^n k_{yi} (h_{xsi})^2 + \frac{(K_{t,spring}L)^2}{m^2\pi^2} \sum_{i=1}^n k_{\phi i} \end{bmatrix} \tag{A2}$$

770

$$P_{crx} = \frac{m^2\pi^2 EI_x}{(K_x L)^2}, \quad P_{cry} = \frac{m^2\pi^2 EI_y}{(K_y L)^2}, \quad \text{and} \quad P_{cr\phi} = \frac{A}{I_0} \left( GJ + \frac{m^2\pi^2 EC_w}{(K_t L)^2} \right)$$

771 Further, the geometric stiffness under reference load  $P$  is:

$$K_g = P \begin{bmatrix} 1 & 0 & y_o \\ & 1 & -x_o \\ sym & & \frac{I_0}{A} \end{bmatrix} \tag{A3}$$

772 The three buckling loads  $P_{cr1}$ ,  $P_{cr2}$ ,  $P_{cr3}$  are found from the eigenvalues ( $\lambda$ 's) as follows:

$$\begin{bmatrix} P_{cr1} & 0 & 0 \\ 0 & P_{cr2} & 0 \\ 0 & 0 & P_{cr3} \end{bmatrix} = \begin{bmatrix} \lambda_1 & 0 & 0 \\ 0 & \lambda_2 & 0 \\ 0 & 0 & \lambda_3 \end{bmatrix} P \tag{A4}$$

773 and the buckling modes from the eigenvectors (columns of  $\Phi$ ):

$$\Phi = \left[ \begin{array}{c} \left\{ \begin{array}{c} u_{cr1} \\ v_{cr1} \\ \phi_{cr1} \end{array} \right\} \\ \left\{ \begin{array}{c} u_{cr2} \\ v_{cr2} \\ \phi_{cr2} \end{array} \right\} \\ \left\{ \begin{array}{c} u_{cr3} \\ v_{cr3} \\ \phi_{cr3} \end{array} \right\} \end{array} \right] \tag{A5}$$

774 Note, for convenience the columns of  $\Phi$  are normalized such that  $\sqrt{u_{cr}^2 + v_{cr}^2 + \phi_{cr}^2} = 1$ . The  
 775 buckling mode shape along the length is defined as:

$$u_\lambda = u_{cr} \sin(\pi z / L), v_\lambda = v_{cr} \sin(\pi z / L), \text{ and } \phi_\lambda = \phi_{cr} \sin(\pi z / L) \quad (\text{A6})$$

776  
 777 Global initial imperfections may be defined based on the mid-height bow ( $u_o$ ) camber ( $v_o$ )  
 778 and twist ( $\phi_o$ ) imperfections:

$$u_{imp} = u_o \sin(\pi z / L), v_{imp} = v_o \sin(\pi z / L), \text{ and } \phi_{imp} = \phi_o \sin(\pi z / L) \quad (\text{A7})$$

779 statistics of measured global imperfections ( $u_o, v_o, \phi_o$ ) of CFS studs are available (Zeinoddini and  
 780 Schafer 2011). Amplification of deflection for any global mode ( $j = 1, 2, 3$ ) follows from

$$\beta_j = \frac{P / P_{crj}}{1 - P / P_{crj}} \quad (\text{A8})$$

781 Specifically, at fastener location  $i$  the mid-height deflection accounting for imperfections, the  
 782 three buckling modes, and the amplification of the deformations is:

$$\delta_{xi} = \sum_{j=1 \text{ to } 3} \beta_j (u_o u_{crj} + \phi_o h_{ysi} \phi_{crj}) \quad (\text{A9})$$

$$\delta_{yi} = \sum_{j=1 \text{ to } 3} \beta_j (\delta_{oy} v_{crj} + \phi_o h_{xsi} \phi_{crj}) \quad (\text{A10})$$

$$\phi_{xyi} = \sum_{j=1 \text{ to } 3} \beta_j (\phi_o \phi_{crj}) \quad (\text{A11})$$

783 and along the length at fastener location  $i$  the deformations are:

$$u_i = \delta_{xi} \sin(\pi z / L), v_i = \delta_{yi} \sin(\pi z / L), \text{ and } \phi_i = \phi_{xyi} \sin(\pi z / L) \quad (\text{A12})$$

784 These displacements may be multiplied times fastener-sheathing stiffness  $k_x, k_y, k_\phi$  at any fastener  
 785 location to determine predicted fastener forces. Given the nature of the deformed shapes, mid-  
 786 height forces typically control.

787 TABLES

788 Table 1 – Condensed summary of test results (ascending order of mean peak load)

Test #	Sheathing		Limit State <sup>1</sup>	Wall Tests Peak Load				Single Stud Tests <sup>2</sup> Peak Load (kN)
	Front	Back		Total (kN)	per stud (kN)	per stud mean	per stud CoV	
2	Bare	Bare	FT and F	250.6	50.1	50.1	-	57.1
12	OSB	Bare	FT	362.8	72.6			
1	OSB	Bare	FT	396.8	79.4			
6	OSB	Bare	FT	410.2	82.0	78.0	0.063	69.6
7	Gyp	Gyp	L	418.4	83.7			
11	Gyp	Gyp	L	429.9	86.0			
4	Gyp	Gyp	L	437.9	87.6	85.7	0.023	95.1
10	OSB	Gyp	L	458.4	91.7			
3	OSB	Gyp	L	470.2	94.0			
8	OSB	Gyp	L	471.4	94.3	93.3	0.015	99.9
5	OSB	OSB	L	471.7	94.3			
9	OSB	OSB	L	487.3	97.5	95.9	-	102.7

(1) Primary limit state observed at peak strength, FT=flexural-torsional, F=weak-axis flexural, L=local buckling

(2) Single stud tests 2.44 m (8 ft) in length as reported in Vieira and Schafer (2011)

789  
790

791

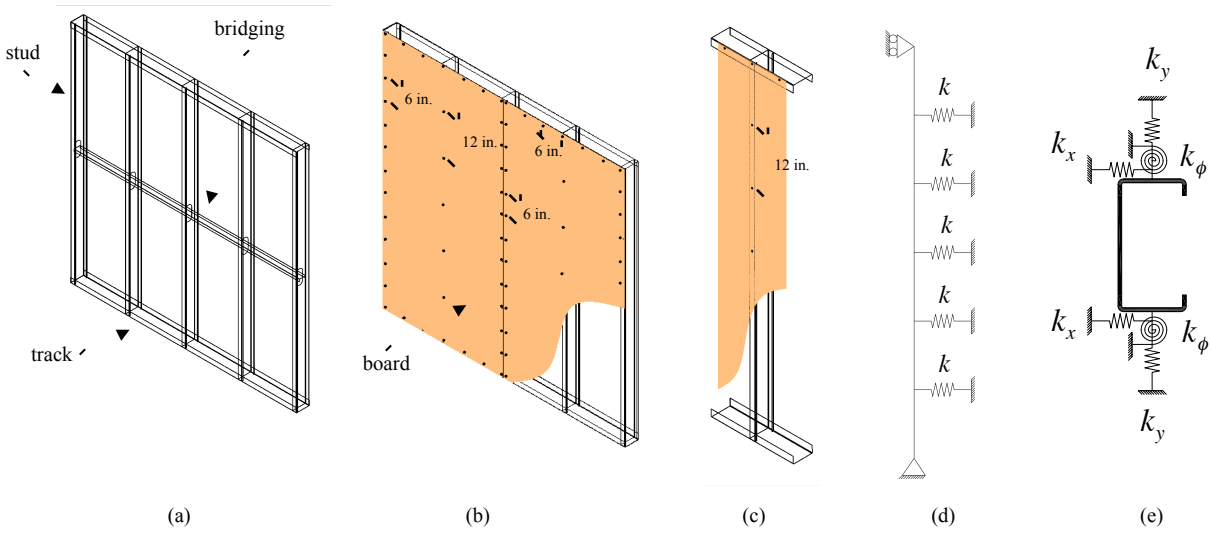
792 Table 2 – Spring foundation stiffness and properties considered

Sheathing Material	$k_x$ (N/mm/mm)	$k_y$ -fully composite (N/mm/mm)	$k_y$ -non-composite (N/mm/mm)	$k_s$ (kN.mm/mm/rad)
OSB	3.185	0.3172	0.001227	0.313
Gypsum	1.172	0.0579	0.000284	0.315

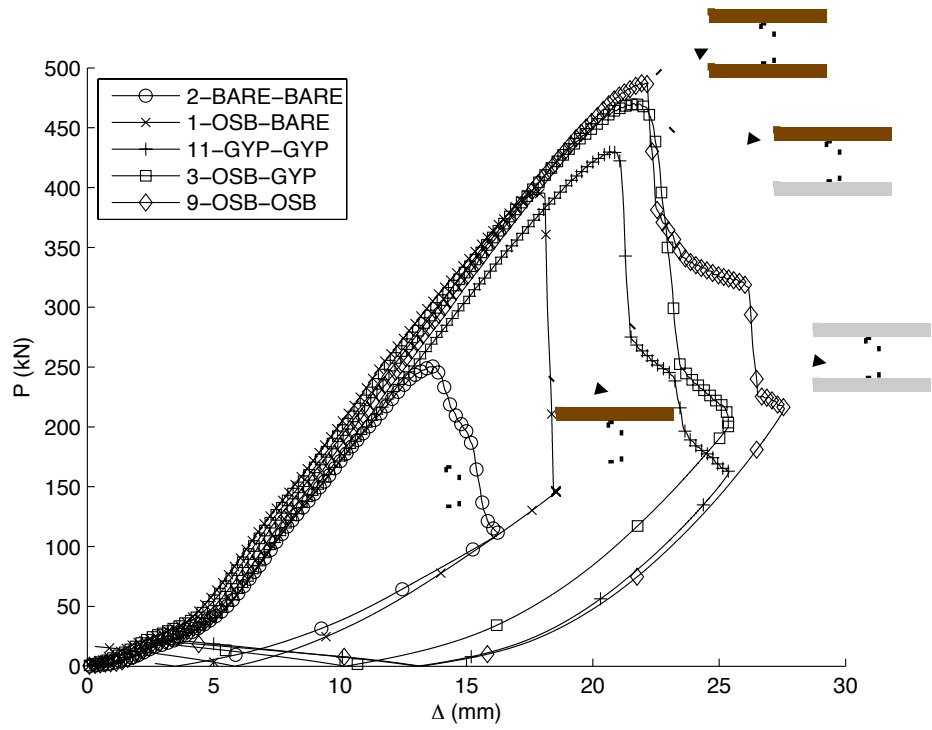
793  $k_x - t_{board} = 1.11$  cm,  $w_{tf} = 61$  cm,  $d_f = 30.5$  cm,  $L = 244$  cm, OSB – G = 1310  
794 MPa,  $k_{x\ell} = 1241$  N/mm,  $k_{xd} = 4490$  N/mm, Gyp – G = 552 MPa,  $k_{x\ell} = 426$  N/mm,  
795  $k_{xd} = 2147$  N/mm  
796  $k_y - b_w = 92$  mm, OSB –  $(EI)_{w-parallel} = 736$  N.m<sup>2</sup>/m, Gyp – E = 993 MPa  
797  $k_y$  – laboratory test  
798  
799

800

801



803  
 804 Figure 1 – Cold-formed steel walls and bracing of the studs: (a) all steel wall, (b) sheathed wall,  
 805 (c) sheathed single stud, (d) schematic of stud with springs as bracing at fastener locations, (e)  
 806 detail of springs bracing the stud cross-section.  
 807



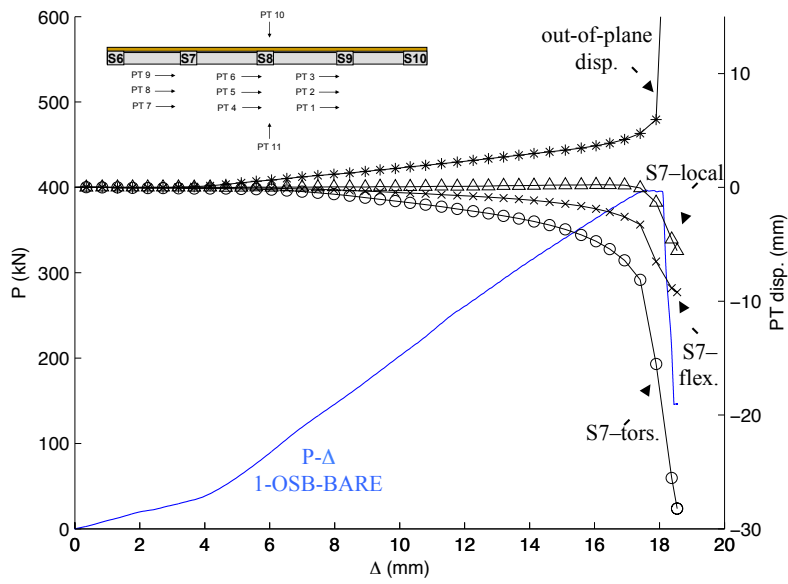
808  
 809 Figure 2 – P-Δ curve of full-scale walls comparing different sheathing combinations (note, Δ is  
 810 overall axial machine displacement, i.e. change in actuator position)



812  
813  
814  
815  
816  
817  
818

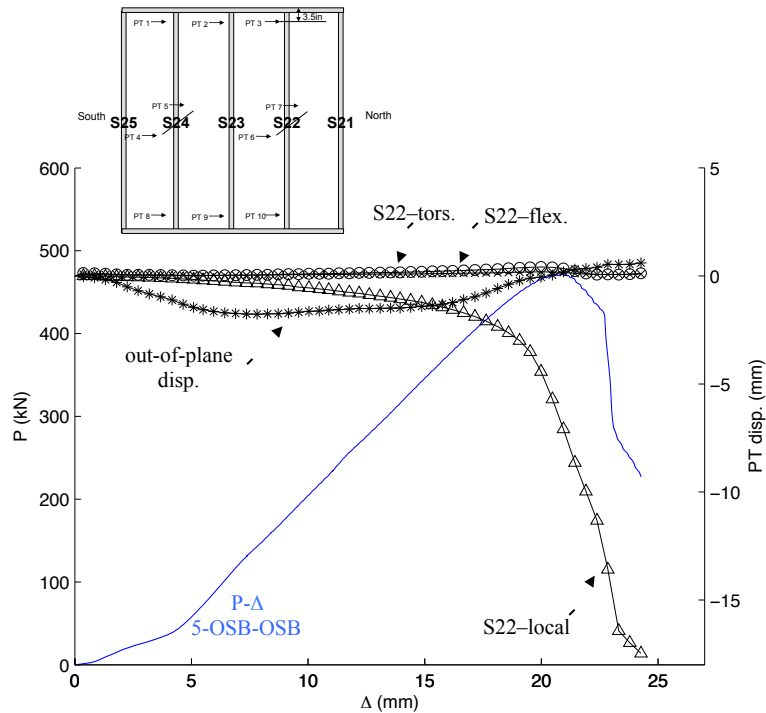
Figure 3 – Tests of sheathed cold-formed steel stud walls under compression: (a) side view of wall in MDOF testing rig before testing; (b) and (c) PT sensors for measuring stud deformations; (d) Gyp-Gyp wall opened after test to show local buckling at the ends; (e) local buckling tearing gypsum board; (f) flexural-torsional buckling of unsheathed Bare-Bare wall; local buckling (g) at the top of OSB-OSB wall, (h) at the bottom of OSB-Gyp wall, (i) followed by distortional buckling on Gyp-Gyp wall.





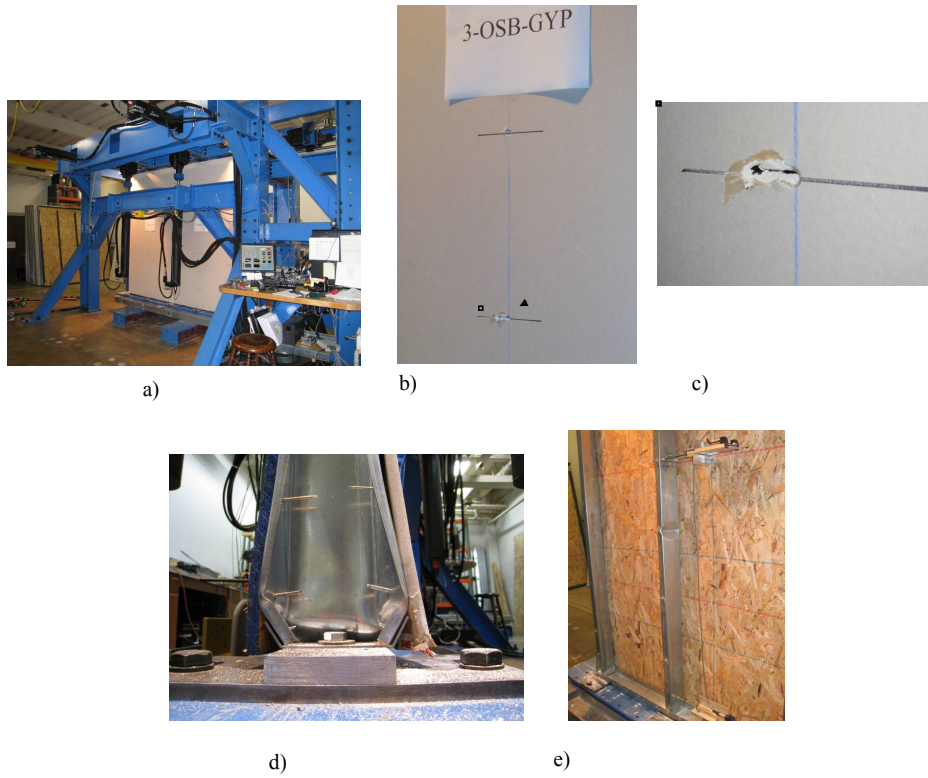
819

820 Figure 4 – Measured PT displacements and axial load vs. axial machine displacement for wall 1-  
 821 OSB-BARE, note dominance of torsion in response  
 822



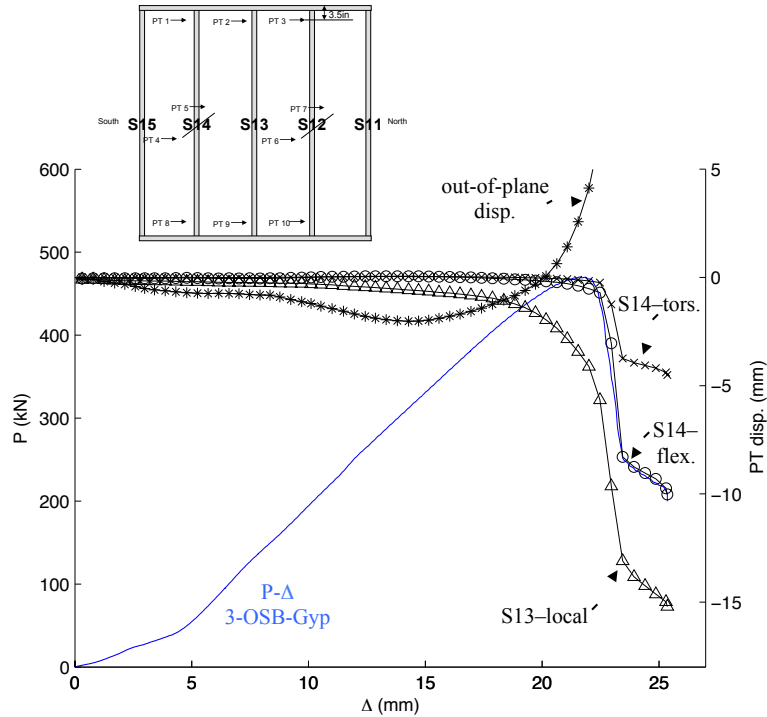
823

824 Figure 5 – Measured PT displacements and axial load vs. axial machine displacement for wall 5-  
 825 OSB-OSB, note dominance of local buckling in response  
 826



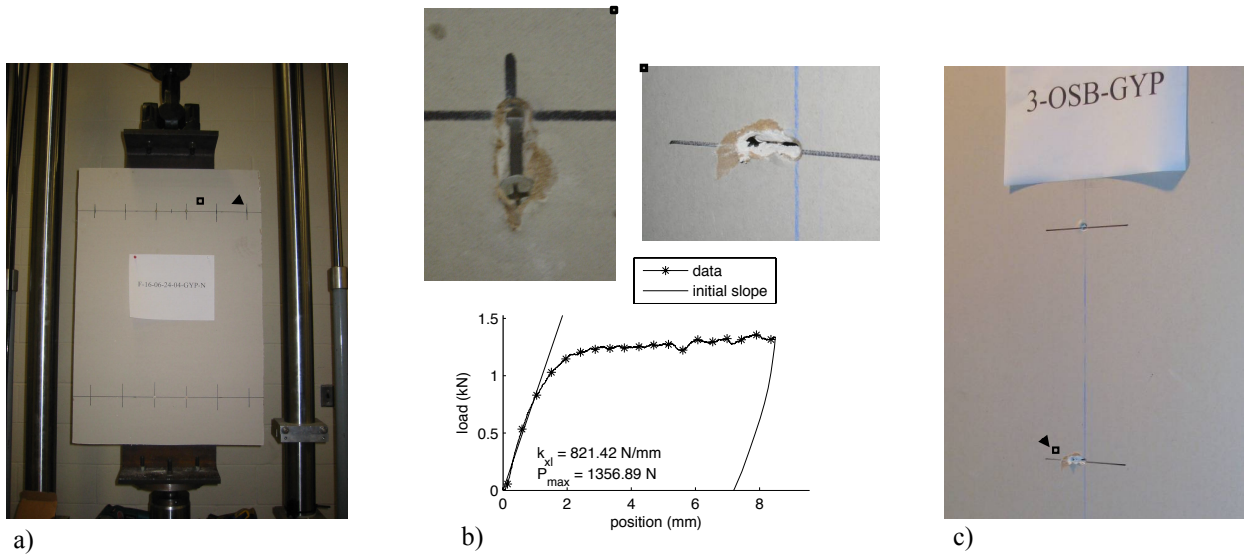
827

828 Figure 6 – Response of specimen 3-OSB-Gyp: (a) side view; (b) bearing failure / screw tearing  
829 out board; (c) close-up view of bearing failure; (d) local buckling; (e) wall opened after test.  
830



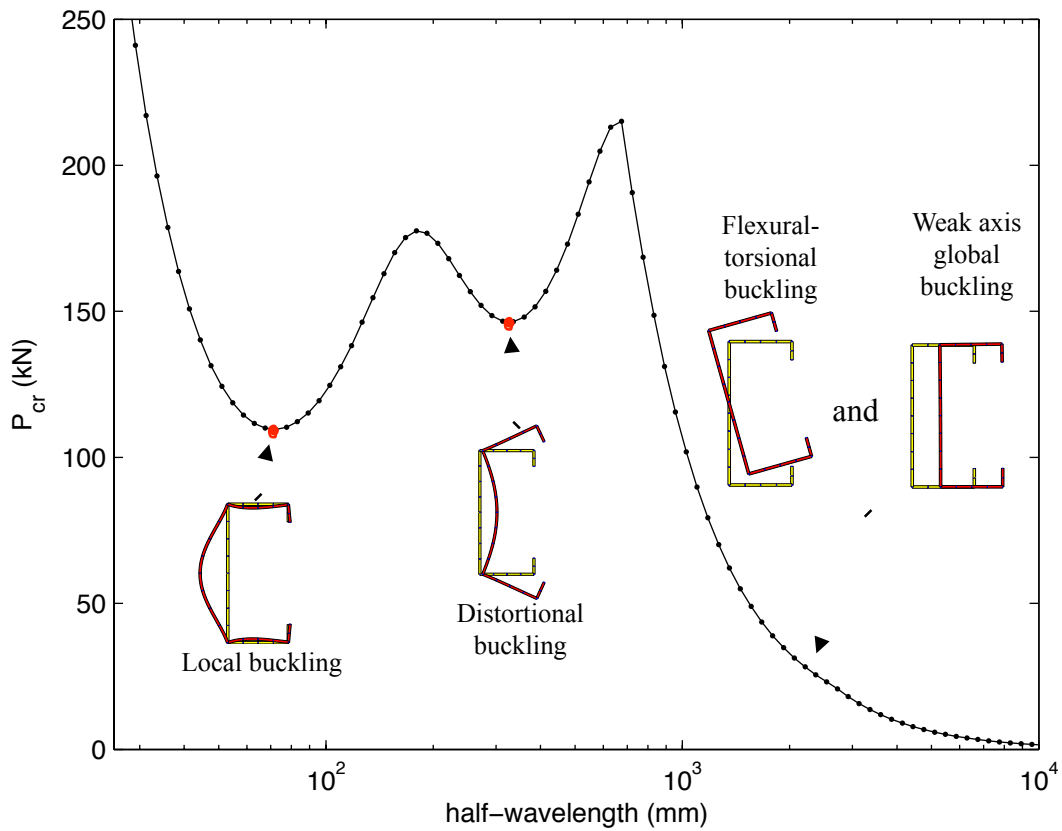
831

832 Figure 7 – Measured PT displacements and axial load vs. axial machine displacement for wall 3-  
 833 OSB-Gyp, note dominance of local buckling and presence of other modes  
 834



835

836 Figure 8 – Small scale test for local lateral stiffness: (a) test setup with gypsum sheathing, (b)  
 837 load-displacement response, local lateral stiffness (per fastener  $k_{x\ell} = 821.42/2 = 410.71\text{N/mm}$ ,  
 838 and peak load (per fastener  $P_{\max} = 1356.89/4 = 339.23\text{N}$ ), (c) similarity in bearing failure for full-  
 839 scale wall with dissimilar sheathing and small scale test for local lateral stiffness.  
 840

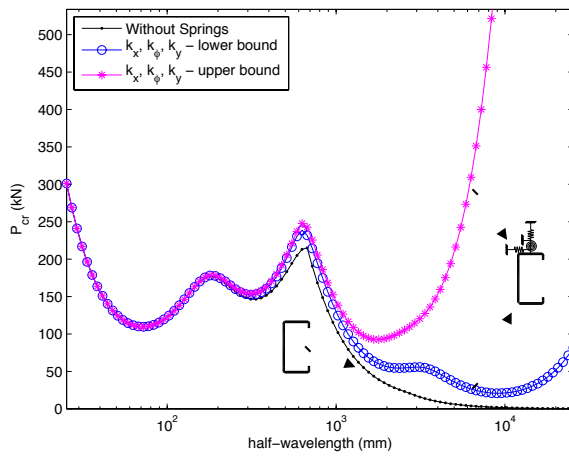


841

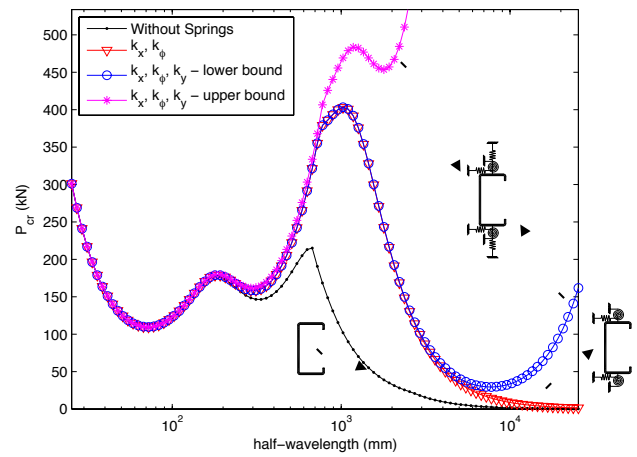
842 Figure 9– Buckling curve and modes for pin-pin, unrestrained 362S162-68 cross-section. (Note,  
 843 dimensions as cataloged (SSMA 2001) except thickness as measured: 1.665 mm (0.0655 in.)).  
 844

845

846



a)



b)

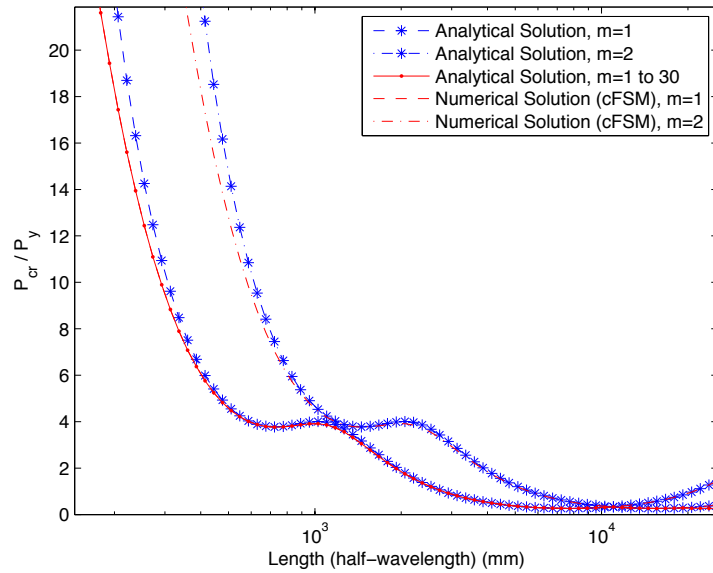
847

848 Figure 10 – Comparison of buckling curves for studs with bracing (spring) restraints: (a) springs  
 849 on one flange only (i.e., OSB-Bare); (b) springs on both flanges (OSB-OSB).  
 850

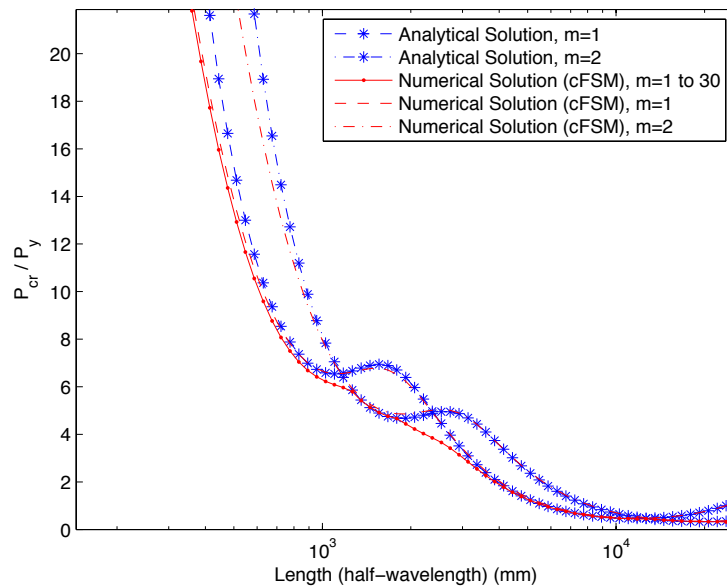
851

852

853

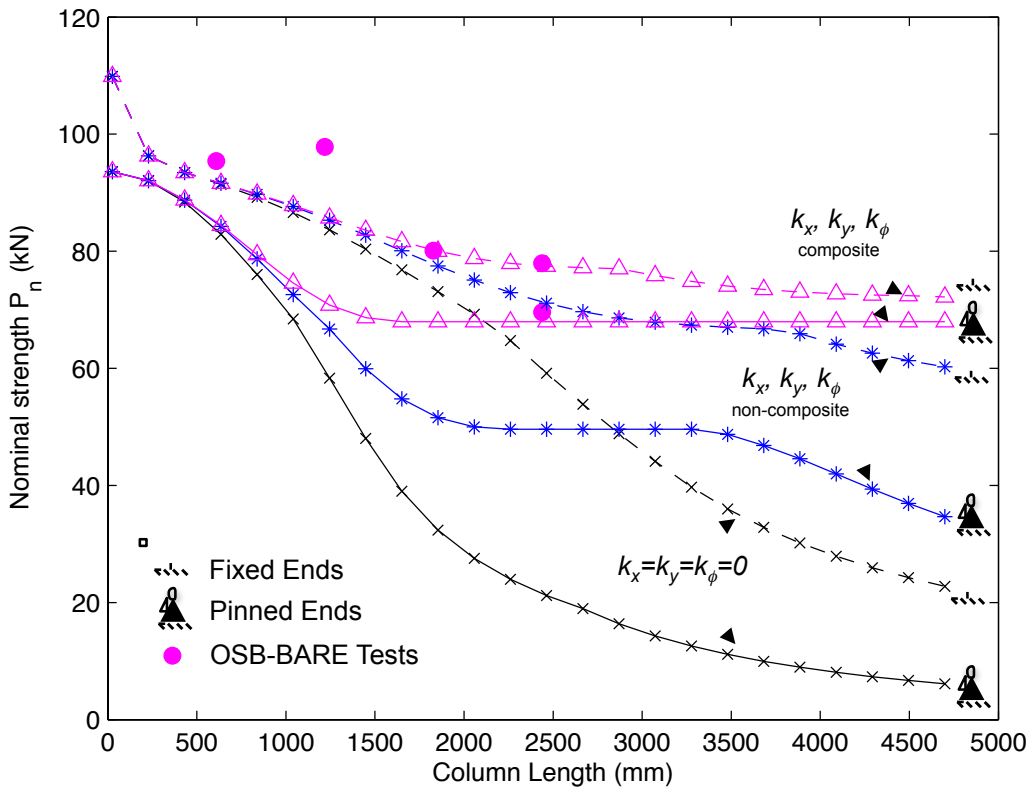


a)



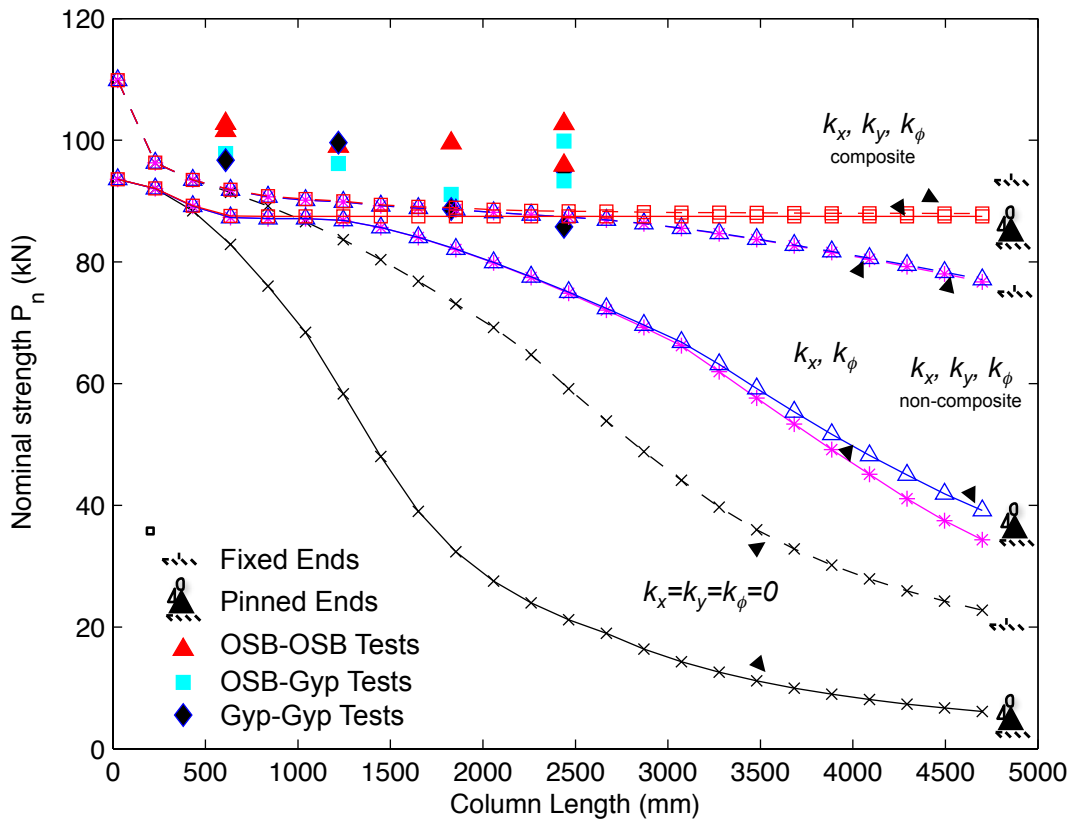
b)

855 Figure 11 – Comparison between numerical and analytical solution for global buckling of a  
 856 362S162-68 column with OSB-OSB springs (Table 2): (a) simply-supported boundary  
 857 conditions, (b) fixed-fixed boundary conditions ( $K_x=K_y=K_t=0.5$  for  $m=1$ ,  $K_x=K_y=K_t=0.7$  for  $m=2$ ,  
 858 and  $K_{x,spring}=K_{y,spring}=K_{t,spring}=\sqrt{3}/2=0.866$  for all  $m$ )



860

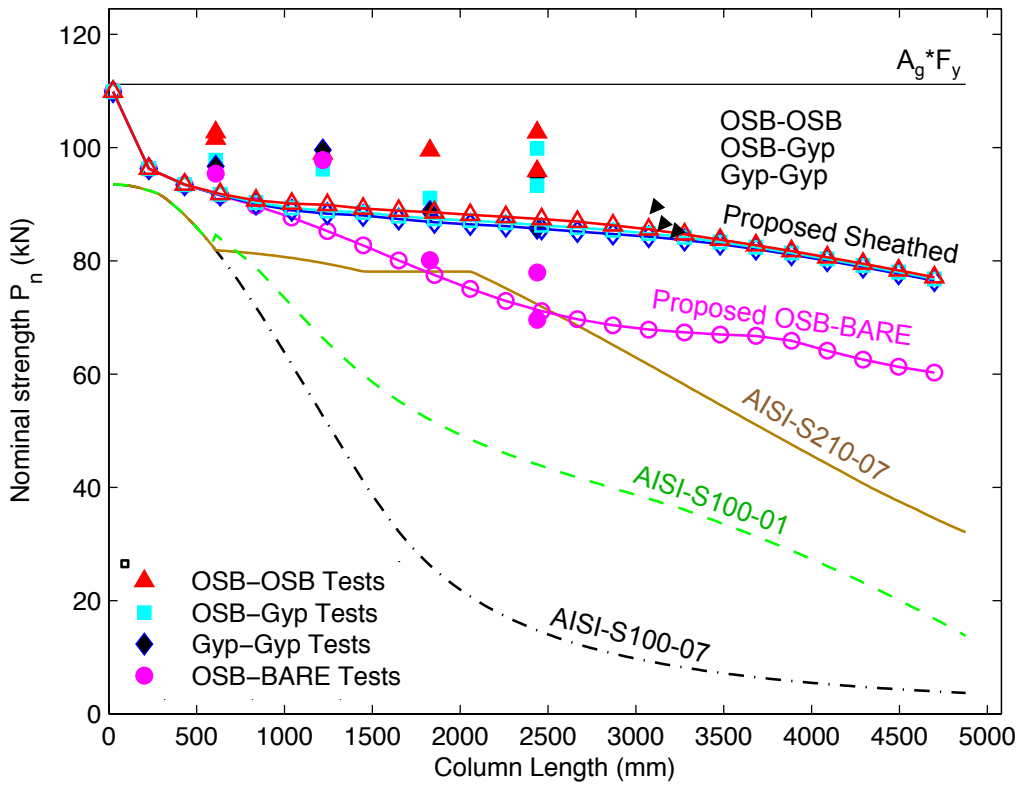
861 Figure 12 – Comparison of test results on one-sided (OSB-Bare) sheathed studs with proposed  
 862 design strengths as a function of end conditions and assumptions about bracing (spring) restraint  
 863 provided by the sheathing (i) ignored  $k_x=k_y=k_\phi=0$ , (ii) non-composite  $k_y$ , and (iii) composite  $k_y$   
 864



865

866 Figure 13 – Comparison of test results on two-sided (OSB-OSB, OSB-Gyp, Gyp-Gyp) sheathed  
 867 studs with proposed design strengths as a function of end conditions and assumptions about  
 868 bracing (spring) restraint provided by the sheathing (i) ignored  $k_x=k_y=k_\phi=0$ , (ii) in-plane only  $k_x$   
 869 and  $k_\phi$ , as appropriate, (iii) in-plane and non-composite  $k_y$ , and (iv) in-plane and composite  $k_y$   
 870  
 871



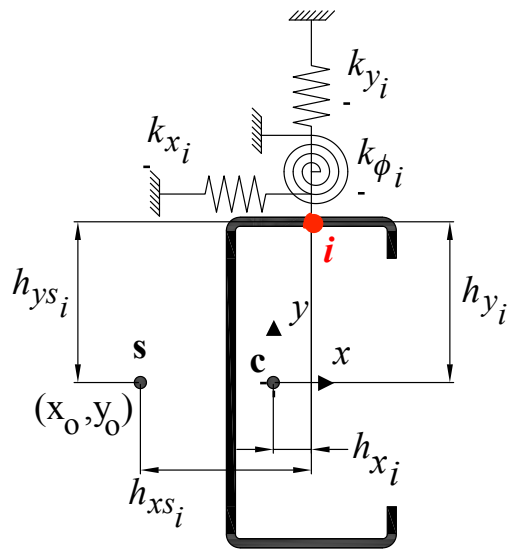


872

873

874

Figure 14 – Comparison of test results to former, current and proposed design methods



875

876

877

Figure 15 – Coordinate system and nomenclature for spring  $i$  on a stud

**Appendix: Peterman, K.D., Schafer, B.W. “Sheathed Cold-Formed Steel Studs Under Axial and Lateral Load.” Submitted to *Journal of Structural Engineering* (Submitted 2 January 2013).**

1  
2  
3  
4  
5  
6  
7  
8  
9  
10  
11  
12  
13  
14  
15  
16  
17  
18  
19  
20  
21  
22  
23  
24

## Sheathed Cold-Formed Steel Studs Under Axial and Lateral Load

K.D. Peterman<sup>1</sup>, B.W. Schafer<sup>2</sup>

1. Graduate Research Assistant, Department of Civil Engineering, Johns Hopkins University,  
Baltimore MD, USA <kdpeterman@gmail.com>

2. Professor and Chair, Department of Civil Engineering, Johns Hopkins  
University, Baltimore MD, USA <schafer@jhu.edu>

### Abstract

This research aims to identify and characterize the behavior of dissimilarly sheathed, load bearing, cold-formed steel studs under axial and lateral load. A series of tests on single studs, set in track, and sheathed with either oriented strand board, gypsum board, or combinations thereof are completed. The tests approximate the behavior of a sheathed stud, within a larger wall. In each test a pre-determined level of axial load (or displacement) is introduced into the stud and a lateral load is then applied until failure. This configuration results in axial load, bending, and (potentially) torsion on the stud. Observed failure modes for studs sheathed on only one face include torsion and/or fastener pull-through. For studs sheathed on both faces, failure modes include torsion, local buckling, fastener pull-through, and bearing (particularly for gypsum sheathed studs). Analysis of the torsional response indicates the important role of the sheathing in limiting torsion and in determining the demands on the member and fastener. The observed member limit states compared favorably with the Direct Strength Method of design even when direct torsion is not explicitly considered. New models for strength prediction in the connection limit states are explored. A model based on the torsional capacity of the fastener-sheathing system limited by first failure in either pull-through or bearing provides the best agreement with the observed testing. Recommendations for design are provided.

## 25 **Introduction**

26 Cold-formed steel (CFS) members are widely used in light-framed construction for both  
27 structural (load bearing) and non-structural members. Vertical CFS members (studs) are  
28 commonly capped in horizontal members (track) and sheathed in wood or gypsum board to  
29 frame the walls. For partition (non-structural) walls it is common practice to rely on the  
30 sheathing to provide bracing for the CFS studs. For structural walls, typically steel bridging  
31 running through holes in the studs provide the required flexural and torsional bracing. Recently,  
32 Vieira and Schafer (2012) explored the use of sheathing to supply bracing to structural studs and  
33 demonstrated that oriented strand board (OSB) or gypsum board can provide sufficient bracing  
34 to axially loaded studs. This research extends that work to sheathed walls with lateral as well as  
35 axial loads applied.

36 Research in the behavior of sheathed CFS stud walls under axial load originated with  
37 Winter (e.g., Green et al. 1947) and focused on determining the stiffness that sheathing could  
38 supply to a stud to restrict weak-axis flexural buckling. This work was followed by examinations  
39 of the role of sheathing shear stiffness (Simman and Pekoz 1976) and the use of gypsum and  
40 plaster board for bracing the studs (Miller and Pekoz 1993,1994, Lee and Miller 2001, Telue and  
41 Mahendran 2001). Vieira and Schafer (2013) demonstrated that sheathing supplies a local  
42 restraint (dominated by deformations at the fastener) and a shear diaphragm restraint (dominated  
43 by the shear modulus of the sheathing material) to the stud, and that if these restraints are  
44 properly incorporated into the elastic buckling analysis of the stud accurate strength predictions  
45 using the Direct Strength Method result.

46 Research on sheathed CFS structural stud walls under out-of-plane lateral load has seen  
47 relatively little study; however, the role of sheathing in restraining CFS floor joists has long been

48 studied (e.g., Winter 1960, Schafer et al. 2009) and is strongly related to the performance of  
49 walls under lateral load. Characterizing the stiffness of the sheathing as it fully or partially  
50 restrains torsion of the joist, due to the fact that in C-sections (e.g. studs or joists) the shear  
51 center and lateral load are not aligned, is the key issue in this previous work. Recent research on  
52 CFS stud walls under lateral load has been focused primarily on the unique problems associated  
53 with blast (Salim et al. 2005, Aviram et al. 2012) and is not the focus here. Work on CFS stud  
54 walls under combined axial and lateral load has seen limited study for a specialized CFS section  
55 (Pham et al. 2006), but no general methods developed. It is worth noting that extensive work has  
56 been conducted on in-plane laterally loaded walls, i.e., CFS sheathed shear walls, including  
57 combined axial and shear tests; however, this mode of behavior is not the focus of the work here.

58         This paper begins with an overview of the setup for the conducted experiments on  
59 sheathed CFS stud walls under axial and lateral load. This is followed by analysis of the  
60 experimental results focusing on the observed limit states and capacities, the member end  
61 conditions, and the lateral load application point. This is followed by torsional analysis of the  
62 assembly to determine the relative torsion between the stud and the fastener-sheathing system.  
63 Next, prediction methods for the member limit states and connector limit states are explored. In  
64 the case of connector limit states new methods are developed and compared to the experiments.  
65 The paper concludes with a discussion of extensions to distributed lateral loads, and a critical  
66 discussion of the developed method for design.

## 67 **Experimental Setup**

68 Consider an isolated, unsheathed (bare) stud, under axial and lateral load as depicted in Figure 1.  
69 The applied loads result in axial force, bending moment, shear, and direct torsion (due to lack of  
70 alignment between the lateral load and the shear center of the stud). Thus, although the applied

71 loads are relatively simple the resulting internal actions can be complicated. For typical end  
72 details and stud length, shear does not control and is thus not studied further here; instead, axial  
73 force, bending moment, and torsion are the focus.

74 Previous research on axially loaded stud walls demonstrated that tests on a single stud  
75 with a tributary width of attached sheathing and track provides the same capacities and limit  
76 states as tests on a full 2.4 x m 2.4 m [8 ft x 8 ft] wall with five studs (Vieira and Schafer 2013).  
77 Therefore, a single stud, with a tributary width of sheathing and track was employed for the  
78 combined axial plus lateral load tests conducted here. However, special attention was paid to the  
79 ends of the track and their connection to the testing rig as the track plays an important role in  
80 resisting the bending and torsion that results from the laterally applied load.

81 As illustrated in Figure 2, the test specimens consisted of a 2.4 m [96 in.] long 362S162-  
82 068 (AISI-S200 (2007) nomenclature) stud, with average dimensions and properties as reported  
83 in Table 1, connected to 0.6 m [24 in.] long 362T125-068 track at top and bottom. The track  
84 bears on three 19 mm [ $\frac{3}{4}$  in.] thick plates, 152 mm [6 in.] long, and 92 mm [3  $\frac{5}{8}$  in.] wide - the  
85 same width as the web of the track, thus insuring the sheathing cannot bear against the plates or  
86 testing rig. At mid-length the track is bolted to the 19 mm [ $\frac{3}{4}$  in.] plate with a 15.8 mm [ $\frac{5}{8}$  in.]  
87 bolt. The track ends are blocked and clamped over a 76 mm [3 in.] length between two 19 mm  
88 [ $\frac{3}{4}$  in.] plates to restrict twist.

89 The entire specimen is mounted in a multi degree of freedom wall testing rig (see Vieira  
90 2011 for full details). The top beam of the rig is actuated and provides axial load to the specimen.  
91 A 152 mm [6 in.] diameter circular bar is affixed to an actuator and supplies a mid-height lateral  
92 load on the specimen. Loading is performed in displacement control at a typical rate of 1.2  
93 mm/min [0.047 in./min] slower rates are used near peak capacity.

94           Where desired sheathing is attached to the stud and track as detailed in Figure 2b. The  
95 sheathing utilized includes 11 mm [7/16 in.] oriented strand board (24/16 rated, exposure 1), and  
96 12.7 mm [1/2 in.] gypsum board (sheetrock). The boards were stored in the laboratory with an  
97 average humidity of 56% and temperature of 22°C (71°F) over 102 days. Simpson Quikdrive  
98 No. 6 x 41 mm [1<sup>5</sup>/<sub>8</sub> in.] fasteners were used for attaching gypsum to the stud while Simpson  
99 Quikdrive No. 8 x 49 mm [1<sup>15</sup>/<sub>16</sub> in.] were used for attaching the oriented strand board (OSB).

100           Seven different sheathing combinations were tested: OSB-OSB (OO), gypsum-gypsum  
101 (GG), OSB-gypsum (OG), gypsum-OSB (GO), OSB-bare (OB), and bare-OSB (BO). In the  
102 nomenclature used herein, the second letter signifies the laterally loaded face of the specimen  
103 (e.g., a GO specimen is loaded on the OSB side). It should be noted that in specimens left bare  
104 (B) on the laterally loaded face, the lateral load is then applied directly to the stud.

105           Vieira et al. (2012) provide results for a similar specimen setup under axial load alone.  
106 Here we find the lateral load that causes failure given an applied axial load of 10%, 40%, 60%,  
107 or 80% of the axial-only capacity, for the seven different sheathing combinations. Complete  
108 details of the test setup including measured drawings of the end details, sensor locations and  
109 numbering, as-measured dimensions of all stud and track, imperfection measurements, etc. are  
110 provided in Peterman (2012).

## 111 **Experimental Results**

### 112 *Peak loads and limit states*

113 The tests were conducted by applying a pre-determined amount of axial load, and then increasing  
114 the lateral load until failure occurred. As the tests were typically conducted in displacement  
115 control the axial displacement (not load) was held constant during the lateral load application;

116 however in two tests the axial load was maintained. The difference in the two loading protocols  
117 and the resulting response is provided in Figure 3. Under lateral load the member shortens  
118 slightly and a constant axial displacement test results in a slowly decreasing axial force.  
119 Regardless of the selected protocol, a failure point, in terms of axial force and lateral force, is  
120 established for each specimen.

121 A summary of the tested capacities and observed limit states for the twenty-seven  
122 specimens is provided in Table 2 along with the previously conducted axial-only tests on  
123 similarly detailed specimens. The peak results are plotted in terms of lateral peak load vs. axial  
124 peak load for the seven different sheathing configurations in Figure 4. The presence of sheathing  
125 leads to a clear increase in capacity for all combinations of axial and lateral load, with bare (BB)  
126 and one-sided sheathed specimens (BO and OB) being the weakest. For the two-sided specimens  
127 with similar sheathing gypsum (GG) is considerably weaker than OSB (OO) and the difference is  
128 greatest in bending dominated (low axial load) cases. For the two-sided specimens with dis-  
129 similar sheathing it is superior to have the loaded face with OSB (GO) as opposed to the loaded  
130 face with gypsum (OG), and this difference is again greatest in bending dominated cases.

131 Examples of the limit states highlighted in Table 2 are provided in Figures 5 and 6.  
132 Figure 5 provides the member limit states: torsion for the bare and one-sided sheathed  
133 specimens, and local buckling (combined with yielding) for the OO and most of the GO and OG  
134 specimens. Figure 6 provides the connection limit states: pull-through for the fasteners on the  
135 laterally loaded face and bearing for the fasteners on the non-loaded face. Fastener limit states  
136 were particularly pronounced in the gypsum sheathed specimens (i.e., GG, GO, OG).



137 ***Member end conditions***

138 To accurately resolve the applied lateral load ( $H$ ) into moment in the specimen, it is  
139 necessary to characterize the end conditions for strong-axis bending. The intent of the detailing  
140 of the track end condition is to simulate a stud in a complete wall system and the expectation,  
141 after previously conducted axial testing (Vieira et al. 2012, Vieira and Schafer 2013), was that  
142 this would supply fixed ends. Although the intent was met and the authors believe the stud-to-  
143 track-to-sheathing end condition is close to field conditions, the expectation of fixed end  
144 conditions in strong-axis flexure was not met.

145 The measured horizontal force ( $H$ ) and mid-height displacement ( $\delta$ ) is compared against  
146 theoretical fixed, pinned, and semi-rigid solutions in Figure 7. For the semi-rigid end conditions  
147 the stud strong-axis rotational end restraint is provided by the torsional stiffness of the short  
148 segment of track with either warping free or warping fixed ends. The track is torsionally weak,  
149 with warping free end conditions for the track the mid-height moment is 99% of the pinned case,  
150 with warping fixed end conditions for the track the mid-height moment is 95% of the pinned  
151 case. As Figure 7 illustrates, for all practical purposes, due to the torsionally weak track, the  
152 boundary condition for major-axis bending of the stud is pinned.

153 ***Lateral load location***

154 As illustrated in Figure 8, load eccentricity from the shear center,  $e$ , changes as the stud  
155 twists. Experimental evidence based on scoring of the load bar against the specimen (Figure 8b)  
156 shows the point of load application moving from approximately mid-flange to the edge of the flat  
157 width of the flange as the twist progresses. As detailed in Figure 8c, for small but finite twist the  
158 distance from the shear center to the termination of the corner radius ( $e = 23.1$  mm [0.91 in.]) is  
159 utilized in this work. This  $e$  is an approximation. The exact  $e$  depends on the specific cross-

160 section and construction details; further, the cross-section does not remain rigid as it twists, and  
161 in addition the load application does not follow the twist of the stud, therefore the resulting  
162 eccentricity decreases as the stud twists. Nonetheless, an estimate of  $e$  is necessary for exploring  
163 the torsional demands.

#### 164 **Torsional Response and Analysis**

165 For an unsheathed (bare) stud loaded laterally (with  $H$ ) eccentric from the shear center  
166 (by a distance  $e$ ) the torsional demand ( $He$ ) is distributed as shown in Figure 1. Warping restraint  
167 provides the primary torsional resistance of the stud. This warping restraint creates additional  
168 longitudinal ( $\sigma_w$ ) and shear stresses in the cross-section. For a known bimoment ( $B$ ) these  
169 longitudinal warping stresses are found from:

$$170 \quad \sigma_w = B\omega / C_w \quad (1)$$

171 where  $\omega$  is the sectoral coordinates,  $C_w$  is the warping torsion constant, and  $B$  is the bimoment.  
172 The distribution of  $\sigma_w$  is proportional to  $\omega$  and is provided for the as-measured 362S162-68  
173 cross-section in Figure 9a. The distribution of  $\sigma_w$  is static, but scales with  $B$ , which may be  
174 determined from appropriate differentiation of the twist, or more generally is available in  
175 numerical beam finite element solutions.

176 For a sheathed stud it is typical in design to assume that the fastener-sheathing system  
177 will supply full torsional resistance to the stud. Thus, it is assumed that the stud does not twist,  
178 the bimoment is zero, and the fasteners carry the full torsional moment. However, in the  
179 experiments the studs experienced finite torsion (Peterman 2012 provides detailed  
180 measurements) most noticeably in the specimens sheathed on one-side only, but also in the two-  
181 sided sheathed specimens.

182 To assess the relative sharing in resisting the applied torsion a structural analysis model is  
183 created in MASTAN using 14 DOF beam finite elements capable of incorporating warping  
184 torsion (McGuire et al. 1999). The 362S162-68 stud is modeled as warping continuous along its  
185 height and warping fixed at its end. Rotational springs of stiffness  $k_\theta$  are included in the model  
186 every 305mm [12 in.] to simulate the fastener-sheathing restraint. A torque is applied at mid-  
187 height, and the resulting torsional moment diagram and torsion in the springs (fasteners) are  
188 summarized in Figure 10a-d as a function of the fastener-sheathing stiffness  $k_\theta$ . The limits are  
189 clear: for small  $k_\theta$  the stud twists significantly, develops a large bimoment (and related stresses)  
190 at mid-height, and sees little of the torsion carried by the springs (fasteners); for large  $k_\theta$  the stud  
191 twist is limited, the bimoment (and related stresses) are smaller, and the applied torsion is carried  
192 directly in the springs (fasteners). For realistic spring (fastener-sheathing) stiffness the behavior  
193 falls somewhere in between these ideal limits.

194 The member and fastener-sheathing attachments relevant for resisting torsion are  
195 summarized in Figure 9b and c. The primary resistance comes from bearing and the associated  
196 lateral springs  $k_{x1}$  and  $k_{x2}$ . Pull-through and its related torsional resistance is determined from a  
197 rotational restraint test, and  $k_{\phi1}$  and  $k_{\phi2}$  incorporate this resistance. The equivalent rotational  
198 spring,  $k_\theta$ , for the fastener-sheathing system is:

$$199 \quad k_\theta = k_{\phi1} + \frac{1}{4}k_{x1}d^2 + k_{\phi2} + \frac{1}{4}k_{x2}d^2 \quad (3)$$

200 The stiffness provided to the stud by the fastener-sheathing combinations are known from  
201 experiments: for OSB  $k_x = 971$  N/mm [5.52 kip/in.] and  $k_\phi = 95309$  N-mm/rad [0.84 kip-in./rad]  
202 and for gypsum board  $k_x = 427$  N/mm [2.43 kip/in.] , and  $k_\phi = 95987$  N-mm/rad [0.85 kip-in./rad].  
203 See Vieira and Schafer 2013 for a summary, Vieira and Schafer 2012 for details on  $k_x$ , and  
204 Schafer et al. 2010 and Vieira 2011 for details on  $k_\theta$ .

205 The stiffness of the sheathing combinations is indicated as vertical lines in Figure 10e. As  
 206 Figure 10e indicates, one-sided sheathing is relatively ineffective, while two-sided sheathing  
 207 provides significant, if incomplete, torsional restraint. To more directly gauge the relative  
 208 effectiveness of the sheathing the member mid-height rotation ( $\theta_{mid}$ ) is estimated from the model.  
 209 The demand torsion,  $He$ , is based on the maximum observed  $H$  for each sheathing type. For the  
 210 bare case (BB)  $\theta_{mid}$  is 9.6 deg., for the one-sided sheathing cases (OB, BO)  $\theta_{mid}$  is a maximum of  
 211 10.1 deg., and for the two-sided sheathing cases (GG, GO, OG, OO)  $\theta_{mid}$  is a maximum of 1.7  
 212 deg. at the peak  $He$  demand.

213 To explore the expected impact of the warping longitudinal stresses on the cross-section  
 214 capacity the bending strength reduction ratio,  $R$ , of AISI-S100 (2012) Section C3.6 is calculated  
 215 for the various sheathing configurations.  $R$  is the ratio of the maximum bending stress to the sum  
 216 of the bending ( $\sigma_b$ ) and warping ( $\sigma_w$ ) stresses, specifically:

$$217 \quad R = \frac{(\sigma_b)_{\max}}{|\sigma_b + \sigma_w|} \leq 1.0 \quad (4)$$

218 The ratio is limited to one, as locations where the bending and warping stresses counteract are  
 219 assumed non-detrimental to the member capacity. From, Eq. (1), and assuming the cross-section  
 220 is in the  $xy$  plane, for the general case:

$$221 \quad R = \frac{My^* / I}{|My / I + B\omega(x, y) / C_w|} \leq 1.0 \quad (5)$$

222 where  $y^*$  is the distance to the extreme fiber, and  $I$  is the moment of inertia. For the specific case  
 223 of a laterally applied mid-height load,  $H$ , the moment  $M = HL / 4$  and the bimoment,  $B$ , can be  
 224 determined from analysis (i.e. Figure 10) and is denoted as  $B = cHe$  where  $c$  is the analysis  
 225 dependent constant and  $He$  the applied torsion. Note, in this configuration the maximum  $B$  and  $M$   
 226 both occur at mid-height. For this specific case, Eq. (5) becomes:

227 
$$R = \frac{Ly^* / 4I}{|Ly / 4I + ce\omega(x,y) / C_w|} \leq 1.0 \quad (6)$$

228 The resulting ratio is independent of  $H$  and only a function of the section, length, and bracing.

229 The bending reduction factor,  $R$ , is supplied for all sheathing configurations in Figure 11.

230 For the bare (BB) case the warping stresses are large, and the minimum  $R = 0.51$  indicating the  
231 expected bending capacity is 0.51 of the pure bending capacity (ignoring torsion). For one-sided  
232 sheathing, (BO, OB) modest relief from torsion is provided, but the minimum  $R$  is still 0.64;  
233 indicating a strong reduction. For two-sided sheathing the reductions are generally small. For the  
234 GG case  $R$  is 0.91 in the tension flange and 0.94 in the compression flange. For the OO case  $R$  is  
235 0.94 in the tension flange and 0.96 in the compression flange. Longitudinal warping stresses  
236 exist in the cases with two-sided sheathing and their absolute magnitude is not small; however,  
237 the maximum location at the tip of the lips, (Figure 9a) is not at the location of maximum  
238 bending stress, and the reduction ratio  $R$  indicates the expected impact is modest. These stress  
239 predictions are approximate as they rely on small deflection analysis, ignore cross-section  
240 deformations, and utilize relatively coarse estimates of the fastener-sheathing stiffness.  
241 Nonetheless, they provide an important relative sense of the importance of the warping torsional  
242 stresses and indicate that they are not a primary concern for studs with two-sided sheathing.  
243 Design methods for the observed member and fastener limit states are addressed in the following  
244 sections.

### 245 **Capacity Predictions for Member Limit States**

246 The member limit states of local, distortional, and global buckling (with appropriate interactions)  
247 are considered in assessing the member capacity. As detailed in Vieira and Schafer (2013)  
248 sheathing greatly influences global buckling, modestly influences distortional buckling, and has

249 little influence on local buckling (due to its short buckling wavelength). To specifically assess  
250 the influence of the sheathing, the stiffness supplied from the fastener-sheathing combination  
251 must be known and included in an elastic stability analysis of the member.

252 The cross-section model including the fastener-sheathing springs of Figure 9b is utilized  
253 in an elastic buckling finite strip analysis. The lateral and rotational springs  $k_x$  and  $k_\phi$  are provided  
254 in the previous section, for OSB  $k_y = 0.374$  N/mm [0.0021 kip/in.], and for gypsum,  $k_y = 0.087$   
255 N/mm [0.00049 kip/in.]. The stiffness values are derived for the specific fastener-sheathing  
256 combinations and may be determined experimentally (stiffness determined at 40% of ultimate),  
257 or using closed-form lower bound solutions as discussed in Vieira and Schafer (2013). The  
258 lower-bound, non-composite action stiffness is employed for  $k_y$ . The per fastener values are  
259 divided by the tributary width of the fasteners (305 mm [12 in.]) to convert from spring stiffness  
260 to foundation stiffness values  $\underline{k}_x$ ,  $\underline{k}_y$ , and  $\underline{k}_\phi$  which are then used in the finite strip analysis.

261 Elastic buckling analysis for pure compression and pure bending is completed for the  
262 finite strip model in CUFSM (Li and Schafer 2010). The local ( $\ell$ ), distortional ( $d$ ), and global ( $e$ )  
263 buckling loads in compression ( $P_{cr}$ ) and bending ( $M_{cr}$ ) are provided in Table 3. With the elastic  
264 buckling values known the nominal strength ( $P_n$  and  $M_n$ ) may be predicted using the Direct  
265 Strength Method formulation of AISI-S100 (2007) Appendix 1. Assuming a simple linear  
266 interaction (as employed in AISI-S100) and ignoring second order-effects the nominal capacity  
267 is compared to the tests via:

268 
$$\frac{P}{P_n} + \frac{M}{M_n} \leq 1 \quad \xrightarrow{M=HL/4} \quad \frac{P}{P_n} + \frac{H}{H_n} \leq 1 \quad (7)$$

269 The resulting linear interaction expression, which is dependent on the sheathing type, is  
270 compared against the test data in Figure 12.

271 In comparing the nominal predictions to the tests in Figure 12, first note that the axial-  
272 only experimental results are from Vieira et al. (2012), and although the nominal cross-section is  
273 the same, the as-measured sections for Vieira's tests were smaller (area and yield stress in  
274 Vieira's tests are both 93% of the as-measured specimens reported here) thus the disagreement  
275 between the predictions and the tests along the axial-only (vertical) axis are due to this difference  
276 in as-measured properties, see Peterman (2012) for further details.

277 For the remaining sections, which have a combination of axial and lateral load, the  
278 predicted member capacities are a conservative approximation of the observed capacities. The  
279 strength prediction for studs sheathed on one-side demonstrates sensitivity of the method to the  
280 sheathing details, the BO case where the fastener-sheathing is connected to the compression  
281 flange provides far greater bending capacity than the OB case. However, while the experimental  
282 results provide a clear difference between the GO, OG, GG, and OO cases the design method  
283 does not and instead predicts essentially all two-sided sheathing cases are able to develop the  
284 moment at first yield, (i.e.  $M_n = M_y$ ). It is worth noting that the GG case is unconservatively  
285 predicted for bending dominant response; indicating a need to consider fastener limit states in  
286 addition to member limit states.

### 287 **Capacity Predictions for Connector Limit States**

288 As discussed in the Torsional Analysis and Response section, it is typical to assume in design  
289 that the full torsional demand ( $He$ ) is carried by the fasteners. However, for practical fastener-  
290 sheathing stiffness the demand on the fasteners is typically less than  $He$ . As Figure 10 shows, for  
291 two-sided sheathing, the demand is around  $0.4He$ . The exact torsional demand on the fasteners  
292 may be determined by a torsional analysis model, similar to that of Figure 10.

293 The torsional demand is carried by the fasteners in a combination of bearing and pull-  
 294 through resistance as depicted in the free-body diagram of Figure 9c. Specifically, if subscript “*i*”  
 295 refers to face 1 and 2, the pull-through resistance supplies a torsional resistance ( $T_{pt}$ ) as the  
 296 section undergoes twist  $\theta$  of:

$$297 \quad T_{pti}(\theta) = k_{\phi i} \theta$$

298 which has a maximum value based on the pull-through capacity ( $P_{pt}$ ) that occurs at  $\theta_{pt}$ :

$$299 \quad (T_{pti})_{\max} = P_{pti} (b / 2) = k_{\phi i} \theta_{pti}$$

300 The torsional resistance developed from the bearing mechanism ( $T_{br}$ ) as a function of twist is:

$$301 \quad T_{bri}(\theta) = k_{xi} (d^2 / 4) \theta$$

302 which has a maximum value based on the bearing capacity ( $P_{br}$ ) that occurs at  $\theta_{br}$ :

$$303 \quad (T_{bri})_{\max} = P_{bri} (d / 2) = k_{xi} (d^2 / 4) \theta_{bri}$$

304 Two models for the torsional capacity are considered. The first model ( $T_1$ ) assumes the capacity  
 305 of the fastener-sheathing system is based on first failure in either pull-through or bearing, on  
 306 either face:

$$307 \quad \theta_f = \min(\theta_{pt1}, \theta_{br1}, \theta_{pt2}, \theta_{br2})$$

$$308 \quad T_1 = T(\theta_f) = T_{pt1}(\theta_f) + T_{br1}(\theta_f) + T_{pt2}(\theta_f) + T_{br2}(\theta_f)$$

309 The second model ( $T_2$ ) is based on fully ductile failure response in the fastener-sheathing system,  
 310 and thus based on the maximum strength:

$$311 \quad T_2 = (T_{pt1})_{\max} + (T_{br1})_{\max} + (T_{pt2})_{\max} + (T_{br2})_{\max}$$



312 Strength in bearing ( $P_{br}$ ) and pull-through ( $P_{pt}$ ), unfortunately, is not generally available.  
313 Bearing strength's upperbound is the screw shear strength, which is available from  
314 manufacturers, but bearing is governed by the sheathing and fastener size. Average experimental  
315 bearing strength ( $P_{br}$ ) from lateral stiffness tests reported in Vieira and Schafer (2012) are 2570  
316 N [578 lbf] for a #8 in OSB and 380 N [86 lbf] for a #6 in gypsum. Pull-through strength's  
317 upperbound is the screw tensile strength, also available from manufacturers (but essentially  
318 irrelevant), as pull-through is governed by the sheathing and the fastener head details. Pull-  
319 through capacities can be determined from the failure load in a rotational restraint test (e.g., per  
320 AISI-TS-1 (2002)) test. The tests detailed in Vieira and Schafer (2012) only provide the stiffness,  
321 the data was revisited as detailed in Peterman (2012), and the average pull-through capacity ( $P_{br}$ )  
322 determined as 1944 N [437 lbf] for a #8 in OSB and 178 N [40 lbf] for a #6 in gypsum.

323 Utilizing the preceding formulation, torsional capacity for models  $T_1$  and  $T_2$  are provided  
324 for the different sheathing configurations in Table 4. To compare against the tests the torsional  
325 capacity must be converted to lateral capacities  $H_1$  and  $H_2$ . This may be done either by the  
326 typical design assumption that all of the torsion is borne by the fasteners,  $T = He$ , or by a torsion  
327 analysis (i.e. Figure 10) which results in a reduced torsion demand,  $T = rHe$ , where  $r$  is  
328 determined from the analysis and is approximately 0.4 for two-sided sheathing cases. Per Table  
329 4, assuming the full torsion demand is borne by the fasteners ( $T = He$ ) leads to unrealistically  
330 low fastener limit state strength, regardless of whether first failure ( $T_1$ ) or maximum capacity  
331 ( $T_2$ ) is employed. A torsional analysis is necessary for determining the proper demand.

332 For similarly sheathed specimens GG or OO first failure ( $T_1$  or  $H_1$ ) and maximum  
333 capacity ( $T_2$  or  $H_2$ ) provide similar strength. For dis-similarly sheathed specimens GO or OG the  
334 gypsum fails much earlier than the OSB and the two models diverge. As Table 4 shows first

335 failure ( $T_I$  or  $H_I$ ) occurs in the gypsum at 1.1 deg. while the OSB does not fail until 24 deg..  
336 Experimental observation of the limit state is more consistent with the first failure model ( $T_I$  or  
337  $H_I$ ), i.e., failure in the gypsum is equivalent to failure of the specimen.

338 The predicted capacity for the model based on first failure ( $T_I$  or  $H_I$ ) utilizing the  
339 analysis-based torsional demand ( $T = rHe$ ) is provided in Table 4 and compared across all tests  
340 and against the member limit states in Figure 12. This model predicts that connector limit states  
341 will not control for the BO, OB, or OO sheathed cases. However, connector limit states may  
342 control in the gypsum sheathed cases GG, GO, or OG. As Figure 12 illustrates the connector  
343 limit state is dominant under moderate bending demands in the GG case, but only controls for  
344 high bending demands in the GO and OG case. The experiments indicated that the GG case was  
345 controlled by connector limits both in terms of observed limit states and capacity. The resulting  
346 failure surface (minimum of the member and connector limit states) provides a rational  
347 progression in its results and is qualitatively similar to the test results.

## 348 **Discussion**

### 349 *Extension to distributed lateral loads*

350 The most common design case for a sheathed stud under axial load and bending is for a  
351 distributed lateral load as opposed to the point load studied here. A torsion analysis, similar to  
352 that described in the Torsional Analysis and Response section (Figure 10) was conducted to  
353 provide preliminary findings for this case. The results are provided in Figure 13. Figure 13e  
354 compares the earlier results for the point torque ( $He$ ) directly to the distributed torque ( $He/L$ ).  
355 The distributed torque allows more fasteners to be involved in resisting the twist and the results  
356 are far more effective. For the same total torque the case with the distributed torque twists less,

357 has lower bimoment (and hence lower warping stresses), and more evenly distributes the demand  
358 to the fasteners compared with a point torque. This is a promising finding, as it suggests that a  
359 torsional stiffness analysis may not be required for design under distributed loads, instead it is  
360 satisfactory to assume the fasteners see their full tributary demand, and that the warping stresses  
361 can be ignored. These assumptions would greatly simplify design.

### 362 ***Recommendations for Design***

363         The method explored for checking the member limit states is relatively sophisticated: all  
364 three buckling classes are explored and the role of sheathing is explicitly included in the elastic  
365 stability analysis. However, it is also approximate: direct torsion stresses are ignored, shear stress  
366 are ignored, stability analysis is only conducted for pure compression or pure bending not for the  
367 actual combined stress states, second-order effects are ignored, inelastic reserve in bending is  
368 ignored, and composite action in bending is ignored. Despite these crude simplifications the  
369 results are useful in a practical sense as the method incorporates the essential increase in strength  
370 that occurs for a sheathed specimen – note the capacity increases 107% in pure bending from the  
371 unsheathed case to the sheathed on both sides case. Even without direct torsional stresses  
372 incorporated the weakness of the section in torsion is included through the stability analysis.  
373 Also, the explored design method does not rely on tools or analysis currently unavailable to  
374 design engineers. Until a more fundamental and detailed prediction method is developed the  
375 approach provided here is recommended for design against the key member limit states in a  
376 sheathed stud.

377         In the method developed for exploring the connector limit states the fasteners are  
378 designed only against the direct torsional demand, not the second-order forces from bracing the  
379 member. This is based on the assumption that the direct torsional demands are greater. This is

380 supported by the axial tests of Vieira and Schafer (2013) that do not exhibit fastener limit states.  
381 A more advanced method would include contributions both from second-order forces (dependent  
382 on bracing stiffness and different for axial and bending) as well as the direct torsional forces  
383 considered here. Alternative mechanisms for resisting torsion were explored in Peterman (2012),  
384 only the most promising models were summarized here. Despite the significant simplifications  
385 utilized here the developed connector limit state model is found to usefully predict the potential  
386 for connector limit states in the tests.

387         The recommended procedure for design of a sheathed stud wall under axial and bending  
388 is as follows. First determines the stiffness and strength of the fastener-sheathing system that will  
389 be providing resistance to the stud. Preferably this is done by test, or alternatively using  
390 simplified closed-formed solutions (see Vieira and Schafer 2013 for a summary). Second, the  
391 member stability in local, distortional, and global buckling must then be assessed. Preferably this  
392 is done by computational analysis (e.g., CUFSM), or alternatively closed-form solutions are  
393 available, but may be involved (e.g., see Vieira and Schafer 2013). Third, the member stability  
394 analyses are used to assess the member limit states using either effective width or Direct Strength  
395 Method approaches. Direct Strength Method is followed herein. Direct torsion was not  
396 considered in the member limit state analyses performed herein, but is included in the fastener  
397 limit states. Fourth, the fastener-sheathing capacities must be determined for pull-through and  
398 bearing limit states. The authors were unable to find generally available methods or industry  
399 reported values for these limit states and thus instead relied on our own direct testing (see Vieira  
400 and Schafer 2012 and Peterman 2012). Fifth, to determine the fastener demands one may assume  
401 all the torsion must be carried by the fasteners, (however this may be too conservative) or  
402 perform a torsional stiffness analysis to determine the proportion carried by the member vs. that

403 carried by the fastener-sheathing combination. Finally, the minimum of the member and fastener  
404 limit states controls the strength.

## 405 **Conclusions**

406 This paper explores the behavior and design of load-bearing cold-formed steel stud walls, where  
407 only sheathing supplies bracing of the stud, under axial and out-of-plane lateral load. A series of  
408 tests were conducted on 2.4 m [8 ft] high 362S162-68 studs, set in 362T162-68 track with special  
409 blocking details. The stud was tested as (a) unsheathed, (b) sheathed on one-side only with  
410 oriented strand board, and (c) sheathed on two sides with all combinations of oriented strand  
411 board and/or gypsum board. The results demonstrate that sheathing has a definitive and positive  
412 impact on the stability and strength of the stud. The unsheathed studs experienced severe twist,  
413 due to the lateral load's lack of alignment with the member shear center, and failed in a torsion  
414 limit state. The studs with sheathing on one-side developed greater capacity, but still suffered  
415 from excessive twist and eventually pull-through of the fasteners through the sheathing. The  
416 studs with sheathing on both sides are generally able to develop member limit states of local  
417 buckling or yielding, and have limited twisting. Connector limit states of pull-through and  
418 bearing are also observed, typically as the specimen strength descends under displacement. The  
419 gypsum sheathed specimens exhibit significantly more damage near the fasteners and are not  
420 able to develop full member capacity in all cases.

421 An analysis of the stud and fastener-sheathing restraint under the torsional demand  
422 induced by the eccentric horizontal load demonstrates how the torsional demand is shared  
423 between the stud and the fastener-sheathing bracing. In all cases the mid-height fastener is not  
424 predicted to carry the full torsional demand. This observation is found to be significant when

425 investigating connector limit states, as it is overly conservative to assume the fasteners carry the  
426 full demand. Further, it is found that the longitudinal warping stresses induced by the torsion in  
427 the member are only significant for the unsheathed and one-sided sheathed studs.

428 Investigation of the design considered both member and connector limit states. The  
429 member limit states of local, distortional, and global buckling were considered. Elastic stability  
430 assessment of the stud must include the restraint from the fastener-sheathing system, and when  
431 this is included the progression in predicted capacity from the unsheathed to two-sided sheathed  
432 cases is reasonable. A new model was developed for assessing the connector limit states, based  
433 on the manner in which fastener pull-through and bearing resist the induced torsional demand.  
434 The total torsional resistance supplied by the fastener sheathing system is included, but first  
435 failure in either pull-through or bearing limits the total connector capacity. The torsional demand  
436 on the fasteners is based on a torsional stiffness analysis as detailed herein. This approach  
437 predicts connector limit states only control for high levels of primary bending in the gypsum  
438 sheathed specimens, consistent with the testing.

439 Extension of the overall design approach to distributed lateral loads (as opposed to a  
440 point lateral load) is provided. Further, the limitations and assumptions of the developed design  
441 method are fully detailed. Significant advancements are still possible as tested capacity exceeds  
442 predicted capacity in many cases; however, for the time being the proposed method provides a  
443 design approach that includes all essential features and provides limit state predictions consistent  
444 with the tests. In summary, it is shown that cold-formed steel stud walls braced by sheathing  
445 alone and subjected to axial and lateral loads can provide the full member capacity (i.e. the local  
446 buckling limited strength) if properly detailed.

447

448 **Acknowledgments**

449 This paper was prepared as part of the American Iron and Steel Institute (AISI) sponsored  
450 project: Sheathing Braced Design of Wall Studs. The project also received supplementary  
451 support and funding from the Steel Stud Manufacturers Association (SSMA). Any opinions,  
452 findings, and conclusions or recommendations expressed in this publication are those of the  
453 authors and do not necessarily reflect the views of AISI, nor SSMA.

454 **References**

- 455 AISI-S100 (2007). "North American Specification for the Design of Cold-Formed Steel  
456 Structural Members." American Iron and Steel Institute, Washington, D.C.
- 457 AISI-S100 (2012). "North American Specification for the Design of Cold-Formed Steel  
458 Structural Members." American Iron and Steel Institute, Washington, D.C.
- 459 AISI-S200 (2007). "North American Standard for Cold-Formed Steel Framing – General  
460 Provisions." American Iron and Steel Institute, Washington, D.C.
- 461 AISI-TS-1 (2002) "Rotational-Lateral Stiffness Test Method for Beam-to-Panel Assemblies"  
462 Cold- Formed Steel Design Manual, 2002 Edition, American Iron and Steel Institute,  
463 Washington, D.C.
- 464 Aviram, A., Mayes, R.L., Hamburger, R.O. (2012). "Enhanced Blast-Resistance of an Innovative  
465 High-Strength Steel Stud Wall System." Proceedings of the 2012 SEAOC Convention, 12 pp.
- 466 Green, G.G., Winter, G., and Cuykendall, T.R. (1947). "Light Gage Steel Columns in Wall-  
467 braced Panels." Cornell University Engineering Experiment Station, 35, 1-50.
- 468 Lee, Y., Miller, T.H. (2001). "Axial Strength Determination for Gypsum-Sheathed, Cold-Formed  
469 Steel Wall Stud Composite Panels." ASCE, Journal of Structural Engineering, 127 (6) 608-615.
- 470 Li, Z., Schafer, B.W. (2010) "Buckling analysis of cold-formed steel members with general  
471 boundary conditions using CUFSM: conventional and constrained finite strip methods."  
472 Proceedings of the 20th Int'l. Spec. Conf. on Cold-Formed Steel Structures, St. Louis, MO.  
473 November, 2010. 17-32.
- 474 Vieira, L.C.M., Schafer, B.W. (2013). "Behavior and Design of Sheathed Cold-Formed Steel  
475 Stud Walls under Compression." ASCE, Journal of Structural Engineering, Preview Manuscript,  
476 (doi: [http://dx.doi.org/10.1061/\(ASCE\)ST.1943-541X.0000731](http://dx.doi.org/10.1061/(ASCE)ST.1943-541X.0000731))
- 477 Miller, T.H., Pekoz, T. (1993). "Behavior of Cold-Formed Steel Wall Stud Assemblies." ASCE,  
478 Journal of Structural Engineering, 119 (2) 641-651.
- 479 Miller, T.H., Pekoz, T. (1994). "Behavior of Gypsum-Sheathed Cold-Formed Steel Wall Studs."  
480 ASCE, Journal of Structural Engineering, 120 (5) 1644-1650.

- 481 Peterman, K.D. (2012). "Experiments on the Stability of Sheathed Cold-Formed Steel Studs  
482 Under Axial Load and Bending." M.S. Thesis. Johns Hopkins University.
- 483 Pham, M.M., Miles, J.E., Zhuge, Y. (2006). "Experimental Capacity Assessment of Cold-  
484 Formed Boxed Stud and C Stud Wall Systems Used in Australian Residential Construction."  
485 ASCE, Journal of Structural Engineering, 132 (4) 631–635.
- 486 Salim, H., Muller, P., Dinan, R. (2005). "Response of Conventional Steel Stud Wall Systems  
487 under Static and Dynamic Pressure." ASCE, Journal of Performance of Constructed Facilities,  
488 19 (4) 267-276.
- 489 Schafer, B.W. Vieira Jr., L.C.M., Sangree, R.H., Guan, Y. (2010) "Rotational Restraint and  
490 Distortional Buckling in Cold-Formed Steel Framing Systems." Revista Sul-Americana de  
491 Engenharia Estrutural (South American Journal of Structural Engineering), Special issue on  
492 cold-formed steel structures, 7 (1) 71-90.
- 493 Simaan, A., Pekoz, T. (1976). "Diaphragm Braced Members and Design of Wall Studs." ASCE,  
494 Journal of the Structural Division, 102 (1) 77-92.
- 495 Vieira Jr., L.C.M., Schafer, B.W. (2012). "Lateral Stiffness and Strength of Sheathing Braced  
496 Cold-Formed Steel Stud Walls." Elsevier, Engineering Structures. 37, 205–213
- 497 Vieira Jr., L.C.M., Shifferaw, Y., Schafer, B.W. (2011) "Experiments on Sheathed Cold-Formed  
498 Steel Studs in Compression." Elsevier, Journal of Constructional Steel Research. 67 (10) 1554-  
499 1566.
- 500 Vieira, L.C.M. (2011). "Behavior and Design of Sheathed Cold-Formed Steel Stud Walls under  
501 Compression." Ph.D. Dissertation. Johns Hopkins University.
- 502 Winter, G. (1960). "Lateral Bracing of Beams and Columns." ASCE, Transactions, Vol. 125  
503 Paper No. 3044, 807-826.
- 504 McGuire, W., Gallagher, R., Ziemian, R. (1999). Matrix Structural Analysis, With MASTAN2.



**List of Tables**

Table 1 Nominal and average (across 27 specimens) measured dimensions for 362S162-68 stud,  
See Peterman (2012) for individual specimen measurements and full statistics

Table 2 Observed failure loads and limit states for previously conducted axial-only test and  
current axial plus lateral load tests reported here

Table 3 Predicted axial and bending member capacity based on average stud dimensions and  
including restraint from sheathing

Table 4 Predicted strength of fastener-sheathing system

Table 1 Nominal and average (across 27 specimens) measured dimensions for 362S162-68 stud,  
See Peterman (2012) for individual specimen measurements and full statistics

Parameter	Nominal	Measured
	(mm)	(mm)
$h$	92.1	93.5
$b_A$	41.3	43.2
$b_B$	41.3	43.0
$d_A$	12.7	16.4
$d_B$	12.7	14.2
$t$	1.811	1.816
$r_{hb-B}$	2.7	8.9
$r_{db-B}$	2.7	7.5
$r_{hb-A}$	2.7	8.8
$r_{db-A}$	2.7	7.8
	(deg.)	(deg.)
$\theta_{hb-B}$	90.0	88.1
$\theta_{db-B}$	90.0	85.3
$\theta_{hb-A}$	90.0	87.3
$\theta_{db-A}$	90.0	83.1
	(MPa)	(MPa)
$F_y$	345	413

Table 2 Observed failure loads and limit states for previously conducted axial-only test and current axial plus lateral load tests reported here

NOMINAL LOADING		SHEATHING (B=BARE, G=GYPSUM, O=OSB)																				
P	H	BB			OB			GG			OG			OO								
		L (m)	P <sub>test</sub> (kN)	LS	L (m)	P <sub>test</sub> (kN)	LS	L (m)	P <sub>test</sub> (kN)	LS	L (m)	P <sub>test</sub> (kN)	LS	L (m)	P <sub>test</sub> (kN)	LS						
100%	0	0.6	87.9	D	0.61	95.4	L	0.6	96.7	L	0.6	97.8	L	0.6	101.6	L						
		1.2	84.6	FT	1.219	97.8	L	1.2	99.6	L	1.2	96.2	L	1.2	99.0	L						
		1.8	60.5	FT	1.829	80.1	FT	1.8	88.7	L	1.8	91.1	L	1.8	99.5	L						
		2.4	57.1	F	2.438	69.6	FT	2.4	95.0	L	2.4	99.9	L	2.4	102.7	L						
L=2.4 m axial + lateral tests		BB			OB			BO			GG			OG			GO			OO		
		P <sub>test</sub> (kN)	H <sub>test</sub> (kN)	LS	P <sub>test</sub> (kN)	H <sub>test</sub> (kN)	LS	P <sub>test</sub> (kN)	H <sub>test</sub> (kN)	LS	P <sub>test</sub> (kN)	H <sub>test</sub> (kN)	LS	P <sub>test</sub> (kN)	H <sub>test</sub> (kN)	LS	P <sub>test</sub> (kN)	H <sub>test</sub> (kN)	LS	P <sub>test</sub> (kN)	H <sub>test</sub> (kN)	LS
~80%P	to failure	-	-	-	-	-	-	-	-	-	77.3	3.4	Y	-	-	-	-	-	-	80.9	4.7	L,PT,Y
Δ <sub>80%P</sub>	to failure	-	-	-	44.1	4.3	T	50.8	3.2	T,PT	64.7	3.2	PT,B,Y	68.0	4.4	L,PT,Y	65.3	5.1	PT,B,Y	66.4	6.0	L,PT,Y
Δ <sub>60%P</sub>	to failure	28.5	2.4	T	28.9	3.4	PT	32.0	3.5	PT	51.6	4.4	PT,B,Y	45.1	5.2	PT,Y	45.2	6.5	B,L,Y	50.9	6.7	L,Y,PT
Δ <sub>40%P</sub>	to failure	10.6	2.6	T	20.3	3.4	PT,T	20.1	4.8	PT,T	30.4	4.8	PT,B	29.8	5.8	L,PT,Y	33.2	6.8	PT,B,Y	33.7	6.9	L,Y
Δ <sub>10%P</sub>	to failure	-	-	-	2.2	5.0	T	-	-	-	7.7	5.5	PT,B	7.7	6.1	L,B,T,Y	8.1	7.3	PT,L,B	10.8	7.4	L,Y

(1) shaded results are from axial only tests of Vieira et al. (2011) on the same nominal stud and similar test setup

(2) limit states (LS): member limit states: L = local buckling, D = distortional buckling, FT = flexural-torsional buckling, F = weak-axis flexural buckling, T = torsion, Y = yielding  
connector limit states: PT = pull-through of the fastener head through the sheathing, B = bearing damage in the sheathing from fastener

Table 3 Predicted axial and bending member capacity based on average stud dimensions and including restraint from sheathing

sheathing	AXIAL					BENDING						
	$P_y$ (kips)	$P_{cr\ell}/P_y$	$P_{crd}/P_y$	$P_{cre}/P_y$	$P_n^1$ (kN)	sheathing	$M_y$ (kN-mm)	$M_{cr\ell}/M_y$	$M_{crd0}/M_y$	$M_{cre0}/M_y$	$C_b M_{cre0}/M_y$	$M_n^2$ (kN)
BB	31.3	1.17	1.30	0.58	<b>67.6</b>	BB	4015	5.70	2.35	0.37	0.48	<b>1927</b>
OB/BO	31.3	1.17	1.34	0.86	<b>85.5</b>	OB	4015	>5.70	>2.35	0.80	1.06	<b>3292</b>
						BO	4015	>5.70	>2.35	>8	>8	<b>4015</b>
GG	31.3	1.17	1.38	2.37	<b>110.4</b>	GG	4015	>5.70	>2.35	>8	>8	<b>4015</b>
OG/GO	31.3	1.17	1.38	2.56	<b>111.4</b>	OG	4015	>5.70	>2.35	>8	>8	<b>4015</b>
						GO	4015	>5.70	>2.35	>8	>8	<b>4015</b>
OO	31.3	1.17	1.39	2.92	<b>112.9</b>	OO	4015	>5.70	>2.35	>8	>8	<b>4015</b>

- (1) calculated per AISI-S100-07 Appendix 1 (DSM) with  $k_x$ ,  $k_y$ ,  $k_\phi$  springs included in CUFSM4 models for finding  $P_{cr\ell}$ ,  $P_{crd}$ ,  $P_{cre}$
- (2) calculated per AISI-S100-07 Appendix 1 (DSM) with  $k_x$ ,  $k_y$ ,  $k_\phi$  springs included in CUFSM4 models for finding  $M_{cr\ell}$ ,  $M_{crd}$ ,  $M_{cre}$
- (3) the number of longitudinal ( $m$ ) terms kept in the CUFSM analysis is 1-10 and 31-37 for P runs, and 1-11 and 39-45 for M runs
- (4) axial capacities assumed fixed end conditions consistent with Vieira and Schafer 2012 findings
- (5) bending capacities assume major-axis pinned end conditions consistent with findings herein
- (6) max moment  $M=HL/4$ , utilized for conversion to P vs. H space for visualizing interaction

Table 4 Predicted strength of fastener-sheathing system

sheathing	fastener torsional capacity calculation				fastener capacity in terms of lateral load H				test H <sup>a</sup> (kN)
	$\theta_f$ (deg)	$T_1=T(\theta_f)$ (kN-mm)	$T_2=\text{sum}(T)$ (kN-mm)	$\theta(T_2)$ (deg)	demand $T=He$		demand $T=rHe^b$		
					$H_1=T_1/e$ (kN)	$H_2=T_2/e$ (kN)	$H_1=T_1/re$ (kN)	$H_2=T_2/re$ (kN)	
BB	-	-	-	-	-	-	-	-	<b>2.62</b>
OB	24.1	40	40	24.1	1.73	1.73	<b>12.06</b>	12.06	<b>4.98</b>
BO	24.1	40	40	24.1	1.73	1.73	<b>12.06</b>	12.06	<b>4.80</b>
GG	1.1	39	42	2.2	1.68	1.84	<b>4.19</b>	4.57	<b>5.47</b>
OG	1.1	61	179	24.1	2.65	7.76	<b>5.87</b>	17.19	<b>6.14</b>
GO	1.1	61	179	24.1	2.65	7.76	<b>5.87</b>	17.19	<b>7.25</b>
OO	3.3	247	316	24.1	10.70	13.69	<b>21.93</b>	28.04	<b>7.38</b>

(a) Maximum horizontal load observed in testing, generally for 10% $P_{axial}$ , see Table 2 for fulltest results.

(b) Demand on fasteners determined from torsional analysis model, for 2 sided sheathing  $r \sim 0.4$ , see Figure 10

## List of Figures

Figure 1 Loading and internal actions for unsheathed (bare) specimen

Figure 2 Typical specimen, tested under applied axial and lateral load (a) end elevation in testing rig, top beam is actuated, and lateral load applied by circular bar, (b) side elevation with fastener spacing and track to testing rig detailed, (c) dimensional nomenclature of tested stud

Figure 3 Force and moment response for gypsum sheathed specimens under different load protocols: constant axial displacement, and constant axial load

Figure 4: Observed axial and lateral failure loads of tested 362S162-68 studs with various sheathing configurations on the two stud flanges (B = Bare, O = OSB, G = Gypsum)

Figure 5 Observed member limit states in axial and lateral load testing

Figure 6 Observed connection limit states in axial and lateral load testing

Figure 7 Horizontal force vs. mid-height horizontal displacement with comparison to fixed, pinned, and semi-rigid end conditions for the short segment of connected track for (a) OO and (b) GO sheathed specimens

Figure 8 Location of laterally applied load (a) top view of load bar showing initial contact location, (b) etching of load bar on stud, showing load location moves to the termination of the flange flat, (c) assumed final location of lateral load for finite twist

Figure 9 As-measured cross-section drawn to scale, with (a) longitudinal stress distribution due to warping alone, (b) rotational/pull-through ( $k_r$ ), lateral/bearing ( $k_x$ ) and composite action/vertical ( $k_y$ ) springs for the unloaded (1) and loaded (2) flanges, (c) torsional free-body diagram for resistance created by fasteners through bearing ( $P_{br}$ ) and pull-through ( $P_{pt}$ ).

Figure 10 Torsional stiffness analysis model for a stud braced with rotational  $k_r$  springs every 305 mm [12 in.] o.c over 2.4 m [96 in.] length and loaded by a point torque at midspan (a) basic model, (b) torsional moment diagram without springs, (c) torsional moment diagram and spring torsion for typical fastener-sheathing spring stiffness, (d) torsional moment diagram and spring torsion for infinitely stiff spring, (e) midspan rotation, midspan bimoment, and midspan torsion in the spring as a function of increasing  $k_r$  (plot normalized to  $T_{app} = 113 \text{ N}\cdot\text{m}$  [1 kip-in.],  $\theta_{bare} = 0.3124 \text{ rad}$ ,  $B_{bare} = 384 \text{ N}\cdot\text{m}^2$  [11.57 kip-in<sup>2</sup>],  $\sigma_{max-bare} = 381 \text{ MPa}$  [55.25 ksi])

Figure 11 Distribution of bending strength reduction ratio  $R$  ( $R = (\sigma_b)_{max} / |\sigma_b + \sigma_w| \leq 1.0$ ) for the five different sheathing configurations. Ratios less than 1 indicate the expected reduction in bending capacity due to the presence of longitudinal warping stresses.

Figure 12 Comparison of observed axial and lateral failure loads of tested 362S162-68 studs with different sheathing configurations against predicted capacity for member limit states (Table 3) and connection limit state (Table 4)

Figure 13 Extension of torsion stiffness analysis of Figure 10 from point torque ( $T_{app} = He$ ) to distributed torque ( $t_{app} = (H/L)e = we$ ), (a) basic model, (b) torsional moment diagram without springs, (c) torsional moment diagram and spring torsion for typical fastener-sheathing spring stiffness, (d) torsional moment diagram and spring torsion for infinitely stiff spring, (e) comparison of mid-height rotation, maximum bimoment, and mid-height torsion in the spring (fastener) as a function of increasing  $k_r$  for point torque vs. distributed torque (plot normalized to  $T_{app} = 113 \text{ N}\cdot\text{m}$  [1 kip-in.],  $T_{trib} = 14 \text{ N}\cdot\text{m}$  [0.125 kip-in.],  $\theta_{bare-point-torque} = 0.312 \text{ rad}$ ,  $B_y = 451 \text{ N}\cdot\text{m}^2$  [12.54 kip-in<sup>2</sup>],  $\sigma_{max}(B_y) = F_y = 413 \text{ MPa}$  [59.9 ksi])

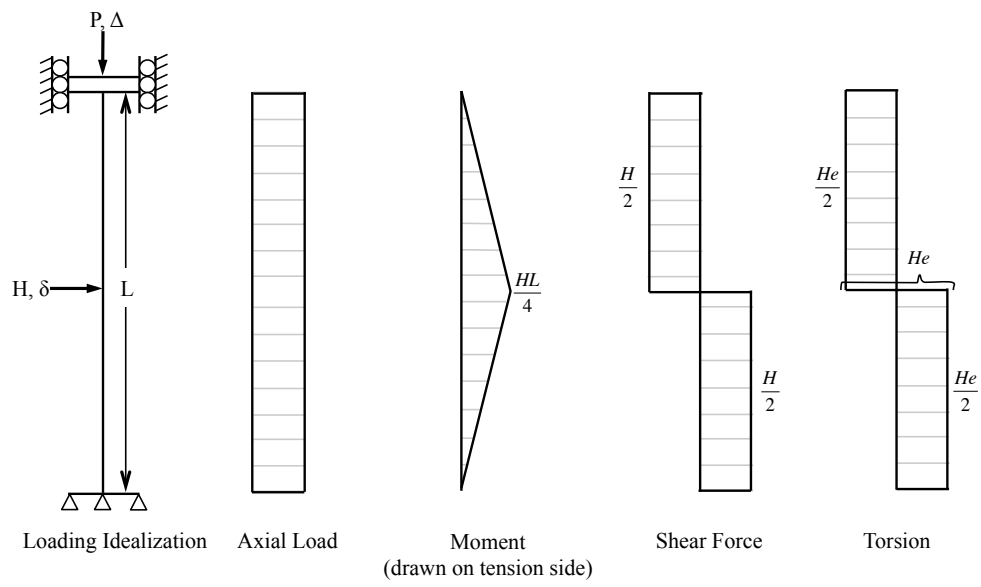


Figure 1 Loading and internal actions for unsheathed (bare) specimen

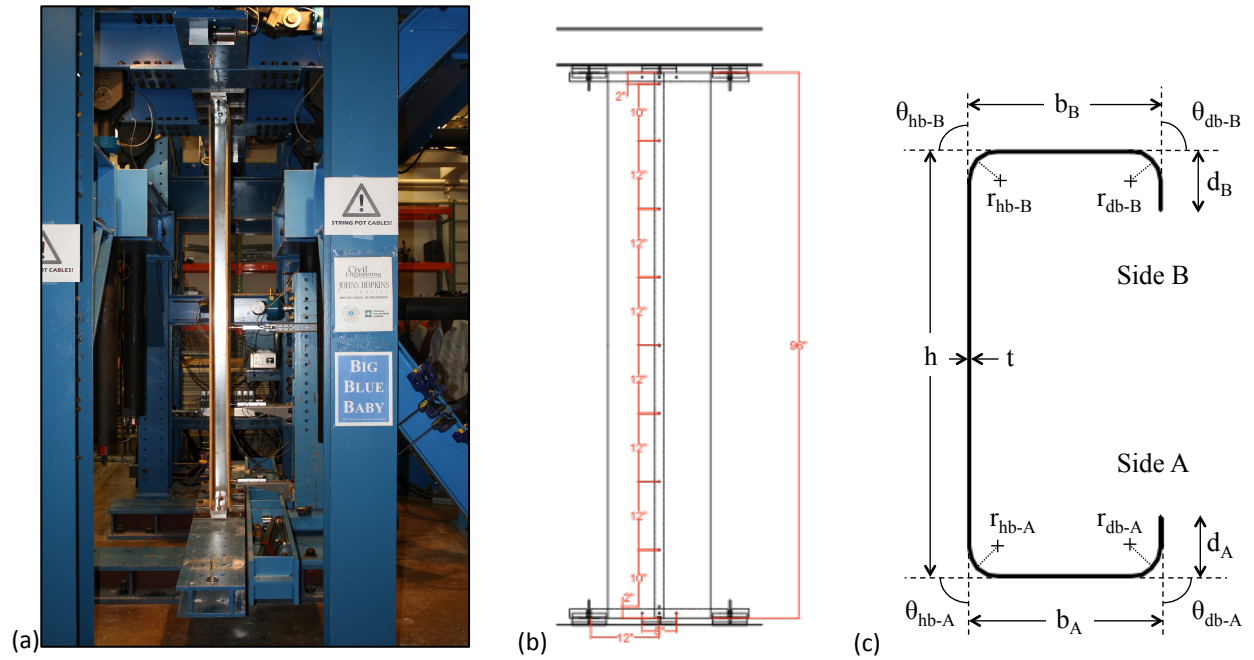


Figure 2 Typical specimen, tested under applied axial and lateral load (a) end elevation in testing rig, top beam is actuated, and lateral load applied by circular bar, (b) side elevation with fastener spacing and track to testing rig detailed, (c) dimensional nomenclature of tested stud



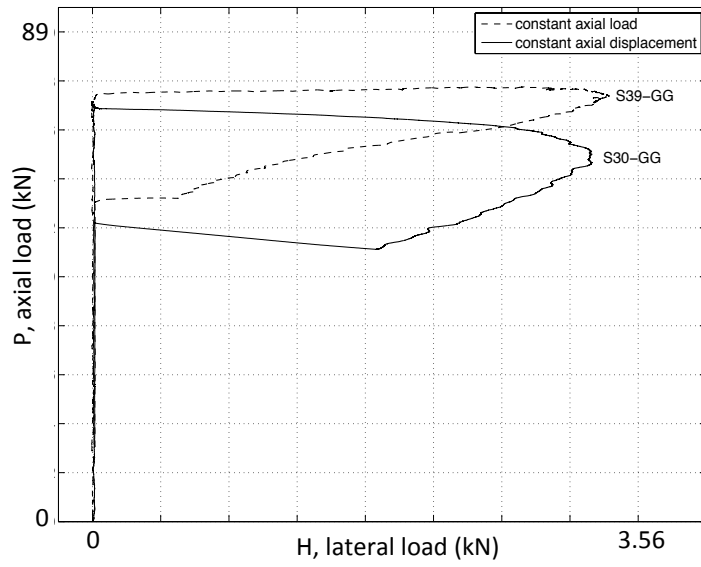


Figure 3 Force and moment response for gypsum sheathed specimens under different load protocols: constant axial displacement, and constant axial load

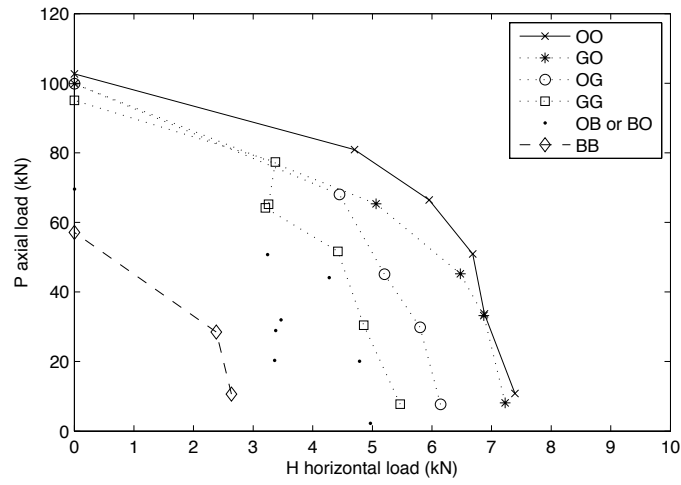
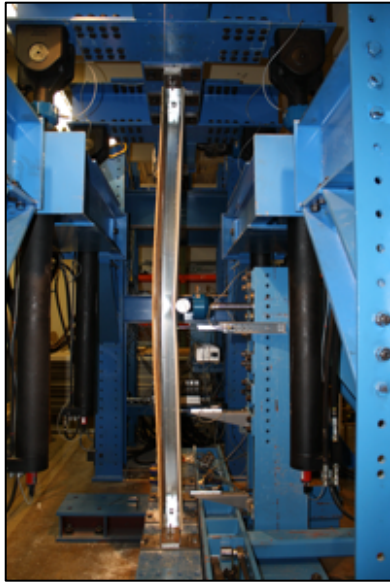


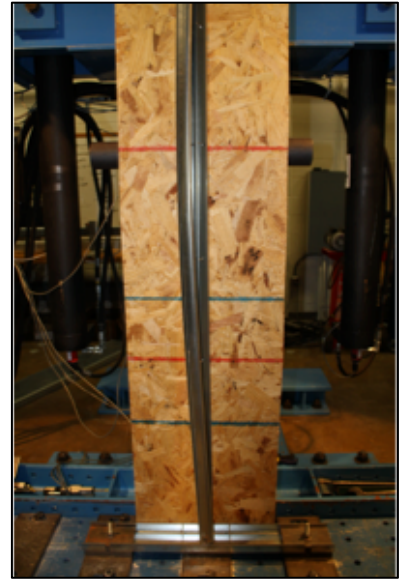
Figure 4: Observed axial and lateral failure loads of tested 362S162-68 studs with various sheathing configurations on the two stud flanges (B = Bare, O = OSB, G = Gypsum)



(a) local buckling (L) limit state in OG specimen, similar for OO specimens

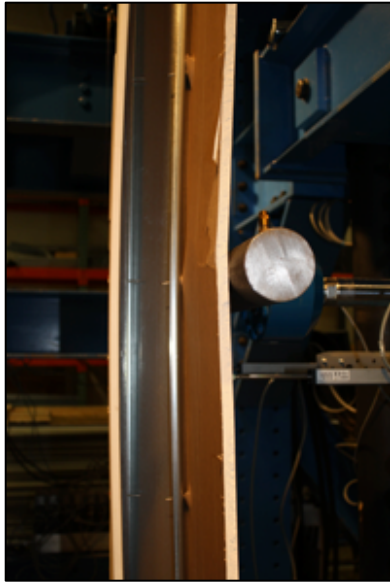


(b) detail of (a) at point of lateral load application, connection damage limited

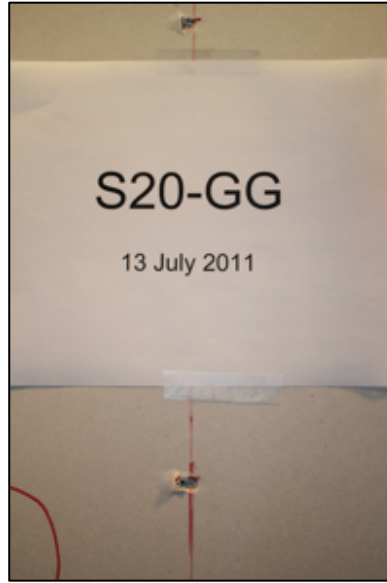


(c) torsion (T) in stud, typical for bare or one-sided sheathing cases, BO case shown

Figure 5 Observed member limit states in axial and lateral load testing



(a) GG specimen exhibiting pull-through (PT) failures on loaded board



(b) same GG specimen as (a) exhibiting bearing (B) failures on non-loaded board



(c) GO specimen exhibiting pull-through (PT) failures on loaded OSB board

Figure 6 Observed connection limit states in axial and lateral load testing

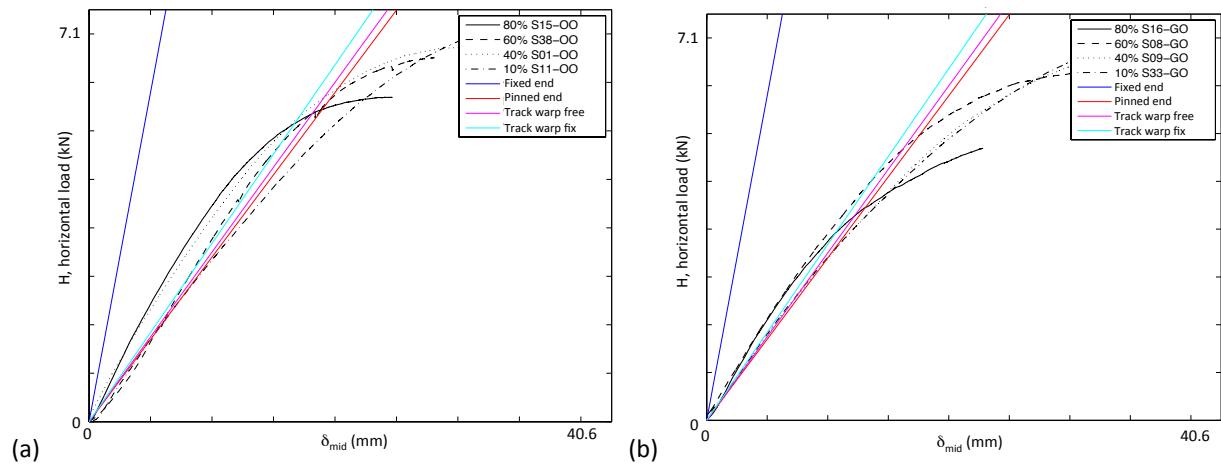


Figure 7 Horizontal force vs. mid-height horizontal displacement with comparison to fixed, pinned, and semi-rigid end conditions for the short segment of connected track for (a) OO and (b) GO sheathed specimens

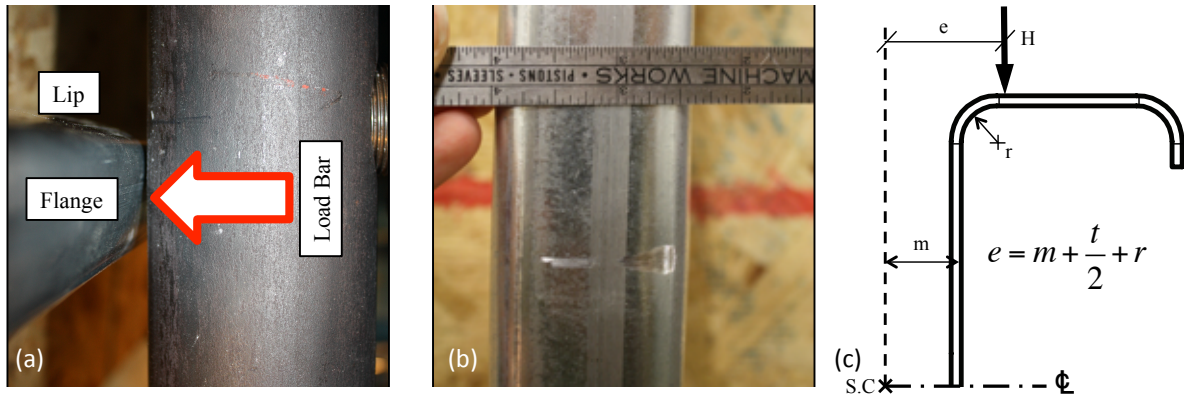


Figure 8 Location of laterally applied load (a) top view of load bar showing initial contact location, (b) etching of load bar on stud, showing load location moves to the termination of the flange flat, (c) assumed final location of lateral load for finite twist

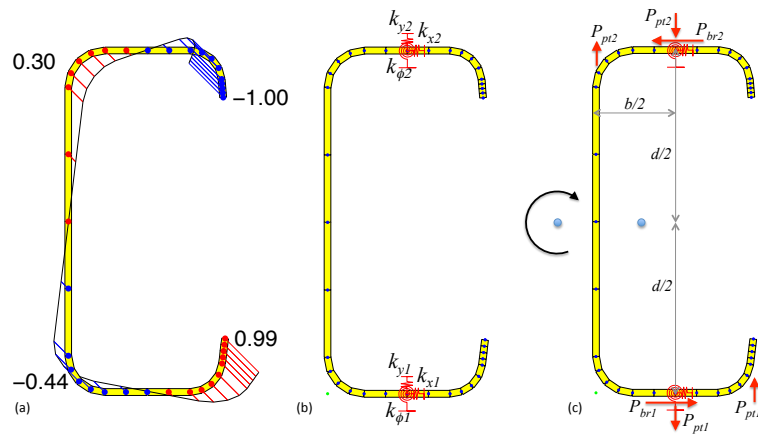


Figure 9 As-measured cross-section drawn to scale, with (a) longitudinal stress distribution due to warping alone, (b) rotational/pull-through ( $k_{\phi}$ ), lateral/bearing ( $k_x$ ) and composite action/vertical ( $k_y$ ) springs for the unloaded (1) and loaded (2) flanges, (c) torsional free-body diagram for resistance created by fasteners through bearing ( $P_{br}$ ) and pull-through ( $P_{pt}$ ).

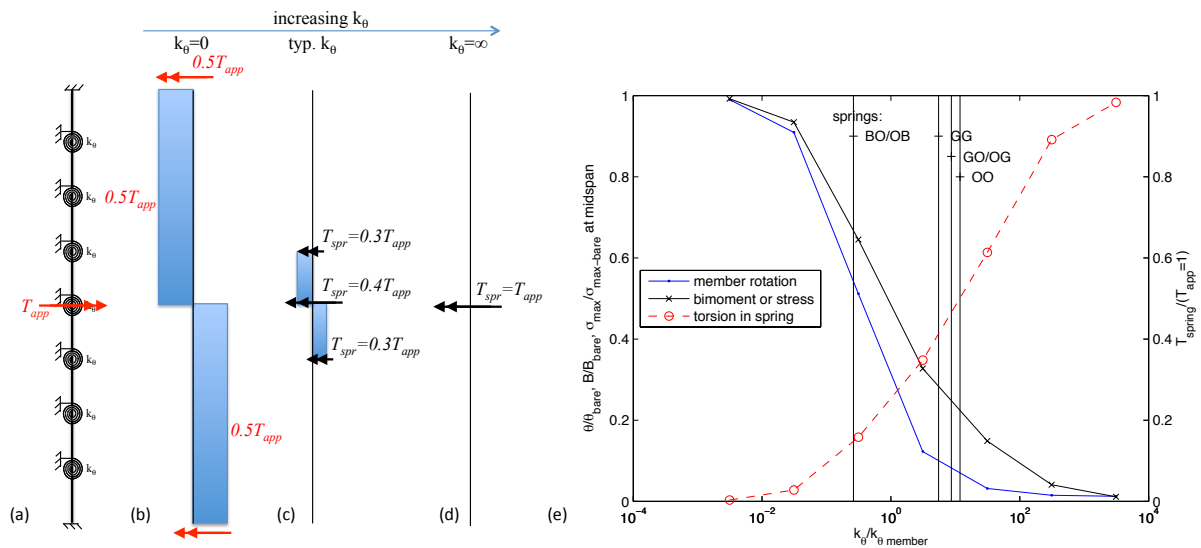


Figure 10 Torsional stiffness analysis model for a stud braced with rotational  $k_\theta$  springs every 305 mm [12 in.] o.c over 2.4 m [96 in.] length and loaded by a point torque at midspan (a) basic model, (b) torsional moment diagram without springs, (c) torsional moment diagram and spring torsion for typical fastener-sheathing spring stiffness, (d) torsional moment diagram and spring torsion for infinitely stiff spring, (e) midspan rotation, midspan bimoment, and midspan torsion in the spring as a function of increasing  $k_\theta$  (plot normalized to  $T_{app} = 113 \text{ N}\cdot\text{m}$  [1 kip-in.],  $\theta_{bare} = 0.3124 \text{ rad}$ ,  $B_{bare} = 384 \text{ N}\cdot\text{m}^2$  [11.57 kip-in<sup>2</sup>],  $\sigma_{max-bare} = 381 \text{ MPa}$  [55.25 ksi])



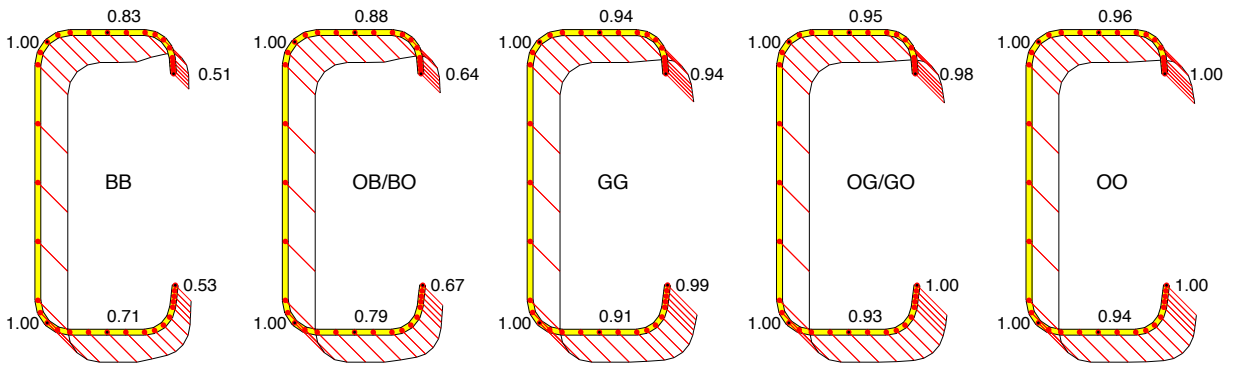


Figure 11 Distribution of bending strength reduction ratio  $R$  ( $R = (\sigma_b)_{\max} / |\sigma_b + \sigma_w| \leq 1.0$ ) for the five different sheathing configurations. Ratios less than 1 indicate the expected reduction in bending capacity due to the presence of longitudinal warping stresses.

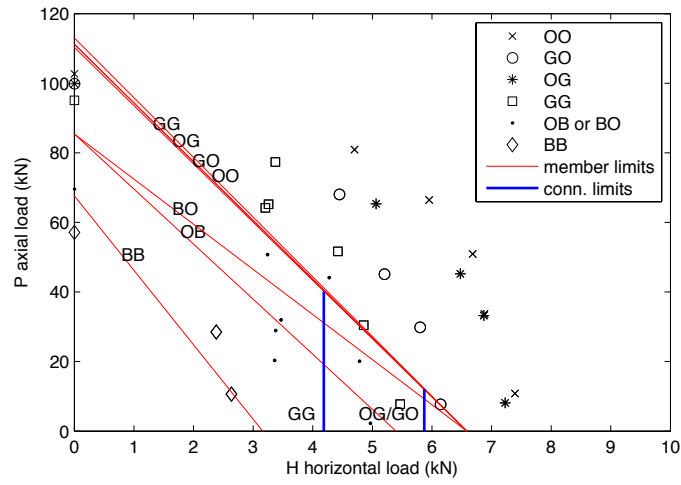


Figure 12 Comparison of observed axial and lateral failure loads of tested 362S162-68 studs with different sheathing configurations against predicted capacity for member limit states (Table 3) and connection limit state (Table 4)

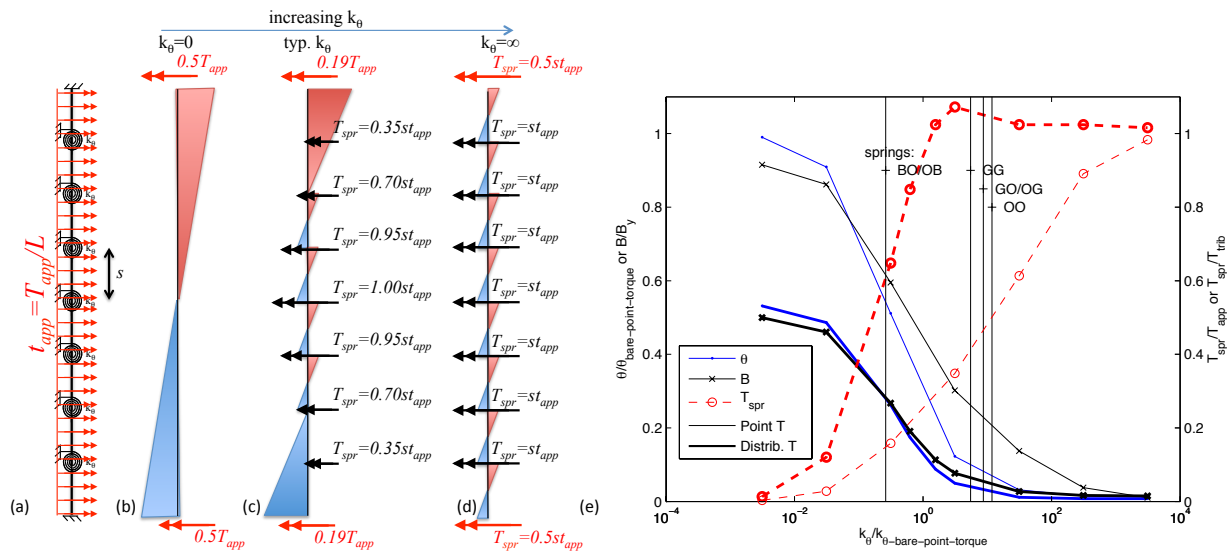


Figure 13 Extension of torsion stiffness analysis of Figure 10 from point torque ( $T_{app} = He$ ) to distributed torque ( $t_{app} = (H/L)e = we$ ), (a) basic model, (b) torsional moment diagram without springs, (c) torsional moment diagram and spring torsion for typical fastener-sheathing spring stiffness, (d) torsional moment diagram and spring torsion for infinitely stiff spring, (e) comparison of mid-height rotation, maximum bimoment, and mid-height torsion in the spring (fastener) as a function of increasing  $k_{\theta}$  for point torque vs. distributed torque (plot normalized to  $T_{app} = 113 \text{ N-m}$  [1 kip-in.],  $T_{trib} = 14 \text{ N-m}$  [0.125 kip-in.],  $\theta_{bare-point-torque} = 0.312 \text{ rad}$ ,  $B_y = 451 \text{ N-m}^2$  [12.54 kip-in<sup>2</sup>],  $\sigma_{max}(B_y) = F_y = 413 \text{ MPa}$  [59.9 ksi])